A BIOPHYSICAL APPROACH TO INVESTIGATE THE HUMAN FE-S CLUSTER ASSEMBLY PATHWAY

A Dissertation

by

NICHOLAS GRAHAM FOX

Submitted to the Office of Graduate and Professional Studies of
Texas A&M University
in partial fulfillment of the requirements for the degree of

DOCTOR OF PHILOSOPHY

Chair of Committee,	David P. Barondeau
Committee Members,	Paul Lindahl
	Wenshe Liu
	James Sacchettini
Head of Department,	David H. Russell

August 2014

Major Subject: Chemistry

ABSTRACT

Iron sulfur (Fe-S) clusters are essential cofactors that function in electron transport, catalyzing substrate turnover, environmental sensing, and initiating radical chemistry. Elaborate multi-component systems have evolved to protect organisms from the toxic effects of free iron and sulfide ions while promoting the efficient biosynthesis of these cofactors. The *in vivo* loss of frataxin (FXN) function results in depleted activity of Fe-S enzymes and is directly linked to the fatal and incurable neurodegenerative disease Friedreich's ataxia (FRDA).

Previously, our lab discovered the cysteine desulfurase and Fe-S assembly activities of the human Fe-S assembly complex (SDU), which consists of the cysteine desulfurase complex NFS1-ISD11 and scaffold protein ISCU2, are greatly stimulated by FXN binding and forming the SDUF complex. This dissertation's objectives were to identify critical FXN interactions for binding and activation of the SDU complex, investigate the interprotein sulfur transfer reaction between NFS1 and ISCU2, and provide mechanistic details of Fe-S assembly on the SDUF complex.

First, surface residues on FXN were substituted with alanine or glycine and the ability of each variant to bind and activate the SDU complex was assessed. These experiments revealed a localized "hotspot" of critical residues on FXN, which could aid in designing small peptide mimics for FRDA therapeutics.

Second, ^{35}S-radiolabeling experiments indicated FXN accelerates the accumulation of persulfide species on NFS1 and ISCU2. The ISCU2 persulfide species

was established as a viable intermediate in Fe-S cluster biosynthesis by tracking the ^{35}S-radiolabel as it converts from a persulfide species to a [2Fe-2S] cluster. Additional mutagenic, enzymatic, and spectroscopic studies suggest conserved ISCU2 residue C104 is critical for FXN-based activation, whereas C35, C61, and C104, are all essential for Fe-S cluster biosynthesis. These results lead to an activation model in which FXN facilitates sulfur transfer from NFS1 to ISCU2 as an initial step in Fe-S cluster biosynthesis and favors helix-to-coil interconversion on ISCU2.

Third, UV-visible, circular dichroism, and Mössbauer spectroscopic studies indicated the SDUF complex synthesizes transient [2Fe-2S] clusters that readily transfer to thiol-containing acceptor molecules. Moreover, these studies revealed competing DTT-mediated transfer and mineralization chemistry that cause complications when studying the mechanism of Fe-S cluster biosynthesis.

DEDICATION

I have been surrounded by some of the most amazing, supportive, and loving people in my life: family, friends, mentors, and professors. Thank you to each of you. I know I am very fortunate and I deeply appreciate each of you.

I have been away from my family for a long time and missed several family gatherings that I wish I could have attended. My family has been very patient and understanding, so I dedicate this to you. Also to my dog Caedo for the long days he spent alone, the excitement he had when I would return and being well behaved to not ruin the apartment. Thank you for all the love and support you have provided. I hope to make you proud.

ACKNOWLEDGEMENTS

First and foremost, I would like to acknowledge my advisor Professor David Barondeau who was abundantly helpful and offered invaluable assistance, support, inspiration, and guidance. I would also like to thank my committee members; Professor Paul Lindahl, Professor Wenshe Liu, and Professor James Sacchettini and my collaborator Professor Frank Raushel for their help, support, and guidance through my career at Texas A&M.

I would like to acknowledge and thank Professor Barondeau, Dr. Chris Putnam, Dr. Chi-Lin Tsai, Dr. Jennifer Rabb, James Vranish, DJ Martin, Rachael Cox, Melissa Thorstad, Shachin Patra, Robert Hoyuela, Deepika Das, Trang Nguyen, and Hyeran Choi for their support, guidance, mentoring, helpful discussions, and suggestions in my research endeavors.

Portions of this research were carried out at the Stanford Synchrotron Radiation Laboratory, a national user facility operated by Stanford University on behalf of the U.S. Department of Energy, Office of Basic Energy Sciences. The SSRL Structural Molecular Biology Program is supported by the Department of Energy, Office of Biological and Environmental Research and by the National Institutes of Health, National Center for Research Resources, Biomedical Technology Program, and the National Institute of General Medical Sciences. Use of the Advanced Photon Source was supported by the U.S. Department of Energy, Office of Science, Office of Basic Energy Sciences, under Contract No. DE-AC02-06CH11357. The Advanced Light Source is supported by the

Director, Office of Science, Office of Basic Energy Sciences, of the U.S. Department of Energy under Contract No. DE-AC02-05CH11231.

NOMENCLATURE

A. vinelandii	*Azotobacter vinelandii*
CD	circular dichroism
DTT	Dithiothreitol
E. coli	*Escherichia coli*
FRDA	Friedreich's Ataxia
FXN	Frataxin (also referred to as FXN, Yfh1 (yeast frataxin), and CyaY (*E. coli* frataxin))
HEPES	N-2-hydroxyethylpiperazine-N'-2-ethanesulfonic acid
IPTG	Isopropyl β–D-thiogalactopyranoside
ISCU2	Human scaffold protein (also referred to as Isu2 (human) and IscU (*E. coli* scaffold protein)
NFS1	Human cysteine desulfurase (also referred to as IscS)
PAGE	Polyacrylamide gel electrophoresis
PLP	Pyridoxal-5'-phosphate
SD	Human NFS1-ISD11 protein complex
SDU	Human NFS1-ISD11-ISCU2 protein complex
SDUF	Human NFS1-ISD11-ISCU2-FXN protein complex
Tris	Tris(hydroxymethyl) aminomethane

TABLE OF CONTENTS

Page

LIST OF FIGURES

Page

LIST OF TABLES

Page

CHAPTER I

INTRODUCTION

Many proteins rely on cofactors in order to be functionally active enzymes. Iron-sulfur (Fe-S) clusters are protein cofactors that are required for many critical cellular functions including oxidative respiration, DNA repair, and the biosynthesis of other cofactors.[1] The most common role for Fe-S clusters is in electron transfer reactions, but additional functions such as substrate turnover, environmental sensing, and protein stabilization are also known. Fe-S clusters with different iron and sulfide stoichiometries, including common rhombic [2Fe-2S] and cubic [4Fe-4S] (Figure 1.1) and more specialized [3Fe-4S], [4Fe-3S], and [8Fe-7S] clusters, are fine-tuned by the protein environment to have the necessary chemical properties for their function. Fe-S clusters are found in each of the three kingdoms of life: Eukarya, Archaea, and

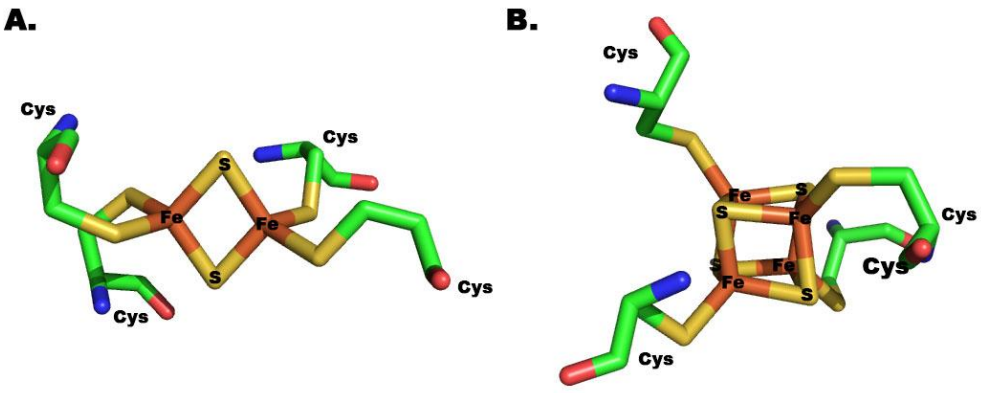

Figure 1.1. Common Fe-S clusters: (a). rhombic [2Fe-2S] and (b). cubic [4Fe-4S].

Eubacteria.[2] Fe-S clusters are also part of more complex enzyme catalysts that are involved in nitrogen fixation, hydrogen production, and CO_2 fixation. Remarkably, the Holm group and others have demonstrated that these biological Fe-S clusters can be self-assembled in solution from iron, sulfide and appropriate sulfur-containing ligands,[3, 4] and it is common to reconstitute recombinant Fe-S cluster proteins using similar conditions. Interestingly, the *in vivo* synthesis of Fe-S clusters does not use this self-assembly chemistry, but synthesizes Fe-S clusters using highly conserved proteins that are part of Fe-S cluster assembly pathways.[5-7] The concentration of iron in yeast mitochondria is between 700-800 μM, which includes about 20 percent nonheme high-spin ferrous iron under anaerobic conditions,[8] which would be very susceptible to redox reactions if not highly regulated. The more prominent Fe-S proteins are associated with Complex I, II, and III for respiration of bacteria and mitochondria, photosystem I and ferredoxin for photosynthesis, aconitase for the citric acid cycle, nitrogenase for azotobactera, and iron regulatory protein 1 (IRP1) involved in iron uptake regulation in mammals.[2] There are three distinct biosynthetic pathways to generate Fe-S cluster in prokaryotes.[2, 9, 10] The NIF system is involved in the nitrogen fixation process that converts N_2 to NH_3 in bacteria.[11, 12] The SUF system is involved in sulfur mobilization and is most predominant during oxidative stress conditions.[13] The Iron-Sulfur Cluster (ISC) assembly machinery is required for the majority of Fe-S cluster proteins, and may perform a general "house-keeping" biosynthetic function.[14] In eukaryotes, Fe-S cluster biosynthesis occurs in the mitochondria using a pathway with similarities to the ISC assembly machinery. This may be due to the mitochondria possibly originated from a

bacterial ancestry.[15] This mitochondrial Fe-S assembly pathway is essential for the biosynthesis of Fe-S clusters found in the mitochondria, but also for Fe-S proteins located in the cytosol and nucleus.

Cluster Assembly Pathway

The general framework for the assembly of Fe-S clusters in eukaryotes is widely studied, but most of the mechanistic details have not been elucidated. There are at least a dozen proteins involved in Fe-S cluster assembly.[2, 5, 16] This process has been best studied in yeast and prokaryotes. The Fe-S biosynthetic pathway in humans is located in the mitochondrial matrix and the core of the iron-sulfur assembly machinery consists of a four protein stable complex of NFS1, ISD11, ISCU2, and frataxin (FXN), called SDUF.[2, 5, 16, 17] The process is shown in Figure 1.2 for the human mitochondria and starts by a membrane potential (pmf)-dependent import of ferrous iron into the mitochondria through the metal transporters mitoferrin. The iron can be stored or delivered to ISCU2 for cluster biosynthesis.[2, 18] ISCU2 is the main scaffold protein involved in obtaining ferrous ion and inorganic sulfide to assemble a cluster and deliver it to an apo target. How iron is delivered to ISCU2 is unclear. Human frataxin (FXN,homolog of yeast Yfh1 or *E. coli* Cyay) has been proposed,[19, 20] along with ISCA,[21] to function as an iron donor for Fe-S cluster biosynthesis. FXN stimulates the cysteine desulfurase reaction and may function as an allosteric activator to regulate the Fe-S assembly complex.[22] FXN also appears to simulate the rate of *in vitro* Fe-S cluster assembly, whereas the bacterial homolog CyaY appears to inhibit Fe-S biosynthesis.[22-24] NFS1 is a cysteine

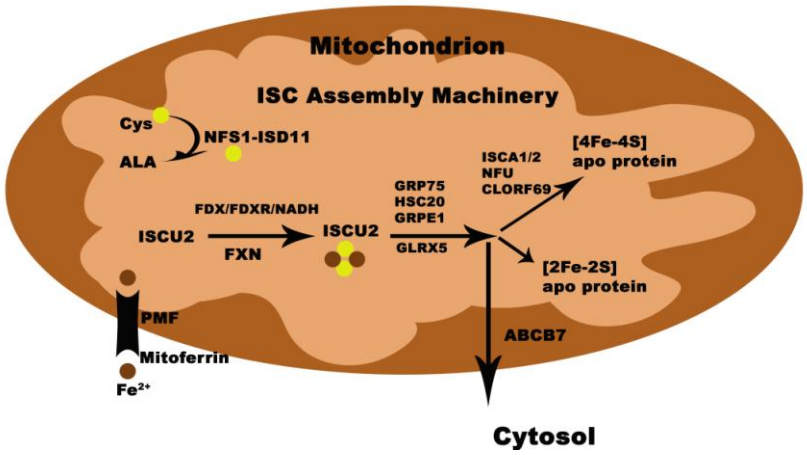

Figure 1.2. A model for eukaryotic ISC assembly machinery in the mitochondrion.

desulfurase (homolog of bacterial IscS) catalyzes the PLP-dependent conversion of L-cysteine to L-alanine (Figure 1.3), generates a persulfide species on a mobile loop cysteine, and delivers the sulfane sulfur to the Fe-S catalytic or scaffold subunit (human ISCU2 or bacterial IscU).[25, 26] The cysteine desulfurase activity is often measured by intercepting this persulfide species using reductive thiol-cleaving reagents such as DTT and quantitating the generate sulfide.[27] ISD11 is a eukaryotic-specific protein that appears to stabilize the cysteine desulfurase and may participate in positioning the mobile loop cysteine for attack of the substrate.[28-32], whereas the ferredoxin/ferredoxin reductase (FDX/FDXR, yeast homolog Yah1/ Arh1) system is thought to provide electrons.[33, 34] *In vitro* Fe-S assembly reactions often use a surrogate electron donor such as DTT rather than the ferredoxin/ferredoxin reductase system. Finally, chaperone and Fe-S carrier proteins appear to facilitate the transfer of intact Fe-S clusters from the Fe-S assembly complex to target proteins.[35, 36]

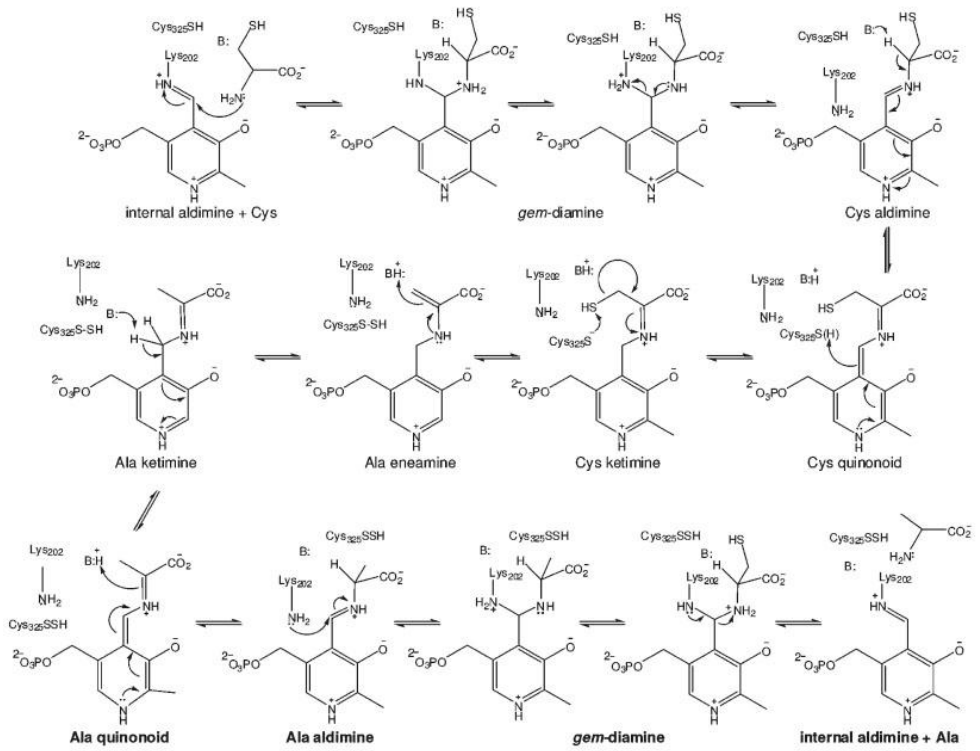

Figure 1.3. Mechanism for the PLP- dependent catalyzed conversion from cysteine to alanine by the cysteine desulfurase enzyme. Reprinted with permission from Behshad, E., and Bollinger, J. (2009) Kinetic analysis of cysteine desulfurase CD0387 from *Synechocystis* sp PCC 6803: formation of the persulfide intermediate, *Biochemistry 48*, 12014-12023. Copyright © 2009 American Chemical Society.

There is much known on the individual components of assembly proteins, but the mechanism for cluster formation is not as well established especially as a complex. There have been two possible mechanisms proposed for the Fe-S cluster assembly mechanisms in the SUF system (Figure 1.4).[37-39] The proposed mechanisms are either an iron first or sulfur first model in assembling a [2Fe-2S] cluster. The binding constants for both ferrous and ferric to the *Thermotoga maritima* IscU and yeast FXN have been determined and are very weak.[40, 41]

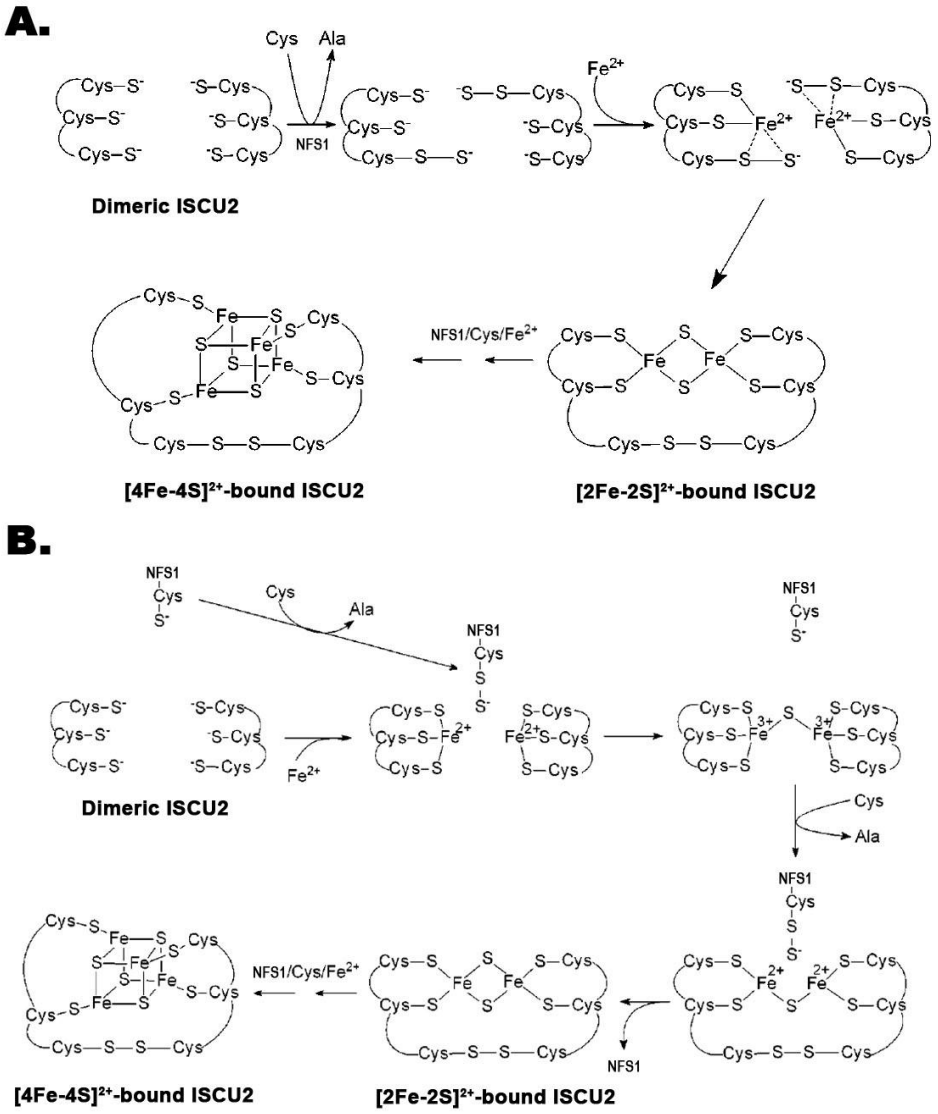

Figure 1.4. Proposed mechanisms for the assembly on Fe-S clusters on the ISCU2 scaffold protein. (A) Iron first mechanism and (B) sulfur first mechanism. Adapted with permission from Krebs, C., Agar, J.N., Smith, A.D., Fazzon, J., Dean, D.R., Huynh, B.H., and Johnson, M.K. (2001) IscA, an alternate scaffold for Fe−S cluster biosynthesis, *Biochemistry 40*, (46) 14069-14080. Copyright © 2001 American Chemical Society.

IscS with IscU, in the absence of DTT, resulted in a persulfide-bound or polysulfide-bound IscU.[42, 43] The iron-first mechanism requires that the first step in cluster

formation is ligation of two ferrous atoms to the three conserved cysteine residues on ISCU2. ISCU2 has been believed to be a dimer in this reaction and may be independent of the complex once sulfur has been transferred from NFS1. Once the iron binds, sulfur is transferred from the cysteine desulfurase in the form of sulfane. This sulfane sulfur must be reduced by 4 electrons, to sulfide, in order to be incorporated in a [2Fe-2S] cluster; 2 of which are contributed from the ferrous iron atoms and 2 of which are proposed to come from ferredoxin. The sulfur-first mechanism is initiated by a cysteine residue on the ISCU2 dimer nucleophilically attacking the persulfidic species generated on the catalytic loop of the cysteine desulfurase, transferring this sulfide to another cysteine on ISCU2 and undergoing another turn over. Ferrous iron than binds and cluster is formed by sequential 2-electron reduction of each sulfane sulfur atom. Sulfur has been shown to be incorporated on the scaffold proteins in the absence of iron, supporting a sulfur first mechanism.[42-44] There is little evidence of very weak iron binding to the complex, but has never been shown to bind ferrous iron with cysteine ligation.[40, 41, 45] Neither the persulfide-bound or polysulfide-bound forms of IscU have been shown to be viable in cluster formation. Human ISCU2 has three conserved cysteine residues (C35, C61, and C104) that are involved with Fe-S cluster assembly and one non conserved cysteine (C96) that is presumed to be not involved in the assembly of an Fe-S cluster. The fourth cluster ligand is unknown but has been suggested to be H103,[46, 47] an ISCU2 ligand formed from ISCU2 dimerization[48] or the mobile loop cysteine (C328) from NFS1.[49] Each of these three conserved cysteine residues on the scaffold protein has been implicated in acting as the sulfur acceptor residue during the sulfur transfer

reaction. Electrospray-ionization mass spectrometry was used to show that the *Azotobacter vinelandii* cysteine desulfurase could deliver a persulfide or polysulfide species to the scaffold protein even if each of three cysteine residues were mutated to alanine resulting in a covalent disulfide bridge between C37 (C35 in human numbering) and the catalytic cysteine of the cysteine desulfurase.[50] The sulfur-first mechanism seems to be the most favorable, but whether a particular cysteine residue on ISCU2 accepts the sulfur atom from NFS1 or multiple cysteine residues, is still debatable. The *E. coli* scaffold protein shows an essential role for C106 (C104 in human numbering) in accepting the persulfide sulfur from the cysteine desulfurase enzyme.[44] The equivalent sulfur transfer experiments have not yet been performed on a eukaryotic system. Most experiments are also performed as individual components and have not in the context of a complex. The pathway of both iron and sulfur throughout the Fe-S cluster biosynthesis has never been shown to be incorporated into an assembled Fe-S cluster and transferred to an apo target.

The prokaryotic scaffold protein IscU combines sulfur generated from cysteine by the cysteine desulfurase, iron, and electrons to synthesize [2Fe-2S] and [4Fe-4S] clusters. Currently, no intermediates in generating [2Fe-2S] clusters are established in the biosynthetic system or self-assembly process, but some details of the conversion of [2Fe-2S] clusters to [4Fe-4S] clusters are known. Inorganic biomimetic chemistry revealed that [4Fe-4S] clusters can be formed by reductively coupling two [2Fe-2S] clusters,[3] whereas studies of the oxygen sensor protein FNR reveal the conversion of persulfide ligated [2Fe-2S] cluster to cysteine ligated [4Fe-4S] cluster upon the addition

of iron.[51] In key early studies on biosynthetic systems, Agar *et al*. demonstrated that [2Fe-2S] clusters can be assembled on IscU in an IscS mediated process,[52] and Foster *et al.* showed that the human ISCU2 D37A variant contains a stable [2Fe-2S] cluster.[53] IscU binds clusters with three conserved cysteines,[50] with experimental support for a semi-conserved histidine,[46, 54] aspartic acid,[55] and a cysteine from another molecule[56, 57] as the fourth ligand. In a remarkable study, the Huynh, Dean, and Johnson groups demonstrated reductive coupling chemistry on an IscU dimeric species with the sequential formation of a single [2Fe-2S] cluster, a second [2Fe-2S] cluster, and then conversion of these [2Fe-2S] clusters to form one [4Fe-4S] cluster per IscU dimer.[48] This reductive coupling chemistry appears to occur at an IscU dimeric interface with each monomer contributing one [2Fe-2S] cluster.

An Fe-S assembly complex appears to be responsible for the synthesis of [2Fe-2S] and possibly [4Fe-4S] clusters for the ISC pathway. A protein complex between bacterial IscS and IscU has been demonstrated in solution,[42, 58] and crystal structures with[56] and without[59] a [2Fe-2S] cluster provide details of the protein-protein interactions and cluster environment. An apparent key to obtaining a crystal structure of the bound [2Fe-2S] cluster was the incorporation of the D35A variant,[56] which was previously shown to stabilize the cluster bound state and/or inhibit cluster transfer.[53, 60, 61] Interestingly, Mössbauer spectroscopic studies suggest the addition of L-cysteine, ferrous iron, and DTT to the bacterial and mammalian Fe-S assembly complexes results in the formation of [2Fe-2S] and [4Fe-4S] cluster species.[62, 63] These results suggest at least two models. In the first model, IscU subunits dissociate after building [2Fe-2S] clusters,

and this dissociated [2Fe-2S]-bound IscU undergoes reductive coupling chemistry to generate [4Fe-4S] clusters. In the second model, [2Fe-2S] clusters synthesized on the Fe-S assembly complex transform to [4Fe-4S] clusters through chemistry that may resemble the [2Fe-2S] → [4Fe-4S] conversion for FNR.[51] The first model is supported by the ability of the scaffold protein to undergo reductive coupling chemistry,[48, 64] whereas the second model is suggested by recent studies of a eukaryotic Fe-S assembly complex.[62]

Human Fe-S Cluster Assembly

Human FXN has been shown to stimulate NFS1 activity (Figure 1.5A). The activity and Michaelis- Menten kinetics was measured by using the methylene blue assay to quantify the amount of sulfide produced from L-cysteine conversion to L-alanine and a persulfide species, which is then released by dithiothreitol (DTT). The reaction is quenched by the addition of *N*,*N*-dimethyl-*p*-phenylenediamine (DMPD) and $FeCl_3$ in 1.2 M HCl (Figure 1.6).[65] Methylene blue is measured by measuring the absorbance at 670 nm to determine the sulfide concentration. Ferrous iron has been shown to stimulate NFS1 activity (Figure 1.5B).[17] Ferrous iron appears to further stimulate NFS1 activity[17] and is unclear if this iron is incorporated in a cluster or could be involved in stabilizing the complex. Ferrous may also stabilize interactions between FXN and ISCU2 in the absence of NFS1/ISD11.[66] The iron may also be bound to ISCU2, presumably to the surface cysteine residues or to the carboxylate-rich region of FXN.[67] The crystal structures of bacterial IscS (homolog of NFS1)[59, 68], bacterial IscU/IscS complex (Figure 1.7A),[69] bacterial IscU (Figure 1.7B, homolog of ISCU2)[47],

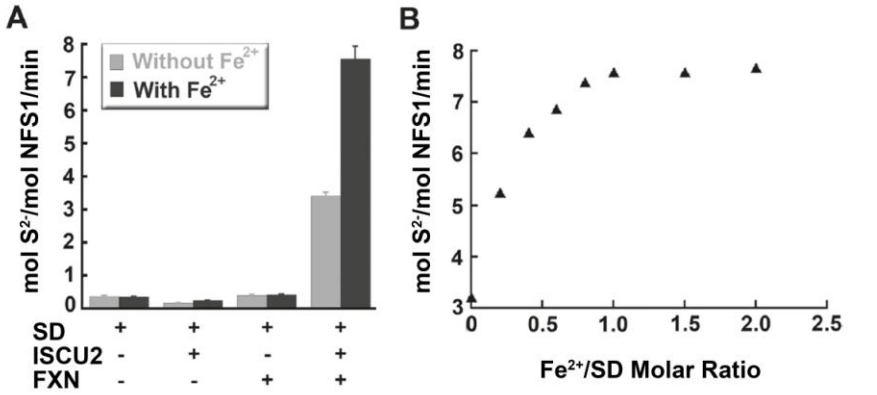

Figure 1.5. Frataxin and ferrous iron stimulates cysteine desulfurase activity. (A) Rates of SD cysteine desulfurase activity were determined by measuring sulfide production in the presence and absence of 3 equivalents of ISCU2 and/or FXN, and either 0 or 10 equivalents of ferrous iron. (B) Rates of sulfide production were determined for SD in the presence of 3 equivalents of ISCU2 and FXN, and increasing amounts of ferrous iron. Reprinted with permission from Tsai, C., and Barondeau, D. P. (2010) Human frataxin is an allosteric switch that activates the Fe-S cluster biosynthetic complex, *Biochemistry 49*, 9132–9139. Copyright © 2010 American Chemical Society.

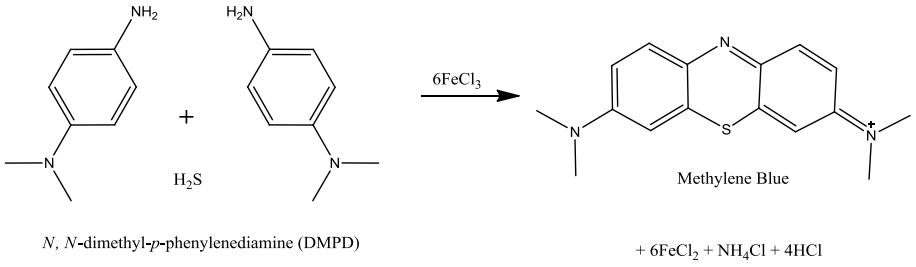

Figure 1.6. Reaction mechanism for methylene blue formation.

and human frataxin (Figure 1.7C) have been previously determined, which may provide structural insight for the human NFS1 and NFS1-ISCU2 complex.[70, 71] There have also been simulations where Cyay (homolog of FXN) may bind the IscS-IscU complex, which can help generate a model for an NFS1-ISCU2-FXN complex.[69] This model could help in elucidating the mechanism for Fe-S cluster biosynthesis.

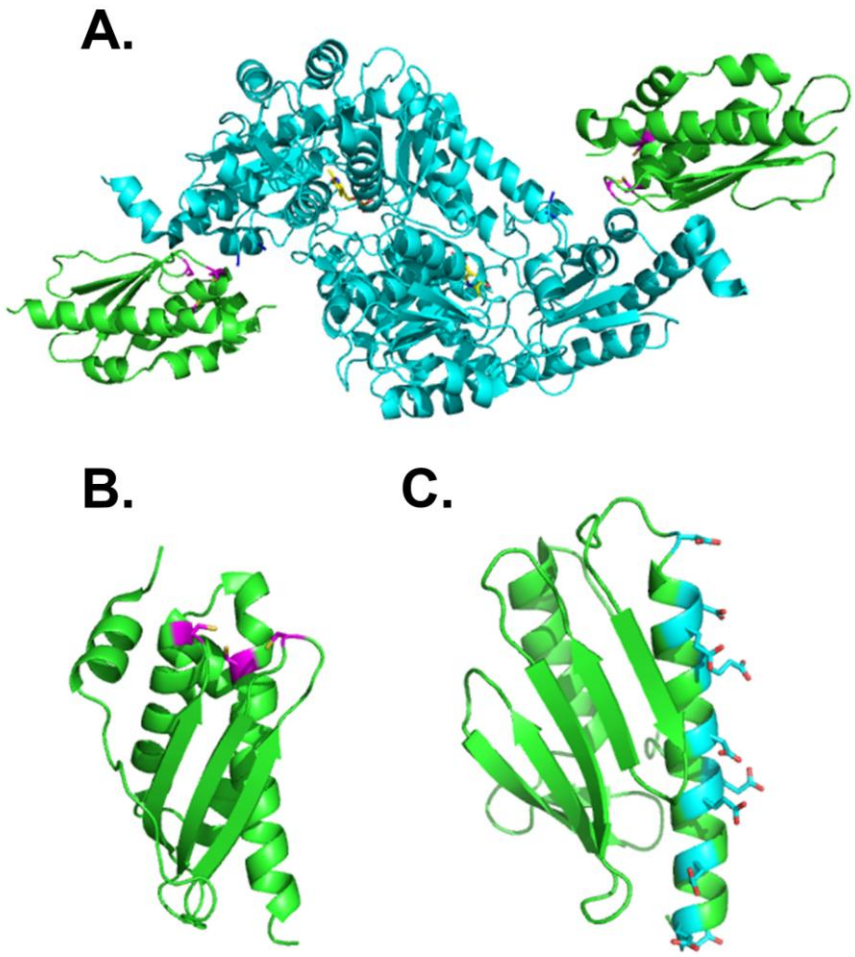

Figure 1.7. Crystal structure of *E. coli* IscS-IscU complex (A, PDB code 3LVL), IscU (B, PDB code 3LVL), and human FXN (C, PDB code 1EKG). In (A) the IscS is in cyan and IscU is in green. In (B) the IscU conserved cysteine residues are highlighted in magenta. In (C) FXN carboxylic patch is highlighted in cyan.

Fe-S Cluster and Health

Deficiencies in the iron-sulfur cluster biosynthetic pathway have been implicated in several human diseases.[16] Friedreich's Ataxias is the most studied disease and is an autosomal, recessive neurodegenerative disorder caused by the deficiency of frataxin.[72] Frataxin is widely suggested to be a chaperone for delivering iron directly to Isu2. Frataxin is well conserved among prokaryotes and eukaryotes. Cellular depletion of frataxin due to lower protein expression or loss of frataxin's functional properties leads to loss of Fe-S protein activities, mitochondrial iron accumulation, and oxidative damage.[73] Mitochondria dysfunction has also been implicated in several human diseases. Nerve cells in the brain and muscles require a great deal of energy, and thus appear to be particularly damaged by mitochondrial dysfunction. Mitochondrial dysfunctions can result in myoclonus epilepsy, strokes, heart failure, muscle weakness, exercise intolerance, dementia, deafness, and blindness. Defects in the Fe-S cluster pathway are associated with cardiomyopathy, neurodegenerative ataxia, and can even contribute to the development of cancer and aging.[74] The prognosis for these disorders ranges in severity from progressive weakness to death.[16, 75]

Here we build upon these observation and present mechanistic details on the assembly of an Fe-S cluster on the human SDUF complex. We designed experiments that support a model in which FXN stabilizes a conformation that both accelerates persulfide formation on NFS1 and also interprotein sulfur transfer from NFS1. We need to determine residues on FXN that are important for this activation and what residues affect binding. To further investigate the mechanism of Fe-S cluster biosynthesis, we

will first need to identify the persulfide accepting cysteine residue on ISCU2 from NFS1, establish that the persulfide formed on ISCU2 in the sulfur transfer reaction is viable in a subsequent Fe-S synthesis reaction, determine the type of Fe-S cluster the human SDUF complex synthesizes, and the transfer to apo targets.

CHAPTER II

HUMAN FRATAXIN ACTIVATES FE-S CLUSTER BIOSYNTHESIS BY FACILITATING SULFUR TRANSFER CHEMISTRY

Introduction

Sulfur is a critical element for all life forms and is found in a variety of protein cofactors including molybdopterins, lipoic acid, thiamin, biotin, and iron-sulfur (Fe-S) clusters. Even though the functions of these cofactors are well understood, mechanistic details are just emerging for how sulfur is incorporated into these biomolecules.[76, 77] A common early step for these pathways is the cysteine desulfurase catalyzed degradation of cysteine to alanine and the generation of a protein-bound persulfide species. This activated sulfur is reductively cleaved by distinct acceptor proteins for the biosynthesis of sulfur-containing cofactors and modification of tRNA.[76] Redox agents such as cysteine and DTT (*in vitro*) can also release the terminal sulfur of the persulfide in an often rate-determining step for the cysteine desulfurase that produces hydrogen sulfide.[25, 27]

Bacteria, archaea, and eukaryotic organelles use one or more of the ISC, NIF, and SUF systems for the biosynthesis of Fe-S clusters. In the ISC assembly system of *Escherichia coli,* the cysteine desulfurase IscS uses a PLP cofactor to assist in cleaving the sulfur-carbon bond of L-cysteine and generating a persulfide intermediate on residue C328.[78] The scaffold protein IscU combines the sulfane sulfur generated by IscS, ferrous iron, and electrons to synthesize Fe-S clusters. Crystal structures of the bacterial IscS-

IscU complex have been determined with[56] and without[59] a [2Fe-2S] cluster bound. The crystal structure of the *E. coli* complex revealed that IscS C328 (equivalent to C381 on human NFS1) is positioned on a highly flexible loop and can potentially traverse the ~30 Å distance between an IscS substrate-PLP adduct and conserved cysteine residues of IscU. Although the functional significance for sulfur transfer is unclear, IscS C328 can form disulfide crosslinks with conserved IscU residues C37[50] and C63[58], consistent with the suggestion based on the IscS-IscU crystal structure[59] that these residues on IscU could function as sulfur acceptor residues during Fe-S cluster biosynthesis. The third conserved cysteine, C106, is somewhat buried on the C-terminal α-helix of IscU.

Research conducted on the bacterial ISC Fe-S assembly system has yet to identify intermediates on the Fe-S assembly complex during cluster biosynthesis or establish if sulfur can be viably transferred from the cysteine desulfurase to the scaffold protein before, after, or simultaneous with iron incorporation. Radiolabeling and mass spectrometry experiments for the ISC system have been used to track interprotein persulfide-based sulfur transfer from IscS to IscU.[42, 43, 50] However, the persulfide (or polysulfide) species that were bound to IscU did not appear to be viable in Fe-S cluster formation. Kinetic data demonstrated that *E. coli* IscU variants C37S and C106S, but not C63S, stimulated sulfide production by IscS,[58] leading to the conclusion that IscU C63 assists in the rate-limiting cleavage of the IscS C328 persulfide species. However, subsequent kinetic experiments failed to observe any IscU-based stimulation of sulfide production by IscS.[24, 63] In contrast, recent experiments monitoring iron-sulfur cluster reconstitution on *E. coli* ferredoxin hinted that IscU residue C106, and not C37 or C63,

has an role in sulfur transfer from IscS to IscU.[79] These experiments have led to proposals that C63[58], C106[79], either C37 or C63[69], or any of the three conserved cysteine residues on IscU[50] can function as the acceptor in the sulfur transfer reaction for the prokaryotic ISC system. Differences in binding affinities for IscU variants to IscS, the facile reactivity of persulfide species with thiol containing molecules, and differences in experimental design such as bypassing IscS (chemical reconstitution), using catalytic amounts of IscS, or using conditions consistent with the IscS-IscU complex, may contribute to these different conclusions.

In eukaryotes, recent evidence suggests Fe-S biosynthesis is catalyzed by an assembly complex that exists in at least two forms: the mostly inactive SDU complex, which contains the subunits NFS1, ISD11, and ISCU2, and the activated SDUF complex, which contains the subunits NFS1, ISD11, ISCU2, and frataxin (FXN).[22, 80] In humans, the 94 kDa homodimeric cysteine desulfurase NFS1 (homolog of IscS) provides sulfur for Fe-S cluster biosynthesis.[25, 81] ISD11 is a eukaryotic-specific protein that interacts, stabilizes, and may activate NFS1.[29, 30, 82-85] Cluster assembly is templated by the scaffold protein ISCU2 (homolog of IscU), whereas FXN stimulates the cysteine desulfurase and Fe-S cluster assembly reactions.[22, 62, 86, 87] Defects in FXN are linked to the neurodegenerative disease Friedreich's ataxia (FRDA),[88, 89] and FXN variants encoded by FRDA missense mutations have compromised ability to bind and activate the Fe-S assembly complex.[86, 87]

The ability of FXN to enhance the cysteine desulfurase and Fe-S assembly activities implies that it is involved in sulfur mobilization and/or transfer chemistry from

the cysteine desulfurase NFS1 to the scaffold protein ISCU2. A ^{35}S-radiolabeling experiment using *Saccharomyces cerevisiae* mitochondria revealed a NFS1 persulfide species under iron depleted conditions and radiolabeled ferredoxin under iron repleted conditions.[85] However, few details are known about the eukaryotic sulfur hand-off mechanism from NFS1 to ISCU2 (see Figure 2.1 for a model of the human NFS1-ISCU2 complex) and the role of FXN in this process. One of the advantages of this experimental system compared to the bacterial ISC systems is the dramatic rate enhancement of the cysteine desulfurase reaction upon FXN binding. Here we build upon this observation and present experiments that support a model in which FXN stabilizes a conformation that both accelerates persulfide formation on NFS1 and also interprotein sulfur transfer from NFS1 to residue C104 on ISCU2 (equivalent to *E. coli* C106) as an early step in Fe-S cluster biosynthesis. Furthermore, we establish that the persulfide formed on ISCU2 in the sulfur transfer reaction is viable in a subsequent Fe-S synthesis reaction, consistent with a sulfur-first mechanism.

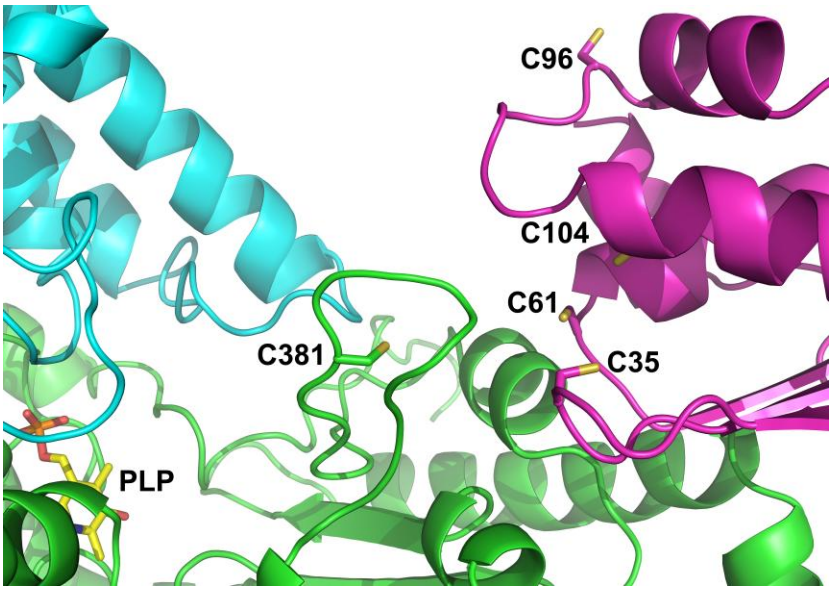

Figure 2.1. Human NFS1-ISCU2 complex modeled from the crystal structure of the analogous IscS-IscU complex (PDB 3LVL). NFS1 subunits are shown in green and cyan, whereas ISCU2 is displayed in magenta.

Experimental Procedures

Protein Expression and Purification

Eight human ISCU2 cysteine variants (C96S, C35A, C35S, C61A, C61S, C104A, C104S, and C35A/C61A) were created by QuikChange site-directed mutagenesis (Stratagene) using a pET11a-ISCU2 plasmid template,[22] and the mutation sites were confirmed by DNA sequencing (Gene Technologies Lab at TAMU). The resulting plasmids containing ISCU2 with the desired mutations were transformed into BL21(DE3) cells and grown at 37 ºC until reaching an OD_{600} of 0.6. Protein expression was induced at 16 ºC with 0.5 mM IPTG and the cells were harvested 16 hours later. The ISCU2 variants along with human NFS1-ISD11 (SD) and FXN were purified as

previously described[22] with the exception of adding 10% glycerol to the buffers for the C61A and C35A/C61A mutants.

Human ferredoxin (FDX, gift from John Markley)[90] was transformed into *E. coli* BL21 (DE3) cells and grown at 37 ºC until reaching an OD_{600} of 0.6. Expression was induced for 16 hours with 0.4 mM IPTG, 1 mM cysteine, and 0.1 mg/mL ferric ammonium citrate. Cells were lysed by sonication and the supernatant was loaded onto an anion exchange column (26/20 POROS 50HQ, Applied Biosystems) and eluted with a linear gradient from 0 to 1000 mM NaCl in 50 mM Tris pH 7.5. Fractions containing FDX were further purified on a Sephacryl S100 (26/60, GE Healthcare) size exclusion column equilibrated in 50 mM Tris, pH 7.4, 50 mM NaCl. Apo FDX was prepared by precipitating the purified FDX with a 10% trichloroacetic acid solution containing 10 mM DTT on ice for 10 minutes, after which the sample was pelleted by centrifugation.[91] The protein pellet was rinsed twice with water and then re-suspended anaerobically in Buffer A (50 mM Tris pH 8.0, 250 mM NaCl).[91] Protein concentration was determined by the Bradford method for reconstituted FDX, and using an extinction coefficient ε_{280} = 2980 $M^{-1}cm^{-1}$ for apo FDX.

SDS-PAGE Analysis of Sulfur Transfer

Reaction mixtures (30 μL) for monitoring sulfur transfer included 3 μM SD, 9 to 120 μM ISCU2, Buffer A and either 0 or 9 μM FXN. A similar experiment was performed in which 9 μM of the FRDA FXN variants N146K, Q148R, I154F, W155R, and R165C, which were purified as previously described,[86, 87] were substituted for native FXN. Samples were incubated in the glovebox for 10 minutes prior to the addition of

100 μM "hot" L-cysteine, prepared by adding 50 Ci/mmol ^{35}S-cysteine (American Radiolabeled Chemicals Inc.) to a 1 mM "cold" cysteine stock solution. After a 2-minute incubation at 37 °C, reactions were terminated by centrifugation through a Micro Bio-Spin P-6 gel filtration column (Bio-Rad). The spin column flow through was combined with non-reducing SDS-PAGE sample loading buffer and then loaded on a non-reducing 14% SDS-PAGE gel. The gel was dried onto chromatography paper in a gel-drying oven at 60 °C under vacuum before a 12-hour exposure to a phosphor screen. ^{35}S label incorporation was visualized using a Phosphorimager (Typhoon Trio, GE Healthcare).

Tracking Sulfur from L-cysteine through the SDUF Complex to a Fe-S Cluster on FDX

To test if the ^{35}S radiolabel from the substrate L-cysteine can be transferred to ISCU2 and then to the [2Fe-2S] cluster of FDX, a sample was prepared that contained 80 μM SD, 240 μM ISCU2, 240 μM FXN, Buffer A in a total volume of 400 μL. The reaction was initiated with the addition of 20 Ci/mmol L-[^{35}S]-cysteine and allowed to proceed for 40 minutes anaerobically at 10 ºC. The sample was then loaded onto a 1 mL HisTrap HP column (GE Healthcare) equilibrated in 50 mM Tris pH 7.5, 200 mM NaCl, and 5 mM imidazole, and eluted with a linear gradient from 5 to 500 mM imidazole. To evaluate ^{35}S-persulfide incorporation, 30 μL of each fraction from the 1 mL HisTrap HP column was centrifuged through a Micro Bio-Spin P-6 gel filtration column (Bio-Rad) and combined with 8 μL non-reducing SDS-gel loading dye and loaded on a 14% SDS-PAGE gel that was dried, exposed, and imaged as described above. Fractions containing labeled NFS1 and ISCU2 were concentrated to 70 μL, of which 20 μL was analyzed for SDUF complex formation using a 6.5% native gel.[22] The remaining 50 μL of

radiolabeled SDUF complex was incubated anaerobically at 10 ºC with 600 μM $Fe(NH_4)_2(SO_4)_2$, 160 μM L-cysteine, and 1 mM DTT for 1 hour. After incubation, the excess reaction components were removed using a Micro Bio-Spin P-6 column that was buffer exchanged into Buffer A. The material that flowed through the Bio-Spin P-6 column was incubated with 200 μM apo FDX anaerobically 10 ºC for 1 hour. The sample was then loaded and eluted from a 1 mL HisTrap HP column as described above, except that absorbance was monitored at 405 nm rather than 280 nm. The flow-through fractions corresponding to non His-tagged FDX were concentrated to 20 μL before loading onto a non-reducing 6.5% native gel. Radiolabel incorporation was analyzed with a phosphorimager as described above.

ISCU2 Binding to and Stimulation of Fe-S Assembly Complex

Protein titrations, monitored by cysteine desulfurase activity measurements, were performed to determine the number of ISCU2 and FXN equivalents to overcome any loss of binding affinity for the SDUF complex due to ISCU2 mutations. For the titration of ISCU2 variants, the reaction mixtures were initiated with 100 μM L-cysteine and included 0.5 μM SD, 2 mM DTT, 10 μM PLP, and Buffer A. Sulfide production was measured using a previously described methylene blue formation assay.[22] The number of equivalents required for each ISCU2 variant (calculated based on the SD concentration) to no longer change or saturate the cysteine desulfurase activities was determined to be 3 (native ISCU2, C35A, and C104A), 30 (C96S), 20 (C35S), 80 (C61A and C61S), 10 (C104S), and 200 (C35A/C61A). Once the saturating amounts of the ISCU2 variants were determined, additional titrations were performed to determine the amount of FXN

needed to maximize the activity of the respective SDU complex. The number of equivalents of FXN was determined to be 3 (native ISCU2), 5 (C96S), 80 (C35A and C35S), 200 (C61A and C61S), 30 (C104A), 50 (C104S), and 400 (C35A/C61A). After determining the number of equivalents of FXN to maximize the cysteine desulfurase activity, additional equivalents of ISCU2 variants were added and the cysteine desulfurase activity was measured. The cysteine desulfurase activity did not further increase confirming saturation of ISCU2 subunits in the SDUF complex.

Michaelis-Menten Parameters for ISCU2 Variant Complexes

Reaction mixtures included 0.5 μM SD, 2 mM DTT, 10 μM PLP, Buffer A, and the saturating amount of ISCU2 variant and FXN (determined above) in the presence or absence of 5 μM $Fe(NH_4)_2(SO_4)_2$. The samples were incubated in a glovebox (mBraun; ~12 °C and < 1 ppm oxygen) for 30 min before initiation of the reaction with L-cysteine. The L-cysteine concentration ranges used were 12.5-400 μM for native, C35A, C35S C61A, C61S, and C96S variants, and 12.5-1000 μM for the C104A, C104S, and C35A/C61A variants. Reaction rates as a function of L-cysteine concentration were fit to the Michaelis-Menten equation using KaleidaGraph software (Synergy Software).

Cysteine Desulfurase and Fe-S Assembly Activities for ISCU2 *Variant Complexes*

The cysteine desulfurase activity for the different SDU complexes were determined in triplicate using a physiological L-cysteine concentration of 0.1 mM with 0.5 μM SD, 2 mM DTT, 10 μM PLP, Buffer A, and saturated amounts of the different ISCU2 variants. Similar experiments were also performed with saturating FXN in the absence or presence of 5 μM $Fe(NH_4)_2(SO_4)_2$. The Fe-S cluster assembly activity was

measured using a standard UV-visible assay[22] and also with a circular dichroism (CD) assay. For the UV-visible assay the reaction mixture contained 8 μM of SD, 5 mM DTT, 200 μM $Fe(NH_4)_2(SO_4)_2$, 100 μM L-cysteine, and Buffer A in a total volume of 0.2 mL. In addition, saturating amounts of the ISCU2 variants with or without saturating amounts of FXN were added to the assay mixture. The ISCU2 variants were incubated for 1 hour with 5 mM DTT in an anaerobic glovebox before addition of the remaining reaction components in an anaerobic cuvette. The reaction was initiated in an anaerobic cuvette by injecting L-cysteine to a final concentration of 100 μM with a gas-tight syringe. Fe-S cluster formation was monitored at 456 nm at room temperature for 3000 seconds at 20 °C and then fit as first order kinetics using KaleidaGraph software. Anaerobic CD monitored Fe-S cluster assembly assays mixtures contained 10 μM of SD, saturating amounts of ISCU2 variants and FXN, 200 μM $Fe(NH_4)_2(SO_4)_2$, 1 mM L-cysteine, and Buffer A in a total volume of 0.4 mL. The reactions were initiated with injection of 1 mM L-cysteine and the ellipticity was measured over the wavelength range 300-600 nm for 60 minutes at 20 °C using a CD spectrometer (Chirascan™).

Results

FXN Increases Sulfur Incorporation on NFS1 and ISCU2

Previously, human FXN binding to the SDU complex was shown to dramatically increase the cysteine desulfurase and Fe-S cluster biosynthesis activities for the assembly complex.[22] To test the hypothesis that FXN activation functions at the step of persulfide species formation on ISCU2, we monitored the transfer of radioactive sulfur from a L-[^{35}S]-cysteine substrate. In this experiment, increasing concentrations of

ISCU2 were added to the SD complex in either the presence or absence of FXN. The samples were incubated for two minutes with the radiolabeled substrate, excess label was removed anaerobically with a desalting column, and then the individual subunits of the SDU or SDUF complexes were analyzed with non-reducing SDS-PAGE (Figure 2.2). Radioactivity associated with NFS1 and ISCU2 under denaturing conditions indicate formation of covalent adducts (likely a persulfide species; see Discussion). Next, the ability of FRDA FXN variants were tested using the same radiolabeling procedure. Samples of the SDU and SDUF complexes were compared to SDUF samples containing the N146K, Q148R, I154F, W155R, and R165C FRDA variants (Figure 2.3). The FRDA variants qualitatively resulted in lower amounts of label incorporation on both NFS1 and ISCU2 under this set of experimental conditions. Together these results indicated a FXN-dependent increase in the radiolabel band intensity, which we have assigned as a persulfide species, associated with both NFS1 and ISCU2, and that this increase in label incorporation is diminished for FRDA variants. Interestingly, the R165C FXN variant was also labeled in this experiment. As this FXN variant labeling is probably a nonphysiological event, it is important to establish that the ^{35}S-label that is incorporated onto ISCU2 is consistent with a physiological event by testing if persulfide-bound ISCU2 species are viable in forming Fe-S clusters.

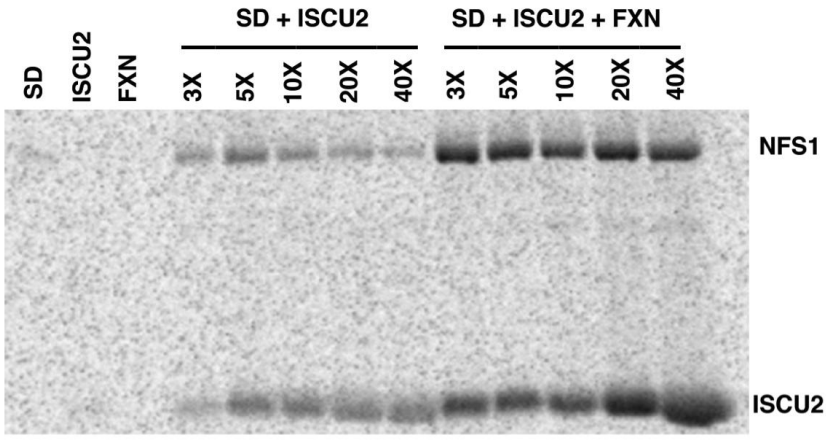

Figure 2.2. FXN enhances sulfur accumulation on NFS1 and ISCU2. Radiolabeled sulfur incorporation from ^{35}S-L-cysteine substrate on NFS1 with subsequent transfer to ISCU2 was monitored by non-reducing SDS-PAGE separation coupled to phosphor imaging. Samples of SD and 3 to 40 equivalents of ISCU2 without FXN and with FXN were incubated for 2 minutes with ^{35}S-cysteine and analyzed by SDS-PAGE. The first three lanes are SD, ISCU2, or FXN controls that were incubated for 2 minutes with ^{35}S-cysteine.

Persulfide-bound Intermediate in Human Fe-S Cluster Biosynthesis

Here, sulfur transfer from NFS1 to ISCU2 and subsequent incorporation into an Fe-S cluster was investigated using the radiolabeled L-cysteine substrate and tracking the ^{35}S progression from the ISCU2 subunit of the SDUF complex to human FDX. Combining SD with three equivalents of both ISCU2 and FXN generated the SDUF complex. The SDUF complex was reacted with L-[^{35}S]-cysteine (see Methods) and applied to a HisTrap column in which non-complexed ISCU2 and/or FXN flowed through the column and proteins associated with 6X-His-NFS1 bound and were eluted with imidazole (Figure 2.4). The radioactivity was correlated with fractions that bound the column (fractions 11-13) and specifically was associated with both NFS1 and ISCU2

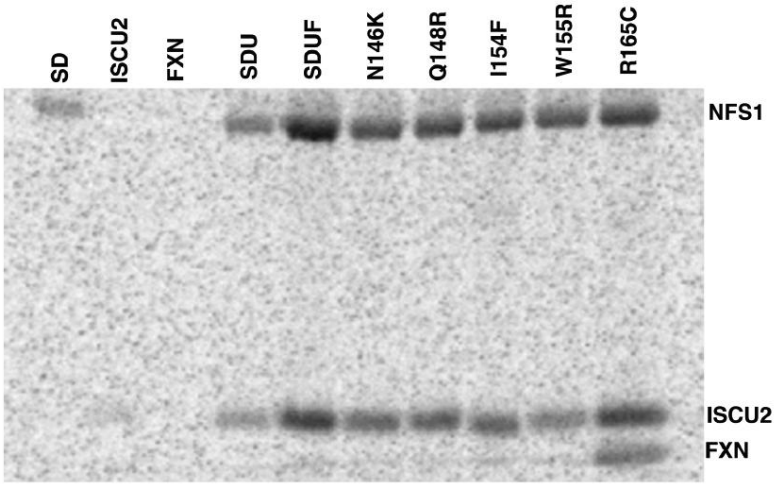

Figure 2.3. FRDA variants decrease the rate of sulfur accumulation on NFS1 and ISCU2. 3 equivalents of ISCU2 and 3 equivalents of FXN variants (native FXN, N146K, Q148R, I154F, W155R, and R165C) were used in a radiolabeling experiment using conditions similar to Figure 2. * This experiment was performed by Dr. Jennifer Bridwell-Rabb

(Figure 2.4B). Very little radioactivity was associated with the non-complexed flow through fractions. A non-reducing native gel showed that the radioactivity was linked to a slower migrating band (Figure 2.4C) that had been previously shown[22] to be associated with the SDUF complex (Figure 2.5). Next, this ^{35}S-labeled SDUF complex (fractions 11-13 from the HisTrap column) was incubated with ferrous iron, non-radioactive L-cysteine, and DTT, which are conditions consistent with synthesizing Fe-S clusters (see below). A desalting column was used to remove the unreacted substrates, the sample was incubated with apo-FDX and loaded onto a HisTrap column, and the fractions were analyzed using a 405 nm filter. Fractions 2 and 3 from the flow through exhibited absorbance at 405 nm (Figure 2.4D), consistent with an Fe-S cluster, and a similar retention time on a native gel as a FDX standard (Figure 2.4E, top). The NFS1

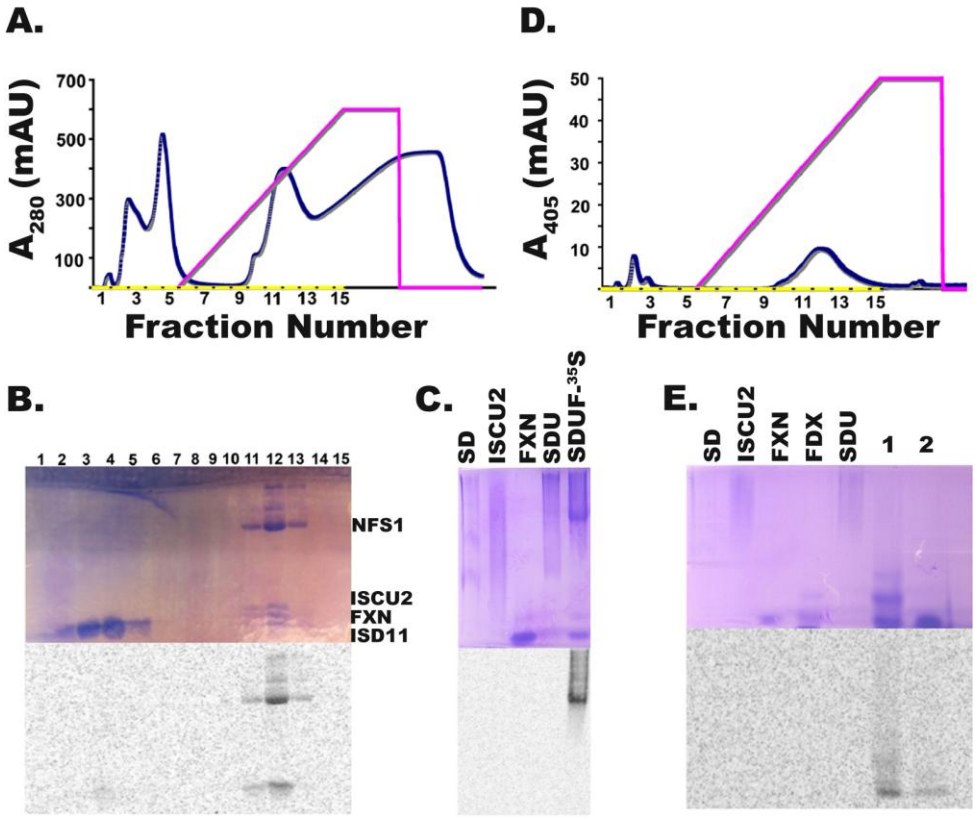

Figure 2.4. ^{35}S-radiolabel tracking from a cysteine substrate to a Fe-S cluster on FDX. The SDUF complex was reacted (see Methods) with L-[^{35}S]-cysteine, and (A) fractionated with a HisTrap column. (B) Fractions were analyzed for protein (top) and radioactivity (bottom) with non-reducing 14% SDS-PAGE, and (C) the fractions 11-13 corresponding to ^{35}S-SDUF were combined and analyzed for protein (top) and radioactivity (bottom) with non-reducing 6.5% Native-PAGE. ^{35}S-SDUF was then reacted with iron (see Methods), and (D) fractionated on a second HisTrap column. (E) Fractions 2-3 from (D) were combined and analyzed with native PAGE in the absence (labeled 1) and presence (labeled 2) of DTT. Standards SD, ISCU2, FXN, FDX, SDU were included for the native gels, proteins were stained using Coomassie blue, and radioactivity was detected using a Phosphorimager. Absorbance (blue) at 280 (panel A) or 405 (panel D) nm was overlaid with a 5-500 mM imidazole gradient (pink).

PLP cofactor also absorbs at 405 nm, as seen in fractions 11-13. Moreover, phosphorimaging analysis revealed the ^{35}S-label was associated with the same fractions and that this label was not released upon the addition of DTT, again consistent with a Fe-S cluster and not a persulfide species bound to FDX (Figure 2.4E, bottom). Thus, these

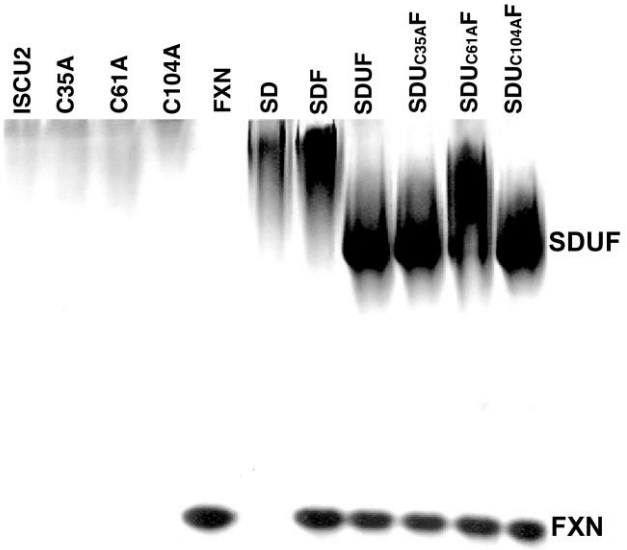

Figure 2.5. Native gel showing complex formation for ISCU2 variants. Non-reducing 6.5% Native-PAGE analysis of protein includes 180 µM ISCU2, 250 uM C35A, 250 µM C61A, 350 µM C104A, 150 µM FXN, 40 µM SD, and SDU (40 µM SD and 120 µM FXN) standards. The variant complexes contained 40 µM SD, 120 µM FXN, and 120 µM ISCU2, C35A, C61A, and C104A, respectively. All samples contained 10 mM DTT, 100 mM HEPES, pH 7.5, 50 mM NaCl, and 10 mM TCEP. The position of the slower migrating band that corresponds to a SDUF complex and FXN were indicated on the right side of the figure. * This experiment was performed by Dr. Chi-Lin Tsai.

data support a persulfide-bound ISCU2 species being a viable intermediate and the terminal sulfur of the persulfide species being converted into the inorganic sulfide of a Fe-S cluster during cofactor biosynthesis.

ISCU2 C104 Variants Disrupt Cysteine Desulfurase Activation by FXN

Here we constructed human ISCU2 variants of the non-conserved cysteine (C96), the conserved cysteine residues (C35, C61, C104), or combinations of the conserved cysteine residues to test the roles of these residues in the sulfur transfer and Fe-S cluster assembly reactions. The conserved cysteine residues were mutated to both serine, which is the best structural mimic of cysteine, and alanine, which has no ability to function in

sulfur transfer or cluster ligation. As these surface mutations could affect the binding affinity of ISCU2 and/or FXN to the SD complex, we determined the ability of these ISCU2 variants to form the SDUF complex using native gel analysis, and the relative binding affinities by monitoring changes in the cysteine desulfurase activity as a function of concentrations of ISCU2 and FXN (see Methods). Native gel analysis revealed that the $SDU_{C35A}F$, $SDU_{C61A}F$, and $SDU_{C104}F$ complexes formed the slower migrating band that is characteristic of the four-protein SDUF complex (Figure 2.5).[22] Interestingly, the slower migrating band is less defined for the C61S variant, suggesting this variant may affect binding more than the other mutants. This conclusion is supported by the kinetic titration experiments. Here the number of equivalents of ISCU2 and FXN that were required to exhibit saturation in the cysteine desulfurase reaction were determined (Table 2.1). In particular, C61 variants appeared to have the largest effect on binding, whereas mutations affecting C104 and the non-conserved C96 had modest binding effects. Saturating amounts of ISCU2 and FXN were used for all subsequent studies to remove complications from changes in binding affinity due to the incorporated ISCU2 mutations.

Next, we determined that assembly complexes that include C104 variants behaved differently than the other cysteine variants in sulfur transfer chemistry. In the absence of FXN, all of the SDU variant complexes exhibited typical unactivated cysteine desulfurase activities that were similar to the native SDU complex (Figure 2.6A). In the presence of FXN, the $SDU_{C96S}F$, $SDU_{C35A}F$, $SDU_{C35S}F$, and $SDU_{C61A}F$ complexes exhibited k_{cat} values similar (9.4 – 11.1 min^{-1}) to the 10.7 min^{-1} for the native SDUF

complex (Table 2.2). The k_{cat} for the $SDU_{C61S}F$ (5.9 min^{-1}) and $SDU_{C35A/C61A}F$ (6.4 min^{-1}) complexes were slightly compromised compared to the native SDUF complex, whereas complexes for the C104A (0.9 min^{-1}) and C104S variants (2.7 min^{-1}) were more similar to samples that lacked FXN (0.8 min^{-1}). Moreover, all SDUF variant complexes, except those that include mutation of C104, exhibit characteristic iron-based stimulation of the cysteine desulfurase activity (Figure 2.6B), which was previously shown to be associated with FXN binding.[22] These data indicated that mutations at position C104, but not the other cysteine residues, were compromised in their FXN-associated stimulation of the cysteine desulfurase reaction and suggested a link between residue C104 and FXN activation.

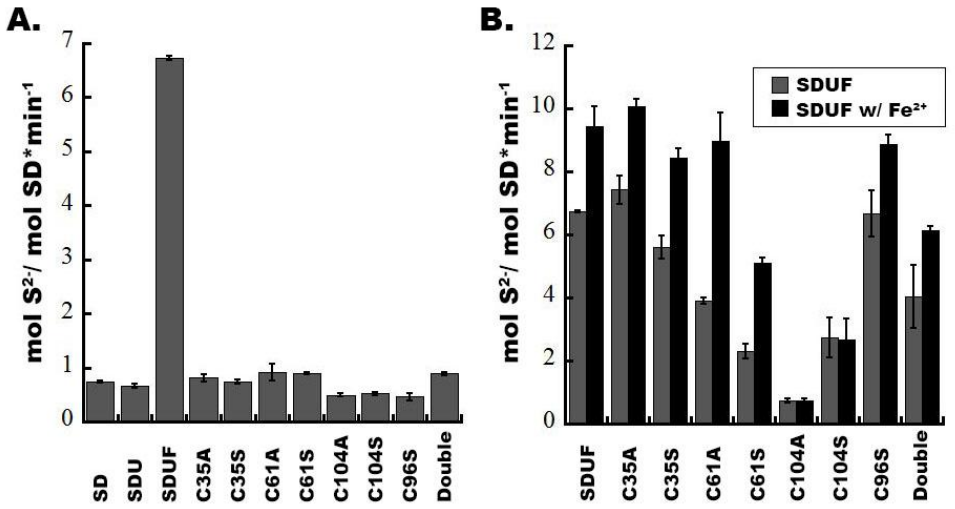

Figure 2.6. Cysteine desulfurase activity for Fe-S assembly complexes containing different ISCU2 variants. (A) Cysteine desulfurase activity for SDU complexes with different ISCU2 variants compared to the native SDUF complex. The double mutant is the ISCU2 variant C35A/C61A. (B) Cysteine desulfurase activity for the SDUF complexes with saturating amounts of FXN and ISCU2 variant in the presence and absence of 10 equivalents of Fe^{2+}. Error bars in A and B are for three independent measurements. All assays performed with 100 μM L-cysteine.
* This experiment was performed by Dr. Jennifer Bridwell-Rabb

Table 2.1. Kinetic Data for ISCU2 Variant Complexes without Fe^{2+}

Complex	ISCU2 equiv	FXN equiv	k_{cat} (min^{-1})	$K_M^{L\text{-}cys}$(mM)	k_{cat}/K_M($M^{-1}s^{-1}$)
SDU	3	NA	0.8 ± 0.1	0.052 ± 0.014	260 ± 70
SDUF	3	3	7.8 ± 0.4	0.015 ± 0.005	8500 ± 3100
$SDU_{C96S}F$	30	5	8.2 ± 0.3	0.018 ± 0.004	7700 ± 1600
$SDU_{C35A}F$	3	80	8.7 ± 0.5	0.024 ± 0.005	6100 ± 1400
$SDU_{C35S}F$	20	80	5.9 ± 0.3	0.014 ± 0.003	7200 ± 1700
$SDU_{C61A}F$	80	200	4.2 ± 0.1	0.010 ± 0.001	6700 ± 930
$SDU_{C61S}F$	80	200	3.0 ± 0.2	0.018 ± 0.005	2800 ± 670
$SDU_{C104A}F$	3	30	1.0 ± 0.1	0.033 ± 0.001	500 ± 170
$SDU_{C104S}F$	10	50	3.2 ± 0.1	0.014 ± 0.002	4000 ± 680
$SDU_{C35A/C61A}F$	200	400	4.5 ± 0.3	0.021 ± 0.007	3600 ± 1200

Table 2.2. Kinetic Data for ISCU2 Variant Complexes with 10 Equivalents of Fe^{2+}

Complex	k_{cat} (min^{-1})	$K_M^{L\text{-}cys}$(mM)	k_{cat}/K_M($M^{-1}s^{-1}$)
SDU	0.8 ± 0.1	0.052 ± 0.014	260 ± 70
SDUF	10.7 ± 0.8	0.019 ± 0.006	9200 ± 3000
$SDU_{C96S}F$	9.9 ± 0.9	0.021 ± 0.008	8000 ± 3200
$SDU_{C35A}F$	11.1 ± 0.6	0.018 ± 0.005	10000 ± 2600
$SDU_{C35S}F$	9.4 ± 0.5	0.020 ± 0.005	7700 ± 2200
$SDU_{C61A}F$	9.6 ± 0.5	0.017 ± 0.004	9300 ± 2300
$SDU_{C61S}F$	5.9 ± 0.2	0.012 ± 0.003	8300 ± 1800
$SDU_{C104A}F$	0.9 ± 0.1	0.023 ± 0.001	640 ± 200
$SDU_{C104S}F$	2.7 ± 0.1	0.016 ± 0.004	2800 ± 670
$SDU_{C35A/C61A}F$	6.4 ± 0.2	0.010 ± 0.002	10600 ± 2300

ISCU2 Conserved Cysteine Residues are Critical for Enzymatic Fe-S Cluster Assembly

We then measured Fe-S cluster formation rates for ISCU2 variants using two different spectroscopic assays. First, the increase in absorbance at 456 nm was used as a measure of the Fe-S cluster biosynthetic activity. The ISCU2 C96S variant, which is the non-conserved cysteine, had a Fe-S cluster assembly activity similar to the native SDU and SDUF complexes (Figure 2.7A), indicating that this residue is neither essential for cluster ligation nor for the mechanism of cluster formation. In contrast, SDUF complexes containing the C35A, C61A, and C104A ISCU2 variants had a dramatic loss of activity relative to native SDUF (Figure 2.7A). Interestingly, there is a low level increase in absorbance for samples containing the C35A, C61A, and C104A variants or the native ISCU2 in the absence of FXN. Second, we monitored the 300-600 nm region using circular dichroism (CD) spectroscopy, which is sensitive to the PLP cofactor and to protein-bound Fe-S cluster species. A CD signal with maxima at 330 and 430 nm

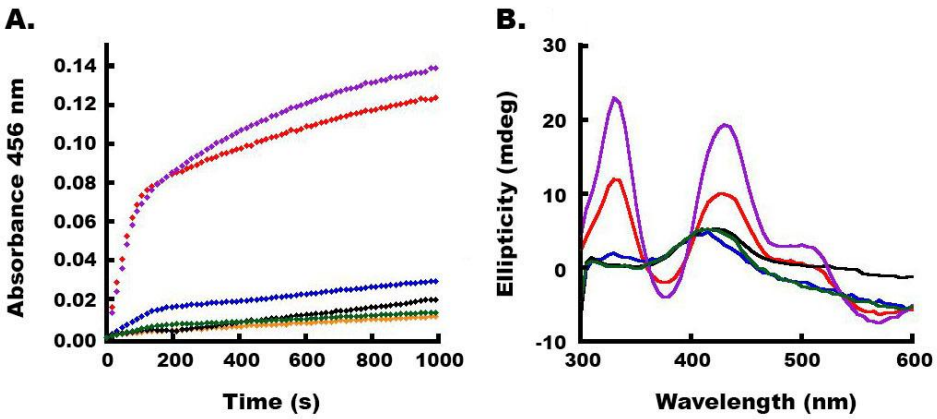

Figure 2.7. Conserved cysteine residues are critical for Fe-S cluster formation on ISCU2. (A) Fe-S cluster formation was monitored at 456 nm by UV-Vis spectroscopy as a function of time. (B) Fe-S cluster formation was monitored by CD spectroscopy and the 60 minute time point is displayed. Samples include SDU (yellow), SDUF (red), $SDU_{C35A}F$ (blue), $SDU_{C61A}F$ (black) $SDU_{C96S}F$ (purple), $SDU_{C104A}F$ (green).

developed for samples of the Fe-S assembly complex containing native ISCU2 or the C96S variant (Figure 2.7B) that appeared similar to [2Fe-2S] cluster bound to bacterial IscU[79]. The development of this Fe-S signal was absent for assembly complex samples that contained the C35A, C61A, and C104A variants. These samples did have a CD signal that maximized at 420 nm, but this signal is due to the PLP cofactor of NFS1 rather than an Fe-S cluster. Together, these data indicate that C96 is not required for the Fe-S assembly reaction, which all three conserved cysteine residues (C35, C61, and C104) are essential for enzymatic Fe-S cluster formation, and suggest that C104 is linked to FXN activation and sulfur transfer chemistry.

Discussion

Despite many excellent studies of the ISC biosynthetic system, details of the sulfur transfer mechanism and intermediates in Fe-S cluster biosynthesis remain

unknown. Currently, two minimalist models have been proposed for Fe-S cluster biosynthesis that differ in the order of substrate addition: the sulfur-first and iron-first mechanisms.[38] In the sulfur-first mechanism, the first step is transfer of the terminal sulfur of a persulfide species on the cysteine desulfurase (bacterial IscS or human NFS1) to a cysteine residue on the scaffold protein (bacterial IscU or human ISCU2).[92] This is followed, in an undefined order, by a second sulfur transfer event, the incorporation of two ferrous irons, and the addition of two electrons to form a $[2Fe\text{-}2S]^{2+}$ intermediate. This model is supported by the ability of *E. coli* and *A. vinelandii* IscS to transfer sulfur from L-cysteine to form persulfide or polysulfide bound IscU.[42, 43] In the Fe-first mechanism, ferrous iron binds to the cysteines of the scaffold protein as an initiating step in forming the $[2Fe\text{-}2S]^{2+}$ intermediate. This model is supported by the ability of the *Thermotoga maritima* IscU to bind ferrous iron[40] and by the stabilization of the *Haemophilus influenza* IscU by binding of divalent metal ions such as zinc to the active site cysteines[93, 94]. However, neither the persulfide-bound nor iron-bound IscU has been demonstrated to be a viable intermediate in Fe-S cluster biosynthesis.

Even less is known about the sulfur transfer mechanism in eukaryotes, and two additional components (FXN and ISD11) are implicated in modulating the cysteine desulfurase activity of NFS1.[22, 29, 30, 82-85] Here our objective was to directly test if a persulfide generated on ISCU2 is viable in forming a Fe-S cluster. Our strategy was to track the ^{35}S-radiolabel from a cysteine substrate to a persulfide species on the human Fe-S cluster assembly complex, and then show that this persulfide species is viable in forming an iron-sulfur cluster on an acceptor protein. The addition of a L-[^{35}S]-cysteine

substrate to the SDUF complex resulted in co-migration of the radiolabel with both NFS1 and ISCU2 on an non-reducing SDS-PAGE gel (Figure 2.4) and addition of reductants such as DTT, GSH, BME, or TCEP decreased the label on NFS1 and ISCU2 (data not shown), consistent with the formation of a covalent adduct. As the labeling experiments were performed under anaerobic conditions and the excess label was removed before analyzing with SDS-PAGE, the covalent adduct is likely a persulfide species rather than a cystine formed by oxidative disulfide bond formation between a radiolabeled cysteine and a cysteine residue on NFS1 or ISCU2. This SDUF complex with a persulfide-bound ISCU2 subunit was then reacted with iron and additional non-radiolabeled cysteine, desalted, and then incubated with apo-FDX. Our results indicate the radiolabel was transferred to FDX and was associated with a DTT-resistant species that absorbs at 405 nm (Figure 2.4), which is consistent with a Fe-S cluster and not a persulfide species. Together these experiments show that a persulfide species can be formed on the ISCU2 subunit of the SDUF complex and this species has properties consistent with an intermediate, which supports a sulfur-first mechanism in eukaryotic Fe-S cluster biosynthesis.

Three conserved cysteines in ISCU2, C35, C61, and C104, are required for efficient Fe-S cluster formation based on absorbance at 456 nm and a CD assay for protein-bound [2Fe-2S] clusters (Figure 2.7), whereas only C104 is required for FXN-activation of the NFS1 cysteine desulfurase activity (Table 2.2). One possibility is that the loss of cysteine desulfurase activity for C104 variants is simply due to loss of protein conformation (switching between order and disorder states). We disfavor this possibility

as the exclusive cause of these effects because of the conservative nature of the substitutions and lack of correlation between cysteine desulfurase activation level and relative ISCU2 and FXN binding to the SD complex (Table 2.1), which is an indirect reporter of conformational state. A second possibility is that C104 functions as a sulfur acceptor in the interprotein sulfur transfer reaction, and the ability to transfer sulfur from NFS1 to C104 ISCU2 (followed by DTT cleavage) is responsible for the enhanced cysteine desulfurase activity. A third possibility is that one of the other cysteines is the sulfur acceptor and the enhanced cysteine desulfurase activity is due to interprotein sulfur transfer from NFS1 to C35 or C61, followed by intraprotein sulfur transfer to C104 and reductive cleavage to generate sulfide. To test this third possibility, we constructed and characterized the C35A/C61A variant and determined that it exhibited a k_{cat} for the cysteine desulfurase activity that was more similar to native ISCU2 than to the C104 variants (Table 2.2). Thus, we favor a model in which C104 acts as a primary rather than secondary sulfur acceptor and this sulfur species partitions in our assays between being intercepted and reductively cleaved to produce sulfide, and functioning as an intermediate in Fe-S cluster formation on the assembly complex. This is a different conclusion than that obtained for the *E. coli* ISC system in which all three conserved cysteines were shown to be dispensable for Fe-S cluster formation using sulfide (chemical reconstitution conditions) as the sulfur source.[79] This apparent contradiction might be explained by differences in reaction conditions that favor the assembly complex and the previous studies that favor the *E. coli* IscU dimer. Dimeric IscU can likely overcome the loss of one of the three conserved cysteines and still ligate a Fe-S

cluster with the remaining four cysteines. In addition, Bonomi *et al.* showed that residue C106 in *E. coli* IscU (equivalent to C104 of human ISCU2) is required for Fe-S cluster formation in assays using IscS and proposes that C106 functions in sulfur transfer chemistry.[79] Despite different experiments and results, we have a similar conclusion and provide data consistent with C104 being the primary sulfur acceptor from NFS1 and the resulting persulfide species on ISCU2 functioning as an intermediate in human Fe-S cluster biosynthesis.

FXN accelerates both the cysteine desulfurase (sulfide production) and Fe-S assembly (increase in absorbance at 456 nm) activities of the human SDU complex.[22] FXN could stimulate the rates of these reactions by inducing a conformational change that (*i*) increases active site accessibility; (*ii*) enhances a step associated with PLP chemistry on NFS1; and/or (*iii*) facilitates interprotein sulfur transfer from NFS1 to ISCU2. The first mechanism suggests a FXN-dependent increase in active site accessibility that allows DTT to intercept a catalytic intermediate and generate sulfide, which could drive non-enzymatic assembly of Fe-S clusters.[3] This explanation would predict that the rates of the cysteine desulfurase and Fe-S assembly reactions should be correlated, which is not true for the $SDU_{C35A}F$ and $SDU_{C61A}F$ complexes that exhibit native like cysteine desulfurase activities (Table 2.2), but compromised Fe-S cluster assembly activities (Figure 2.7). The second mechanism, involving enhancement of persulfide formation on NFS1, suggests that FXN but not FRDA FXN variants should increase the level of ^{35}S radiolabel accumulation on NFS1, which was observed (Figure 2.2 and 2.3). Previous results[22] and data provided here (Table 2.2) indicate that FXN

affects the K_M for L-cysteine in the cysteine desulfurase reaction, and is consistent with recent results in *Saccharomyces cerevisiae*.[95] The third mechanism, involving a FXN-dependent acceleration of interprotein sulfur transfer, is more difficult to separate from acceleration of a rate-limiting formation of a persulfide on NFS1, despite the increase in accumulation of the ^{35}S radiolabel on ISCU2 (Figure 2.2). However, the fact that the cysteine desulfurase k_{cat} values for the C104 ISCU2 variants were reduced to levels similar to the Fe-S assembly complex without FXN suggest that this residue is involved in the sulfur transfer chemistry and FXN-activation (Table 2.2). Taken together, these data are consistent with a role for FXN in accelerating both the persulfide formation on NFS1 as well as interprotein sulfur transfer to ISCU2.

We propose that a key aspect of the cysteine desulfurase and Fe-S assembly by the human Fe-S assembly complex revolves around the accessibility of ISCU2 C104 (Figure 2.8), which is reminiscent of the ordered and disorder equilibrium for *E. coli* IscU proposed by the Markley lab.[96, 97] The crystal structure of the trimeric *Aquifex aeolicus* IscU reveals a distinct helix-to-coil transition for the vicinity of C104 based on the presence (subunit B) or absence (subunits A and C) of a Fe–S cluster.[54] Similarly, we propose a pre-equilibrium mixture between non-functional (helix) and functional (coil) states in the C104-containing helix of ISCU2 that shifts upon FXN binding from the non-functional to functional form to facilitate sulfur transfer from NFS1 C381 to ISCU2 C104. The proposed helix-to-coil transition could also expose the LPPVK motif (residue 97-101 in ISCU2) to adopt a flexible conformation promoting the binding of chaperones

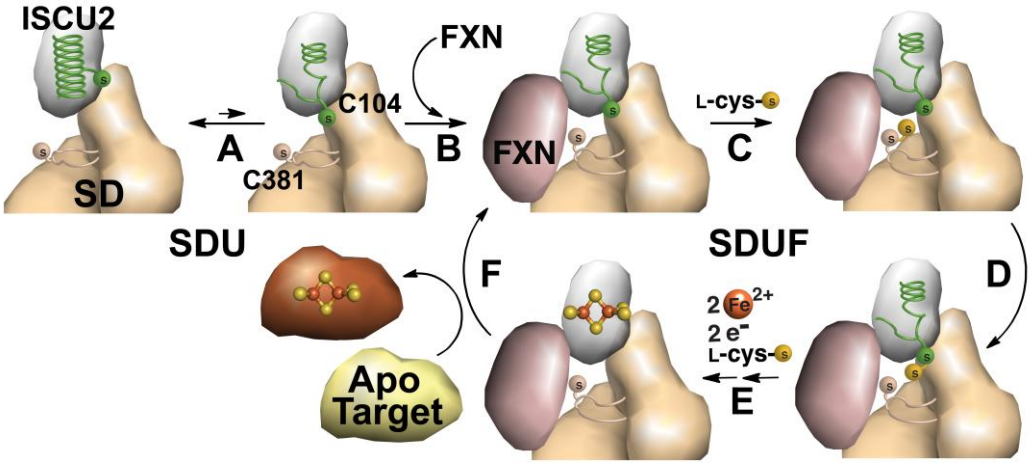

Figure 2.8. Cartoon model of FXN activation of the Fe-S assembly complex. (A) SDU complexes exist as an equilibrium mixture between a stable inactive (helix) and less stable active (coil) conformation. (B) FXN binds to the coil conformation for the C-terminal helix and shifts the equilibrium from the inactive to active form. (C) NFS1 reacts with L-cysteine to form a persulfide species on residue C381. (D) Sulfur is transferred from NFS1 to ISCU2 residue C104. (E) Addition of the remaining substrates results in [2Fe-2S] cluster formation on ISCU2. (F) The Fe-S cluster is transferred to an apo target and the active SDUF assembly complex is reformed. This last step may involve subunit dissociation and/or chaperone proteins.

involved in cluster transfer.[98, 99] At this stage it is unclear if and what triggers holo-ISCU2 dissociation from the Fe-S assembly complex and what assembly state interacts with molecular chaperone and target proteins. Our *in vitro* results and our model suggest FXN functions as an allosteric regulator that controls Fe-S cluster assembly. Such a function would be consistent with the generally accepted role for FXN in Fe-S cluster assembly and explain the loss of Fe-S enzyme activity phenotype upon FXN depletion. Future experiments will focus on testing and expanding upon this model with the ultimate goal of developing new strategies to treat FRDA.

Conclusion

In summary, we provide data that support a role for human FXN in accelerating the PLP-based chemistry of the cysteine desulfurase NFS1 and also in the interprotein sulfur transfer between NFS1 and scaffold protein ISCU2. Our results are consistent with ISCU2 residue C104 being the sulfur acceptor and the resulting intermediate being an early step in Fe-S cluster assembly. We propose a testable activation model in which FXN facilitates a helix-to-coil activation model for sulfur transfer. These *in vitro* results suggest FXN may have a physiological function as a regulator and that FXN levels control Fe-S cluster assembly. Such a function would be consistent with the generally accepted role for FXN in Fe-S cluster assembly and explain the loss of Fe-S enzyme activity phenotype upon FXN depletion. Future experiments will focus on testing and expanding upon this model with the ultimate goal of developing new strategies to treat FRDA.

CHAPTER III

THE HUMAN FE-S ASSEMBLY COMPLEX GENERATES TRANSIENT [2FE-2S] CLUSTER INTERMEDIATES THAT READILY TRANSFER TO THIOL-CONTAINING TARGET MOLECULES

Introduction

Iron-sulfur (Fe-S) clusters are protein cofactors that are required for many critical cellular functions including oxidative respiration, DNA repair, and the biosynthesis of other cofactors.[1] The most common role for Fe-S clusters is in electron transfer reactions, but additional functions such as substrate turnover, environmental sensing, and protein stabilization are also known. Fe-S clusters with different iron and sulfide stoichiometries, including common rhombic [2Fe-2S] and cubic [4Fe-4S] and more specialized [3Fe-4S], [4Fe-3S], and [8Fe-7S] clusters, are fine-tuned by the protein environment to have the necessary chemical properties for their function. Spectroscopic features can often distinguish these different classes of Fe-S clusters. For example, $[2Fe-2S]^{2+}$ clusters exhibit characteristic electronic absorbance (315, 400, and 456 nm) and circular dichroism (CD) (330 and 430 nm) peaks and diagnostic Mössbauer parameters (δ = 0.25-0.30 mm/s and ΔE_Q = 0.7-0.8 mm/s), whereas $[4Fe-4S]^{2+}$ clusters have broad electronic absorbance spectra (peak at ~400 nm), are often CD silent, and exhibit Mössbauer signals with very different parameters (δ = 0.40-0.45 mm/s and ΔE_Q = 1.1-1.5 mm/s).[3, 44, 100-103] Remarkably, the Holm group and others have demonstrated that these biological Fe-S clusters can be self-assembled in solution from iron, sulfide and

appropriate sulfur-containing ligands,[3, 4] and it is common to reconstitute recombinant Fe-S cluster proteins using similar conditions. Interestingly, the *in vivo* synthesis of Fe-S clusters does not use this self-assembly chemistry, but synthesizes Fe-S clusters using highly conserved proteins that are part of Fe-S cluster assembly pathways.[5-7]

The prokaryotic ISC, NIF, and SUF systems enzymatically build Fe-S clusters from substrates L-cysteine, iron, and electrons. As biological Fe-S clusters have been shown to self-assemble in solution, these enzymatic systems may not be necessary to form the specific Fe-S bonds, but to control the iron and sulfur reactivity/toxicity and regulate the amounts of different types of clusters that are synthesized. Here we focus on the ISC pathway. The prokaryotic ISC pathway is probably the best studied and is analogous to the eukaryotic Fe-S biosynthetic pathway that is located in the mitochondrial matrix and includes at least a dozen proteins.[2, 5, 16] A cysteine desulfurase (human NFS1 or bacterial IscS) catalyzes the PLP-dependent conversion of L-cysteine to L-alanine, generates a persulfide species on a mobile loop cysteine, and delivers the sulfane sulfur to the Fe-S catalytic or scaffold subunit (human ISCU2 or bacterial IscU).[25, 26] The cysteine desulfurase activity is often measured by intercepting this persulfide species using reductive thiol-cleaving reagents such as DTT and quantitating the generate sulfide.[27] Isd11 is a eukaryotic-specific protein that appears to stabilize the cysteine desulfurase and may participate in positioning the mobile loop cysteine for attack of the substrate.[28-32] Human frataxin (FXN) stimulates the cysteine desulfurase reaction and may functions as an allosteric activator to regulate the Fe-S assembly complex.[22] FXN also appears to simulate the rate of *in vitro* Fe-S cluster assembly,

whereas the bacterial homolog CyaY appears to inhibit Fe-S biosynthesis.[22-24] FXN has also been proposed,[19, 20] along with IscA,[21] to function as an iron donor for Fe-S cluster biosynthesis, whereas the ferredoxin/ferredoxin reductase system is thought to provide electrons.[33, 34] *In vitro* Fe-S assembly reactions often use a surrogate electron donor such as DTT rather than the ferredoxin/ferredoxin reductase system. Finally, chaperone and Fe-S carrier proteins appear to facilitate the transfer of intact Fe-S clusters from the Fe-S assembly complex to target proteins.[35, 36]

The prokaryotic scaffold protein IscU combines sulfur generated from cysteine by the cysteine desulfurase, iron, and electrons to synthesize [2Fe-2S] and [4Fe-4S] clusters. Currently, no intermediates in generating [2Fe-2S] clusters are established in the biosynthetic system or self-assembly process, but some details of the conversion of [2Fe-2S] clusters to [4Fe-4S] clusters are known. Inorganic biomimetic chemistry revealed that [4Fe-4S] clusters can be formed by reductively coupling two [2Fe-2S] clusters,[3] whereas studies of the oxygen sensor protein FNR reveal the conversion of persulfide ligated [2Fe-2S] cluster to cysteine ligated [4Fe-4S] cluster upon the addition of iron.[51] In key early studies on biosynthetic systems, Agar *et al*. demonstrated that [2Fe-2S] clusters can be assembled on IscU in an IscS mediated process,[52] and Foster *et al.* showed that the human ISCU2 D37A variant contains a stable [2Fe-2S] cluster.[53] IscU binds clusters with three conserved cysteines,[50] with experimental support for a semi-conserved histidine,[46, 54] aspartic acid,[55] and a cysteine from another molecule[56, 57] as the fourth ligand. In a remarkable study, the Huynh, Dean, and Johnson groups demonstrated reductive coupling chemistry on an IscU dimeric species with the

sequential formation of a single [2Fe-2S] cluster, a second [2Fe-2S] cluster, and then conversion of these [2Fe-2S] clusters to form one [4Fe-4S] cluster per IscU dimer.[48] This reductive coupling chemistry appears to occur at an IscU dimeric interface with each monomer contributing one [2Fe-2S] cluster.

An Fe-S assembly complex appears to be responsible for the synthesis of [2Fe-2S] and possibly [4Fe-4S] clusters for the ISC pathway. A protein complex between bacterial IscS and IscU has been demonstrated in solution,[42, 58] and crystal structures with[56] and without[59] a [2Fe-2S] cluster provide details of the protein-protein interactions and cluster environment. An apparent key to obtaining a crystal structure of the bound [2Fe-2S] cluster was the incorporation of the D35A variant,[56] which was previously shown to stabilize the cluster bound state and/or inhibit cluster transfer.[53, 60, 61] Interestingly, Mössbauer spectroscopic studies suggest the addition of L-cysteine, ferrous iron, and DTT to the bacterial and mammalian Fe-S assembly complexes results in the formation of [2Fe-2S] and [4Fe-4S] cluster species.[62, 63] These results suggest at least two models. In the first model, IscU subunits dissociate after building [2Fe-2S] clusters, and this dissociated [2Fe-2S]-bound IscU undergoes reductive coupling chemistry to generate [4Fe-4S] clusters. In the second model, [2Fe-2S] clusters synthesized on the Fe-S assembly complex transform to [4Fe-4S] clusters through chemistry that may resemble the [2Fe-2S] → [4Fe-4S] conversion for FNR.[51] The first model is supported by the ability of the scaffold protein to undergo reductive coupling chemistry,[48, 64] whereas the second model is suggested by recent studies of a eukaryotic Fe-S assembly complex.[62]

Here our objectives were to utilize spectroscopic methods to determine intermediates associated with the synthesis of Fe-S clusters by the human assembly complex. Previously, the kinetics of enzymatic Fe-S cluster formation was measured using the increase in absorbance due to sulfur-to-iron charge transfer bands.[22, 23, 46, 96] The human Fe-S assembly complex consisting of NFS1, ISD11, and ISCU2 subunits (named SDU) exhibited low cysteine desulfurase activity and a slow increase in absorbance at 456 nm that was attributed to the Fe-S synthesis reaction.[22] Addition of FXN generated the SDUF complex, which exhibited greatly enhanced rates for the cysteine desulfurase and Fe-S cluster assembly reactions.[22] Here we apply UV-visible, circular dichroism, and Mössbauer spectroscopy to reveal details of the Fe-S cluster assembly reaction on the SDUF complex and competing DTT-mediated transfer and mineralization chemistry that have implications for the mechanism and study of Fe-S cluster biosynthesis.

Experimental Procedures

Protein Expression and Purification

NFS1-ISD11 (named SD), ISCU2, and FXN were purified as previously described.[22] Briefly, plasmids that contain the genes for human SD, ISCU2, and FXN were individually transformed into BL21(DE3) cells and grown at 37 °C until reaching an OD_{600} of 0.6. Protein expression was induced with either 0.5 mM (ISCU2 and FXN) or 0.1 mM (SD) IPTG, the temperature was reduced to 16 °C, and the cells were harvested 16 hours later. The SDUF complex exhibited a cysteine desulfurase activity of 11 mol sulfide/(mol NFS1)(min), which is similar to previously published values.[22, 24]

The plasmid PET9a encoding human ferredoxin (FDX; gift of John Markley)[90] was transformed into *E. coli* BL21 (DE3) cells and grown at 37 ºC until an OD_{600} of 0.6. Expression was induced with 0.4 mM IPTG, 1 mM cysteine, and 0.1 mg/mL ferric ammonium citrate, and the cells were harvested 16 hours later. The cells were lysed by sonication, the soluble proteins were loaded onto an anion exchange column (26/20 POROS 50HQ, Applied Biosystems), and eluted with a linear gradient from 0 to 1000 mM NaCl in 50 mM Tris pH 7.5. Fractions containing FDX were further purified[91, 104] on a Sephacryl S100 (26/60, GE Healthcare) size exclusion column equilibrated in 50 mM Tris, pH 7.4, 50 mM NaCl. Apo FDX was prepared by precipitating purified FDX with 10% trichloroacetic acid, incubating with 10 mM DTT on ice for 10 minutes, pelleting the sample, rinsing the pellet with water two times, and resuspending the pellet anaerobically in 50 mM Tris pH 8.0, 250 mM NaCl.[104] Unless otherwise stated, anaerobic experiments were performed in a Mbraun glovebox at ~12 °C with an argon atmosphere and O_2 < 1 ppm as monitored by a Teledyne Model 310 analyzer.

Fe-S Cluster Formation Assays

The Fe-S cluster assembly assay mixtures under five different experimental conditions (Standard, DTT-free, Stoichiometric, Catalytic and Acceptor) were prepared anaerobically and transferred to an anaerobic cuvette for UV-visible (Agilent UV-Visible 8453) and circular dichroism (CD; Chirascan™) data collection at 20 ºC. Standard assay conditions include 10 μM SD, 30 μM ISCU2, 30 μM FXN with 4 mM DTT, 100 μM cysteine and either 250 μM or 400 μM $Fe(NH_4)_2(SO_4)_2$. The DTT-free conditions were the same as the standard conditions except the L-cysteine concentration

was increased to 1 mM, samples lacked DTT, and the $Fe(NH_4)_2(SO_4)_2$ concentration was changed from 400 to 250 μM. Stoichiometric conditions included 10 μM SD, 10 μM ISCU2, 30 μM FXN with 1 mM cysteine and 250 μM $Fe(NH_4)_2(SO_4)_2$. Catalytic conditions included 0.5 μM SD, 30 μM ISCU2, and 30 μM FXN with 250 μM $Fe(NH_4)_2(SO_4)_2$ and 1 mM cysteine. The Acceptor conditions included 4 μM SD, 30 μM ISCU2, 30 μM FXN, 90 μM apo FDX, 250 μM $Fe(NH_4)_2(SO_4)_2$, 1 mM cysteine with or without 4 mM DTT. Extinction coefficients of 16 $mM^{-1}cm^{-1}$ at 400 nm[105, 106] and 5.8 $mM^{-1}cm^{-1}$ at 456 nm[48] were used to quantitate [4Fe-4S] and [2Fe-2S] clusters, respectively.

Protein Assembly State Analysis

Sample mixtures of 50 μM SD plus 150 μM ISCU2 with (SDUF) or without (SDU) 150 μM FXN were incubated anaerobically for 20 minutes at 10 °C with 1.5 mM DTT and 500 μM of $Fe(NH_4)_2(SO_4)_2$, L-cysteine, or both $Fe(NH_4)_2(SO_4)_2$ and L-cysteine. Samples were applied to an anaerobic S-200 column (GE 26/60 Sephacryl S-200 High Resolution) equilibrated with 50 mM HEPES pH 7.8, 250 mM NaCl (Buffer A). In second set of experiments, NFS1 was alkylated by incubating 50 μM SD with 1 mM iodoacetamide for 1 hr at 12 °C, quenched with 10 mM cysteine, and modifications to C381 was confirmed by mass spectrometry. Alkylated or non-alkylated SD was reacted for 15 minutes at 12 °C with 50 μM ISCU2, 50 μM FXN, 200 μM $Fe(NH_4)_2(SO_4)_2$, 1.5 mM DTT, and 200 μM Na_2S, and applied to the S-200 column. In a third set of experiments, 100 μM SDUF was prepared by addition of 100 μM SD with 300 μM ISCU2 and 300 μM FXN and was reacted for 45 min at 12 °C with 1 mM

$Fe(NH_4)_2(SO_4)_2$, 1 mM L-cysteine, and 3 mM DTT in the presence and absence of 500 μM apo FDX, and applied to the S-200 column. The reaction without apo FDX was repeated and the High Molecular Weight Species (HMWS) was isolated from the S-200 column. The HMWS sample was split and (*i*) incubated for 10 min with 4 mM DTT; and (*ii*) incubated for 40 min with 500 μM apo FDX and 4 mM DTT. Both samples were applied to a S-200 column. The HMWS eluted at the void volume for the S-200 column (8 mL), the SDU and SDUF complexes eluted at 12 mL, and uncomplexed ISCU2, FXN, and FDX eluted at 16 mL. Calibration with molecular weight standards confirmed that the protein samples eluted at volumes consistent with their known molecular masses. Sulfide production was measured using methylene blue assay,[22, 107, 108] whereas iron quantitation was achieved with a Ferrozine assay.[109-112]

Mössbauer Analysis of Fe-S Species

Mössbauer was used to analyze three HMWS samples, an Fe-S assembly reaction coupled to CD spectroscopy, and an Fe-S assembly reaction with and without DTT. The first HMWS sample was prepared by reacting 600 μM SD with 6 mM L-cysteine, 6 mM ^{57}Ferric citrate, and 1.8 mM DTT for 45 min at 12 °C, and isolating the HMWS using a S-200 column equilibrated in Buffer A. The second HMWS sample was prepared identically but Mössbauer spectras were collected at 5 and 100 K. In the third HMWS sample 2.4 mM cysteine was slowly added (10 μM per minute) to a solution of 600 μM SDUF, 2.4 mM ^{57}Ferric citrate, and 10 mM glutathione, the sample was incubated at 12 °C for 1 hour, and applied to the S200 column. In the Fe-S assembly reaction coupled to CD spectroscopy, 8 μM SD, 200 μM ISCU2, and 8 μM FXN was

combined with 500 μM $^{57}Fe^{2+}$ and 1 mM L-cysteine in a total volume of 8 mL, and a portion was removed to monitor reaction progress at 20 °C with CD spectroscopy. ^{57}Ferrous was made by the reduction of a 80 mM ^{57}Ferric citrate stock solution by dithionite that was carefully monitored by Mössbauer spectroscopy to generate 100% reduced iron with no excess dithionite. After 45 minutes, the rest of the 8 mL sample was concentrated to 800 μL, diluted to 3 mL, and re-concentrated to 800 μL three times before analysis by LC-ICP-MS (see below) and Mössbauer spectroscopy. In the final sample, 10 μM SD, 1300 μM ISCU2, 1.5 mM $^{57}Fe^{2+}$ and 10 mM L-cysteine were combined in a total volume of 1600 μL. The ferrous was slowly added to Fe-S assembly reaction (375 μM per hour). The sample was incubated for 1 hour at 12 °C and then split split in half. Half of the sample was incubated with 10 mM DTT for 1 hour and then both samples were separately analyzed by LC-ICP-MS (see below) and Mössbauer spectroscopy. Low-field Mössbauer spectra were collected using a model MS4 WRC spectrometer (SEE Co, Edina MN) at 5K and analyzed using WMOSS software (SEE Co, Edina MN). The parameters are reported relative to α-Fe foil at 298 K.

LC-ICP-MS Analysis

A Superdex 200 (10/300, GE Healthcare) was equilibrated with 50 mM Tris-HCl, 150 mM NaCl, pH 7.4 buffer. The buffer was prepared in double-distilled deionized trace-metal-free water. The elution flow rate was 0.5 mL/min^{-1}, controlled by a Bio-Inert HPLC (Agilent Technologies). A variable wavelength diode array detector (Agilent Technologies) was positioned post column and set to 280 nm. The entire system was housed in a ~7 °C Mbraun glovebox with O_2 < 3 ppm. The post detector flow was

split using a micro splitter valve (Upchurch Scientific, USA) with ~30% directed to the ICP-MS and the remainder to a 1260 Infinity Analytical-Scale Fraction Collector (Agilent Technologies). The 7700x ICP-MS (Agilent Technologies) was used in collision cell mode (He: 4.3 mL min^{-1}) with platinum cones and skimmer to minimize polyatomic inferences. The instrument was optimized daily using manufacturer's tuning solution. The sample was introduced through a standard Micromist nebulizer (Glass Expansion, Australia). ^{56}Fe and ^{57}Fe were monitored with a dwell time of 100 ms.

Results

Standard Assay Conditions Generate Fe-S Species not Associated with SDUF Complex

Fe-S assembly complexes were prepared anaerobically in a glovebox, placed in a sealed cuvette, and assayed for Fe-S cluster assembly activity under five different sets of conditions: Standard, DTT-free, Stoichiometric, Catalytic and Acceptor (see Methods). A Standard Fe-S assembly reaction, which includes substrates L-cysteine and $Fe(NH_4)_2(SO_4)_2$, and uses DTT as the electron source, was initiated by the addition of L-cysteine with a gas-tight syringe, and the absorbance spectrum was monitored as a function of time. The absorbance spectrum at the end of the reaction exhibited a broad absorbance peak that maximized at 400 nm that is reminiscent of [4Fe-4S] clusters (Figure 3.1A). Examining the change in absorbance at 400 nm revealed an immediate increase in absorbance that appears to saturate at > 20 minutes (Figure 3.1B). CD spectra for the SDUF sample under Standard conditions revealed a peak at 420 nm and a slight decrease in 300-350 nm ellipticity over time (Figure 3.2A). Control reactions that lacked

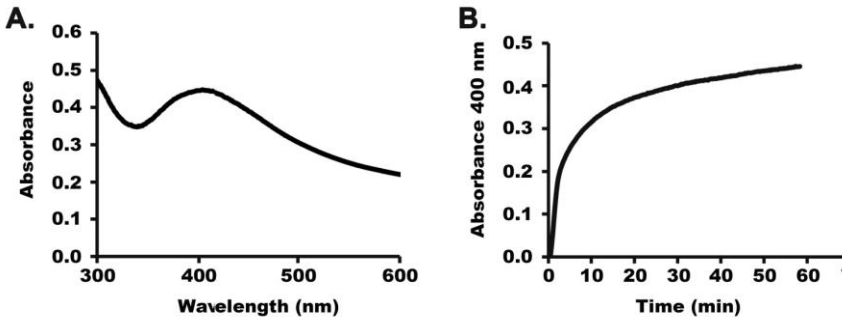

Figure 3.1. Fe-S cluster formation for SDUF complex in the presence of DTT. (A) Final Fe-S cluster absorbance spectrum and (B) kinetics monitored at 400 nm for reaction of SDUF (1:3:3 SD:ISCU2:FXN) with L-cysteine, Fe^{2+}, and DTT under Standard conditions (see Methods).

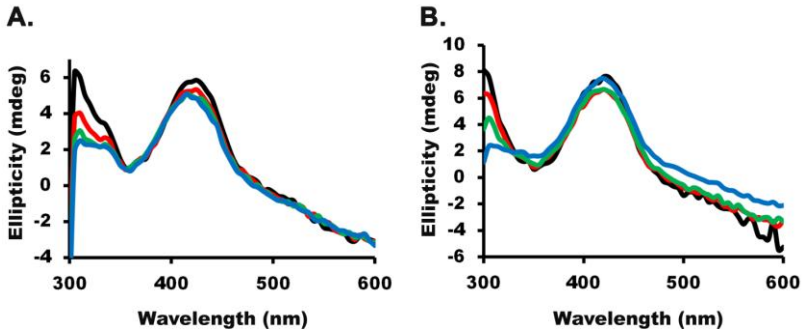

Figure 3.2. SDUF Fe-S assembly reactions in the presence of DTT exhibit PLP but not Fe-S CD features. CD spectra overlaid for the Fe-S assembly reaction under Standard conditions in the presence (A) and absence (B) of iron. Complete assembly reactions in (A) were collected at 0 (black), 20 (red), 40 (green), and 90 (blue) minutes. Control reactions in (B) included 10 mM EDTA and revealed changes due to the PLP cofactor at 0 (black), 10 (red), 20 (green), and 40 (blue) minutes.

iron (Figure 3.2B) revealed these changes were due to the PLP cofactor. Samples of the SD complex and *E. coli* IscS also exhibit the 420 nm peak. Previously, [2Fe-2S], but not [4Fe-4S], clusters were shown to exhibit characteristic strong CD features for bacterial IscU.[36, 40, 44] The electronic absorbance and CD spectroscopic data are therefore consistent with the SDUF complex facilitating rapid formation of a [4Fe-4S] cluster (or Fe-S species with similar spectroscopic properties) and provide no evidence for an [2Fe-2S] intermediate under Standard conditions. A [4Fe-4S] cluster assignment would result in similar concentrations (Table 3.1) of [4Fe-4S] clusters (27 μM) and ISCU2 (30 μM) and suggest saturation of the ISCU2 binding sites. However, as the concentration of SD was only 10 μM, this indicates at least some Fe-S species not associated with the SDUF complex. Based on these data our initial hypothesis was that SDUF reactions under Standard conditions generated [4Fe-4S] clusters associated with uncomplexed monomeric ISCU2.

Discovery of Fe-S Associated High Molecular Weight Species (HMWS)

To test our initial hypothesis, Fe-S assembly assays under Standard conditions were coupled to anaerobic analytical size exclusion analysis to determine protein species (uncomplexed ISCU2 or SDUF) associated with Fe-S clusters. Unexpectantly, Fe-S assembly reactions using either the SDU or SDUF complex resulted in the formation of a high molecular weight species (HMWS) that elutes at the void volume (7-11 mL) of the analytical S-200 column (Figure 3.3). The HMWS only formed for SDU and SDUF samples if iron and cysteine were included in the reaction mixture (Figure 3.3), and the rate of HMWS formation was increased by DTT (data not shown). Iron and sulfide co-

Table 3.1. Quantification of the Fe-S Cluster Generated from the SDUF Complex

Reductant	SD µM	ISCU2 µM	Fe^{2+} µM	Cys mM	Cluster µM
DTT	**10**	**30**	**400**	**0.1**	**27**
Cys	**10**	**30**	**250**	**1.0**	**125**

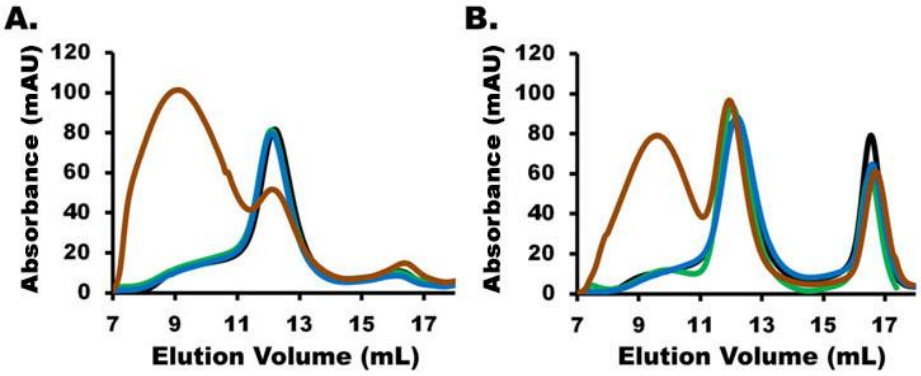

Figure 3.3. Discovery of HMWS formation during Fe-S assembly reactions. Fractions from anaerobic S-200 column for SDU (A) and SDUF (B) samples and addition of DTT (black), Fe^{2+} and DTT (green), cysteine and DTT (blue), or cysteine, Fe^{2+} and DTT (gold). HMWS elutes at void volume (~8mL), native SDUF, SDU, and SD complexes elute at ~12 mL, and uncomplexed ISCU2 and FXN elute at 16 mL. The spectrums from S-200 column were monitored at 280 nm.

eluted from the S-200 column primarily with the HMWS rather than SDU, SDUF, or uncomplexed ISCU2, and the HMWS was associated with brown color, which is consistent with an Fe-S species. Thus, the electronic absorbance spectroscopic features (Figure 3.1A) generated by the SDUF complex under Standard Fe-S assembly reaction

conditions are likely associated with the HMWS. Next, we tested if the HMWS could be a large assembly complex of possible physiological significance by evaluating the ability of this species to insert an Fe-S cluster into apo human Ferredoxin (FDX). Addition of excess apo FDX at the beginning of the experiment resulted in a decrease in the HMWS absorbance peak and an increase in the native assembly complex and FDX absorbance peaks compared to the control reaction (Figure 3.4A). The absorbance at 405 nm was monitored for these fractions and indicated protein species associated with either Fe-S clusters or the PLP cofactor. Thus, it appears that the addition of apo FDX at the start of the experiment resulted in: (*i*) enzymatic assembly or chemical reconstitution of Fe-S clusters on FDX that bypassed HMWS formation; and/or (*ii*) formation of the HMWS that converted back to the Fe-S assembly complex by transferring Fe-S clusters to FDX. To test if the HMWS can transfer a cluster to apo FDX, we isolated the HMWS and split it into two fractions, incubated one fraction with DTT and the other with both DTT and apo FDX, and separately analyzed the fractions with anaerobic S-200 chromatography. The apo FDX fraction exhibited a decrease in absorbance at 405 nm for the HMWS peak and an increase in absorbance for the native assembly complex and FDX (Figure 3.4B). The ability of the HMWS to build and transfer Fe-S cluster species to apo acceptor proteins is consistent with the HMWS being part of the biosynthetic assembly pathway or participating in a chemical reconstitution reaction.

The HMWS appears to be an Fe-S material that associates with cysteine-containing proteins. Interestingly, the HMWS that formed from SDU or SDUF under Standard Fe-S assembly reaction conditions exhibited little ISCU2 and no FXN on SDS-

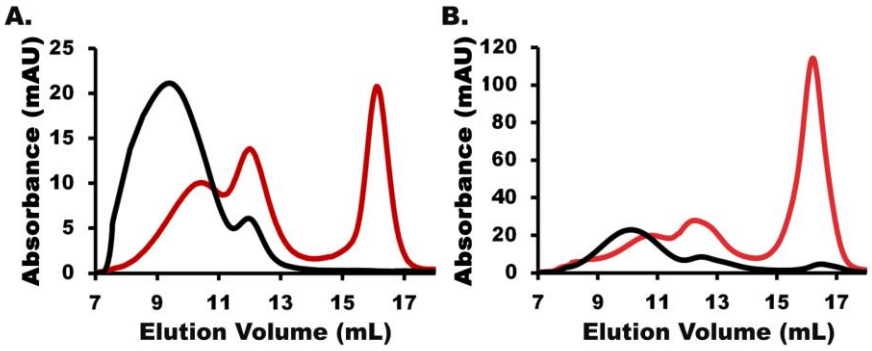

Figure 3.4. HMWS diminished by addition of apo FDX. (A) S-200 chromatographic analysis of SDUF Fe-S assembly reaction under Standard conditions in the absence (black) or presence (red) of apo FDX. (B) S-200 analysis of isolated HMWS incubated with DTT (black) or apo FDX (red). The absorbance was monitored at 405 nm which is sensitive to Fe-S clusters and the PLP cofactor.

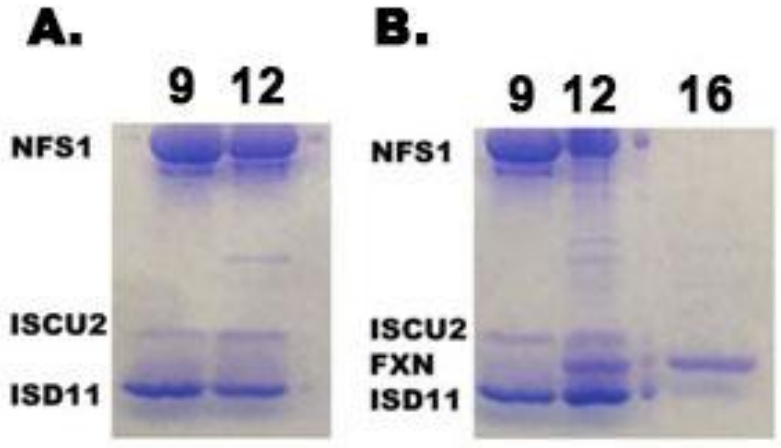

Figure 3.5. Discovery of HMWS formation from Figure 3 during Fe-S assembly reactions. Fractions from anaerobic S-200 column for SDU (A) and SDUF (B). HMWS elutes at void volume (~8mL), native SDUF, SDU, and SD complexes elute at ~12 mL, and uncomplexed ISCU2 and FXN elute at 16 mL. The SDS-PAGE analysis of HMWS (lane 1, fraction 9), native complexes (lane 2, fraction 12) and uncomplexed ISCU2 and FXN (lane 3, fraction 16) from the S-200 column.

PAGE (Figure 3.5). As a control, the same Fe-S assembly reaction was repeated with SD and a similar HMWS was generated (Figure 3.6A). Further, generation of the HMWS is not specific to the human cysteine desulfurase as assays with *E. coli* IscS generated similar results (Figure 3.7). This suggests the HMWS is associated with the cysteine desulfurase. Since the ISUC2 scaffold protein is not a required component for the formation of the HMWS, the HMWS is likely the product of an iron and sulfide dependent chemical reconstitution process rather than some type of physiological supermacromolecular transfer complex. The cysteine desulfurase could be required simply to produce sulfide in these reactions. This hypothesis was tested in two ways. First, we substituted sulfide for L-cysteine and demonstrated that the HMWS is still formed in the presence, but not absence, of ferrous iron (Figure 3.6B). Second, a sample in which the cysteines on NFS1 were alkylated was incubated with sulfide and ferrous iron. In this case, the HMWS failed to form (Figure 3.6B), indicating the formation of the HMWS requires iron, sulfide, and proteins with unmodified cysteines. Moreover, iron and sulfide quantitation for the HMWS from the SDUF Fe-S assembly reaction under Standard conditions revealed more iron and sulfide (9 Fe^{2+} and 10 S^{2-} per NFS1) than expected for a standard biological Fe-S cluster. This suggested some type of NFS1-solubilized Fe-S mineral. To further test this hypothesis, the Standard Fe-S assembly reaction was allowed to reach saturation before being spiked with additional cysteine, which initiated further Fe-S synthesis (Figure 3.8). The saturation behavior in this assay was evidently not due to forming a specific cluster-bound intermediate on ISCU2, but

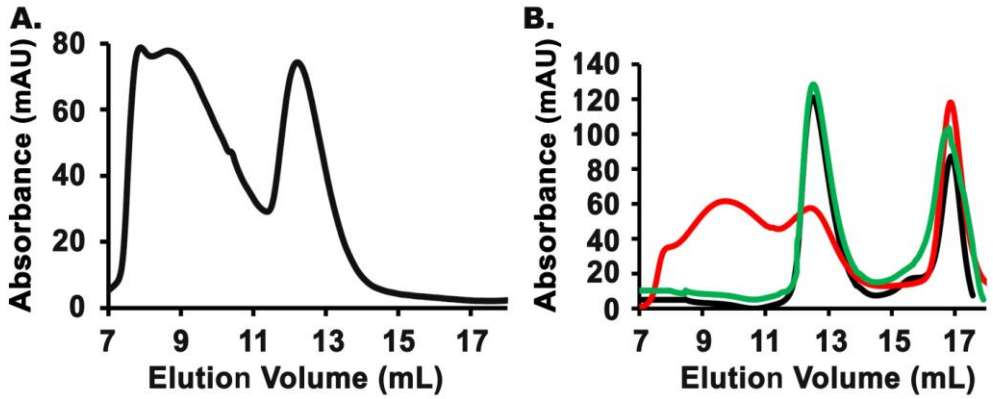

Figure 3.6. HMWS is formed under conditions inconsistent with enzymatic Fe-S cluster biosynthesis. (A) The SD complex was reacted with DTT, Fe^{2+}, and L-cysteine. (B) The SDUF complex was incubated with DTT and reacted with S^{2-} (black), Fe^{2+} and S^{2-} (red), and, after alkylating NFS1 (see Methods), with Fe^{2+} and S^{2-}. All samples applied to an anaerobic S-200 column and absorbance at 280 nm was measured. The HMWS, cysteine desulfurase, and uncomplexed ISCU2 and FXN are in fractions 7-11, 11-13, and 16-17, respectively.

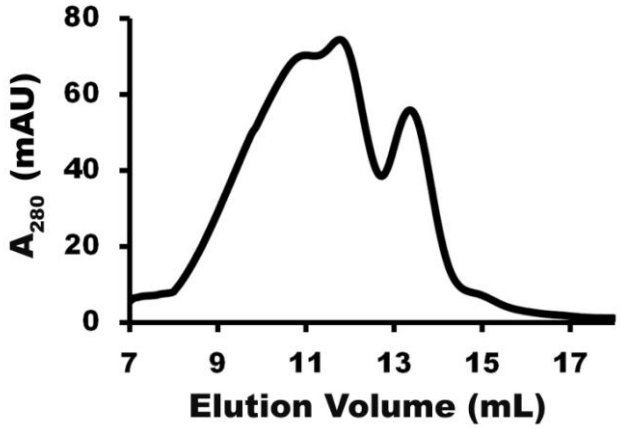

Figure 3.7. *E. coli* IscS forms the HMWS during Fe-S assembly reactions. IscS was reacted with DTT, Fe^{2+}, and L-cysteine and applied to an anaerobic S-200 column. The HMWS and cysteine desulfurase elute in fractions 9-12, and 13-14, respectively.

instead due to running out of substrate for formation of Fe-S species. Together, these data suggest a mineralization process that associates with cysteine-containing proteins.

Mössbauer spectroscopy supports the assignment of the HMWS as an Fe-S mineral. Interestingly, the HMWS exhibited electronic absorbance and CD spectroscopic properties reminiscent of [4Fe-4S] clusters, the ability to transfer Fe-S clusters to the [2Fe-2S] cluster binding protein FDX, and properties consistent with a solubilized Fe-S mineral. Mössbauer spectroscopy was used to further clarify the type of Fe-S cluster bound to the HMWS. Fe-S assembly reactions were performed with SD and SDUF under Standard conditions, the HMWS was isolated with a S-200 column, and the samples were frozen anaerobically for Mössbauer analysis. The HMWS from both SD and SDUF samples exhibited a high spin ferrous signal and a quadruple doublet with approximate parameters of δ = 0.35 mm/s and ΔE_Q = 0.67 mm/s (Figure 3.9). The Mössbauer parameters for the quadruple doublet did not match the parameters for a $[2Fe\text{-}2S]^{2+}$ or a $[4Fe\text{-}4S]^{2+}$ cluster but were more consistent with those of a $[2Fe\text{-}2S]^{2+}$ cluster. The Mössbauer spectra for a separate HMWS sample exhibited superparamagnetic behavior in which an unresolved peak collapsed to a quadruple doublet at higher temperatures (Figure 3.10). In addition, incubation of the HMWS with excess dithionite did not result in an EPR active S = ½ state (data not shown), which argues against a standard $[2Fe\text{-}2S]^{2+}$ or $[4Fe\text{-}4S]^{2+}$ cluster. These spectroscopic properties are consistent with the HMWS being a solubilized Fe-S mineral, and are similar to properties of material isolated from chemical reconstitution reactions.[113] Together these results suggest that Fe-S biosynthetic and reconstitution assays that

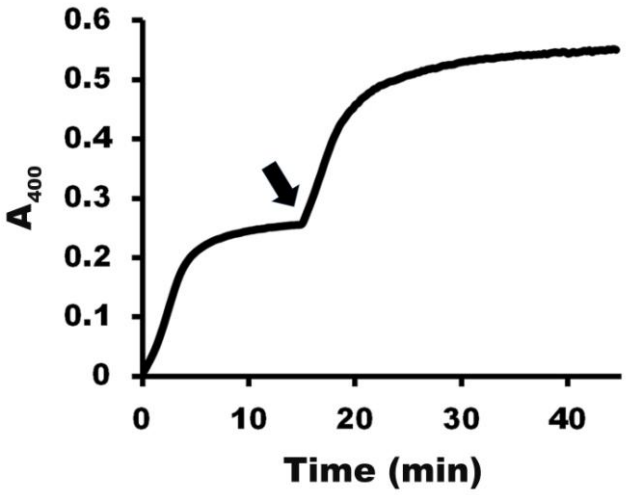

Figure 3.8. SDUF Fe-S assembly reactions are limited by L-cysteine in the presence of DTT. The SDUF Fe-S assembly reactions appear to saturate under Standard conditions. Addition of L-cysteine (arrow) results in additional Fe-S assembly.

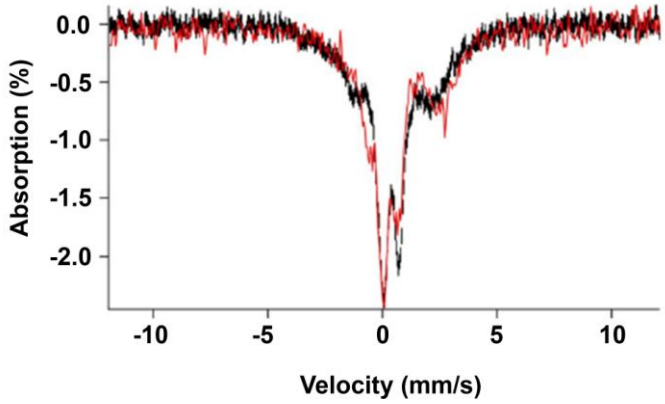

Figure 3.9. Mössbauer spectra determined for the HMWS. SDUF (red) and SD (black) Fe-S assembly reactions were performed under Standard conditions, the samples were applied to an anaerobic S-200 column, and the samples were frozen for Mössbauer analysis. The intensity is matched to show the overlap of the spectra. The HMWS was five times more concentrated for the SD sample than the SDUF sample.

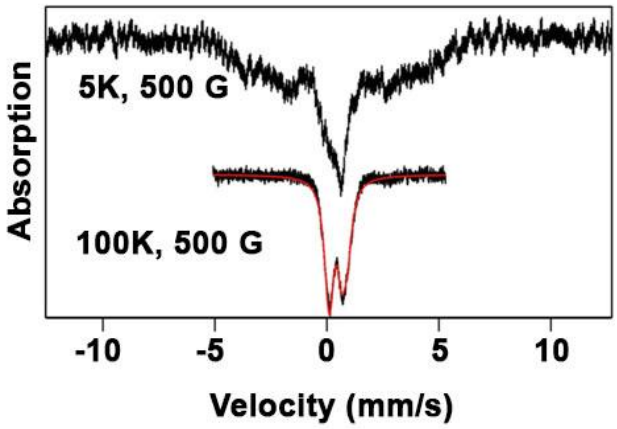

Figure 3.10. Mössbauer spectra determined for the HMWS. SD Fe-S assembly reactions were performed under Standard conditions and applied to an anaerobic S-200 column, and then frozen for Mössbauer analysis. The Mössbauer showed supermagnetic properties at low temperature that collapsed into a central doublet at high temperature indicating a mineral.

include or produce sulfide will likely generate Fe-S minerals and that this material will interact with cysteine-containing proteins to form HMWS.

Generation of [2Fe-2S] Clusters Associated with Uncomplexed ISCU2

The discovery of the HMWS material complicates kinetic analysis of enzymatic Fe-S cluster assembly using electronic absorption spectroscopy, as the mineral-like material and biological Fe-S clusters both exhibit sulfur-to-iron charge transfer bands that absorb in the 400-500 nm region. Further, simple desalting columns are ineffective at separating the Fe-S assembly complex and HMWS. In contrast, the 300-600 nm region of the CD spectrum is sensitive to the binding of [2Fe-2S] clusters to IscU,[40, 42, 44] whereas control mineralization reactions between ferrous or ferric iron with sulfide and DTT do not significantly contribute to this region of the spectrum (Figure 3.11). Alternate Fe-S assembly reaction conditions were also tested that minimize the

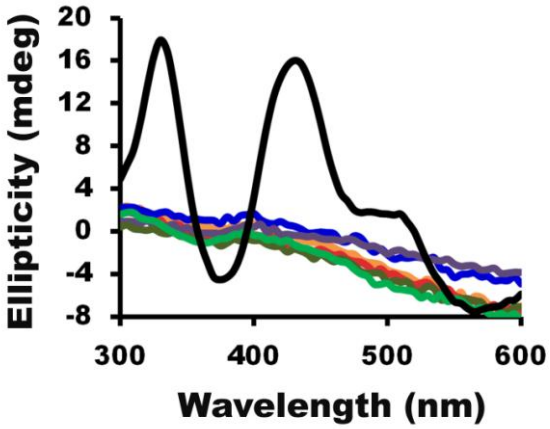

Figure 3.11. [2Fe-2S] clusters, but not Fe-S minerals, exhibit significant CD signals. The CD spectra are overlaid for reaction of $Fe(NH_4)_2(SO_4)_2$ and Na_2S (orange), $FeCl_3$ and Na_2S (red), $Fe(NH_4)_2(SO_4)_2$, Na_2S, and DTT (blue), $FeCl_3$, Na_2S, and DTT (purple), $Fe(NH_4)_2(SO_4)_2$, Na_2S, and cysteine (dark green), and $FeCl_3$, Na_2S, and cysteine (light green). The ISCU2-Fe-S is displayed in black.

generation of sulfide and Fe-S mineralization. The cysteine desulfurase activity is a direct measure of the sulfide generation ability of the Fe-S assembly complex. First, we explored Fe-S assembly reactions using the SDU complex, which is 10 fold less active than SDUF in the cysteine desulfurase reaction.[22] Second, we tested alternate reductants that are less efficient at sulfide generation than DTT. The cysteine desulfurase activity of the SDUF complex is five-fold lower using 1 mM L-cysteine than with standard reactions with 100 µM cysteine and 4 mM DTT (data not shown).

SDU Fe-S assembly reactions under Standard conditions result in competing [2Fe-2S] cluster formation and Fe-S mineralization pathways. The increased cysteine desulfurase activity for the SDUF complex (compared to SDU) under Standard conditions promotes Fe-S mineralization chemistry and may partially explain the ~25 fold greater rate of increase in 456 nm absorbance, which is attributed to Fe-S

assembly.[22] We show SDUF Fe-S assembly reactions under Standard conditions (above) generate the HMWS and spectroscopic features (Figure 3.1A and 3.2A) inconsistent with formation of a [2Fe-2S] cluster. In contrast, early time points for the SDU Fe-S assembly reaction revealed electronic absorption spectral features consistent with a [2Fe-2S] cluster (Figure 3.12A). At later time points, [4Fe-4S]-like features dominated the spectra (Figure 3.12A) and resulted in features similar to the SDUF sample (Figure 3.1A). The SDU sample, in contrast to SDUF, also exhibited a CD signal (Figure 3.12B) with peaks at 330 and 430 nm that are consistent with an [2Fe-2S] cluster bound to bacterial IscU.[44] Together this data leads to a model in which (*i*) the increase in the 400-500 nm electronic absorbance features are due to both [2Fe-2S] cluster and Fe-S cluster mineralization chemistry; (*ii*) the rate of mineralization is related to the ability of the complex to generate sulfide; and (*iii*) the competing Fe-S cluster mineralization chemistry overwhelms the [2Fe-2S] spectral features for the SDU sample at later time points (Figure 3.12A). To further test this model, we performed assays with an alternate reductant (L-cysteine) that is not as efficient at generating sulfide.

The SDU and SDUF Fe-S assembly complex samples generate [2Fe-2S] clusters under DTT-free conditions. The DTT-free Fe-S cluster assembly reaction includes 250 μM Fe^{2+} and 1 mM L-cysteine, which may function both as a substrate for generating sulfur and as a reductant to provide electrons for Fe-S cluster biosynthesis. The SDUF Fe-S assembly reaction exhibited different electronic absorbance spectra in the presence (Figure 3.12A) and absence (Figure 3.13A) of DTT. The final absorbance spectrum for

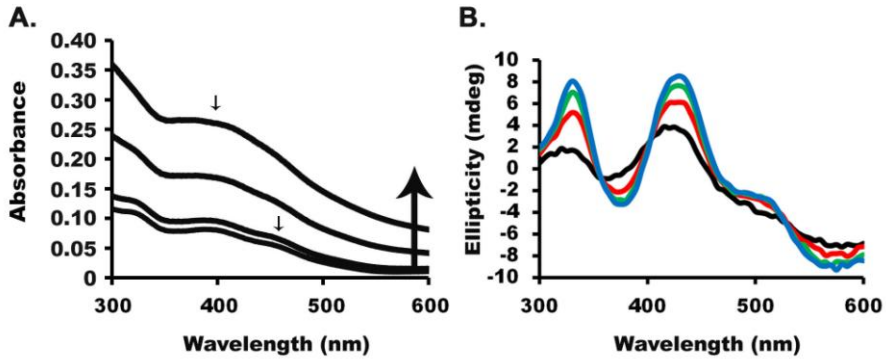

Figure 3.12. The SDU complex forms [2Fe-2S] clusters under in the presence of DTT. The SDU Fe-S assembly reaction was performed under Standard conditions. (A) The electronic absorbance spectra revealed [2Fe-2S] features (arrow at 456 nm) in early time points and a [4Fe-4S]-like peak (arrow at 400 nm) at later time points. The spectra were recorded 5, 10 30, and 60 minutes after initiating the reaction with L-cysteine. (B) The CD spectra revealed the development of characteristic [2Fe-2S] peaks. The spectra were collected at 0 (black), 20 (red), 40 (green), and 90 (blue) minutes.

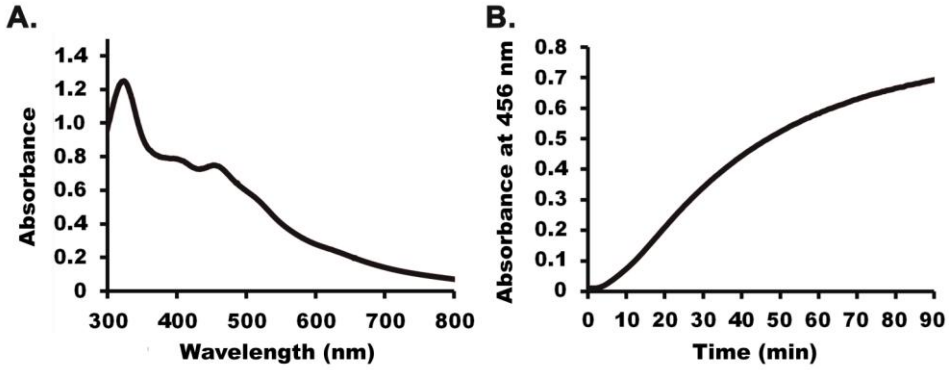

Figure 3.13. Fe-S cluster formation for SDUF complex in the absence of DTT. (A) Final Fe-S cluster absorbance spectrum and (B) kinetics monitored at 456 nm for reaction of SDUF (1:3:3 SD:ISCU2:FXN) with L-cysteine and Fe^{2+} under DTT-free conditions (see Methods).

the SDUF DTT-free reaction had features consistent with a [2Fe-2S] cluster (Figure 3.13A), rather than the peak at 400 nm that was attributed primarily to the HMWS. Measuring the SDUF Fe-S cluster formation rate under DTT-free conditions revealed the

rate of Fe-S cluster formation (Figure 3.13B) was an order of magnitude slower than under Standard conditions (Figure 3.1B) and that the kinetic trace appeared to have a sigmoidal or lag phase of indefinite length (Figure 3.13B). We further interrogated the DTT-free Fe-S cluster assay using CD spectroscopy. Interestingly, both SDU (Figure 3.14A) and SDUF (Figure 3.14B) samples exhibited CD features consistent with a [2Fe-2S] cluster. Moreover, the [2Fe-2S] cluster CD signal intensity does not diminish at later time points, suggesting the [2Fe-2S] clusters are not converted to [4Fe-4S] clusters or other Fe-S species with different CD signals during the experiment. Since the [2Fe-2S] cluster could be bound either to the Fe-S assembly complex or to uncomplexed ISCU2, additional experiments were performed under Catalytic (1:60 NFS1:ISCU2) and Stoichiometric (1:1 NFS1:ISCU2) conditions. Increasing the concentration of uncomplexed ISCU2 was predicted to not change the CD signature if the [2Fe-2S] cluster was a stable intermediate bound to the assembly complex. In contrast, the CD spectrum showed a significant change for the Catalytic reaction (Figure 3.14C), but very little change for the Stoichiometric reaction (Figure 3.14D). Thus, there appears to be a correlation between the amount of uncomplexed ISCU2 and the intensity of the Fe-S CD signal.

The SDUF Fe-S assembly complex generates non-protein Fe-S species under DTT-free conditions. Spectral comparisons for SDUF Fe-S assembly reactions under DTT-free conditions indicated the CD signal appeared to saturate after about 1 hour, whereas the electronic absorbance signal continued to increase at later time points (Figure 3.15A). This suggests at least two different Fe-S protein or small molecule

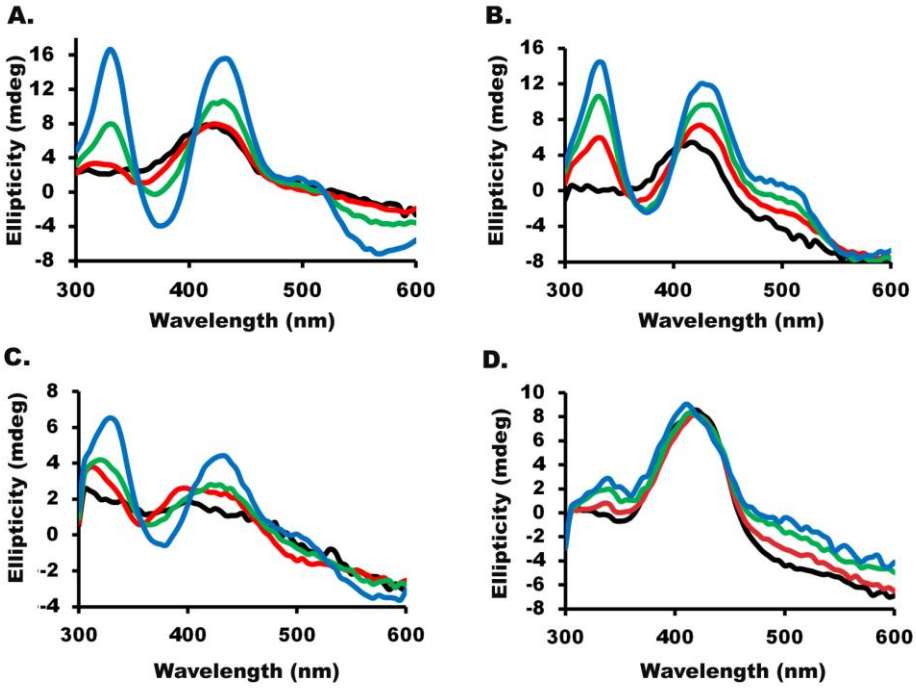

Figure 3.14. SDU and SDUF complexes generate [2Fe-2S] clusters in the absence of DTT. CD spectra measured for using DTT-free conditions with (A) SDU (1:3 SD:U), (B) SDUF (1:3:3 SD:U:F), (C) Catalytic amount of SD (1:60:60 SD:U:F), and (D) Stoichiometric (1:1:3 SD:U:F) conditions. Time points are 0 (black), 20 (red), 40 (green), and 90 (blue) minutes after initiating the reaction with L-cysteine.

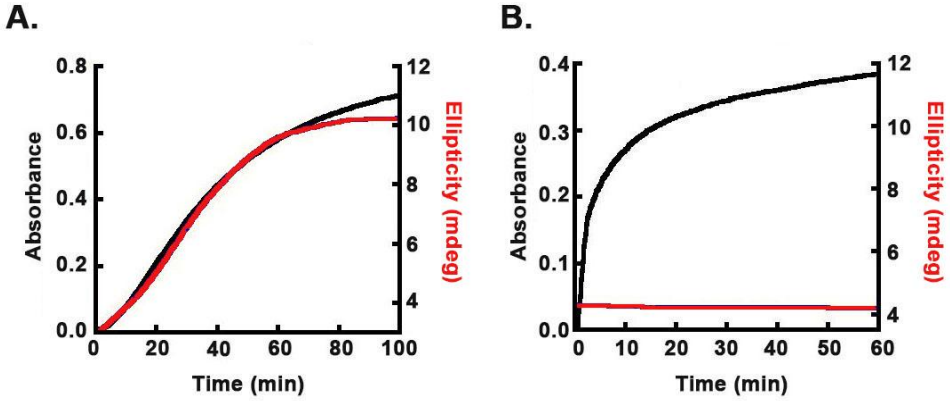

Figure 3.15. SDUF Fe-S assembly reactions compared in the presence and absence of DTT. (A) In DTT-free conditions the kinetics are overlaid for the Fe-S assembly reactions and the electronic absorbance at 456 nm (black) and CD at 430 nm (red) are shown. (B) In Standard conditions the kinetics are overlaid for the Fe-S assembly reactions and the electronic absorbance at 400 nm (black) and CD at 430 nm (red) are shown.

species are being formed under these conditions. Quantitation of the final absorbance from the SDUF DTT-free Fe-S assembly reaction indicated a significantly higher concentration of [2Fe-2S] cluster (125 μM) than ISCU2 (30 μM), and that this reaction is limited by the amount (250 μM) of iron (Table 3.1). Spiking a reaction that appeared complete with iron resulted in additional cluster synthesis (Figure 3.16). The non-protein bound Fe-S species may convert to the HMWS as even under DTT-free conditions the spectral properties for the SDUF reaction converted in a few hours from a characteristic [2Fe-2S] signal to features dominated by the absorbance signal previously assigned to the HWMS (Figure 3.17A). S-200 chromatographic analysis confirms HMWS formation after 3.5 hours (Figure 3.17B) that corresponds to the change in the absorbance spectra. These results revealed that the SDUF complex under DTT-free Fe-S assembly conditions generated (*i*) Fe-S species with CD parameters consistent with ISCU2 bound [2Fe-2S] clusters; (*ii*) additional Fe-S species with absorbance features consistent with [2Fe-2S] clusters that are not associated with ISCU2 (possibly bound to L-cysteine); and (*iii*) the slow conversion of the non-protein bound [2Fe-2S] clusters to HMWS.

The SDUF complex generates [2Fe-2S] clusters on uncomplexed ISCU2. Here we combined Mössbauer spectroscopy with LC-ICP-MS analysis to confirm the molecular species (SDUF or uncomplexed ISCU2) that was associated with the [2Fe-2S] cluster. The LC-ICP-MS is a custom-designed system in which an FPLC is located in an anaerobic glovebox that splits the eluent after column chromatography between a UV-Vis detector and ICP-MS. An SDUF Fe-S assembly reaction under Catalytic (no DTT) conditions was initiated by the addition of L-cysteine to a sample containing ^{57}Fe, a

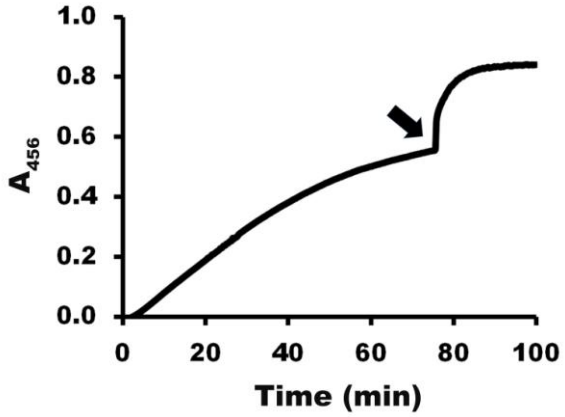

Figure 3.16. SDUF Fe-S assembly reactions are limited by iron in the absence of DTT. The SDUF Fe-S assembly reactions appear to saturate under DTT-free conditions. Addition of Fe^{2+} (arrow) results in additional Fe-S assembly.

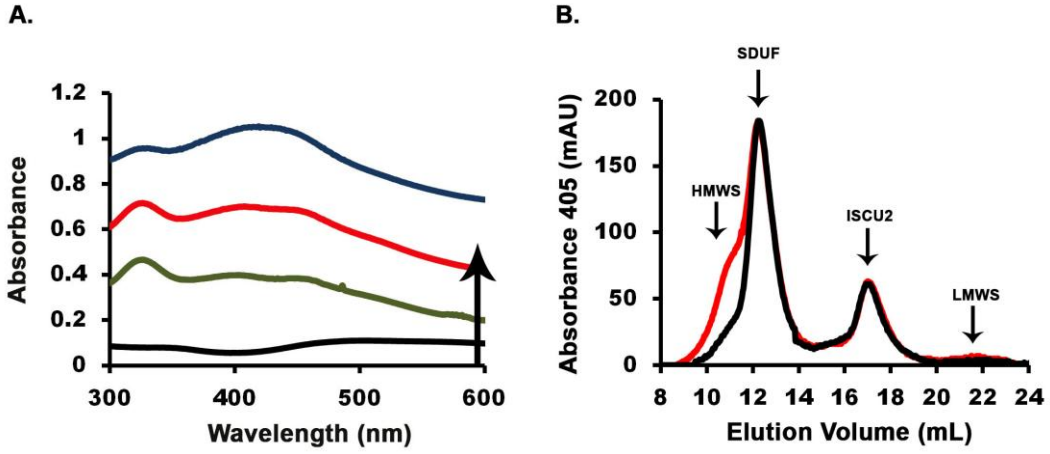

Figure 3.17. (A) The SDUF Fe-S cluster assembly assay was measured under DTT-free conditions over the time course of 5 hours: 0min (black), 2 hrs (green), 3.5 hours (red), and 5 hours (blue). The [2Fe-2S] cluster-like feature seems to fade in to [4Fe-4S] cluster-like feature at later time points. (B) An analytical S-200 monitored reaction similar to (A) was monitored for 1.5 hrs (black) and 3.5 hours (red). The HMWS starts to form at the 3.5 hr mark indicated by shoulder between 10-11 mL. The small molecule thiols shows a weak 405 nm absorbance indicated by LMWS.

portion of the sample was placed in an anaerobic CD cuvette to monitor reaction progress, and the rest of the sample was desalted upon reaction completion to remove excess reagents before splitting the sample for LC-ICP-MS and Mössbauer analysis. A portion of the sample was applied to an anaerobic S-200 size exclusion column attached to the LC-ICP-MS. The eluent from the column was partitioned between an ICP-MS to determine the iron concentration, and a UV-Vis detector to determine the absorbance at 280, 400 and 456 nm. The iron counts along with the absorbance at all three wavelengths coincided primarily with the retention time of monomeric ISCU2, with some counts associated with SDUF (Figure 3.18). Mössbauer analysis revealed parameters (δ= 0.30 mm/s and ΔE_Q= 0.72 mm/s) consistent with a $[2Fe\text{-}2S]^{2+}$ cluster with no significant population of free iron, [4Fe-4S] cluster, or Fe-S mineral (Figure 3.19), suggesting that the species on uncomplexed ISCU2 and the SDUF complex is a $[2Fe\text{-}2S]^{2+}$ cluster. Together these data suggest a model in which [2Fe-2S]-SDUF intermediates undergo subunit dissociation or cluster transfer chemistry to generate uncomplexed [2Fe-2S]-ISCU2 species in the absence of Fe-S target proteins.

DTT Mediated [2Fe-2S] Cluster Conversion and Transfer Chemistry

The SDUF complex generates [2Fe-2S] clusters that can be converted to [4Fe-4S] clusters by the addition of DTT. Spectral comparisons under Standard conditions (above) showed a rapid increase in the [4Fe-4S]-like HMWS absorbance signal that continues to increase at later time points, yet no significant CD signal due to an Fe-S species (Figure 3.15B). One possible explanation for the lack of a CD signal is that DTT facilitates the reductive coupling of two $[2Fe\text{-}2S]^{2+}$ clusters to generate a CD silent [4Fe-

$4S]^{2+}$ cluster. To test this hypothesis, we determined if DTT can mediate conversion of ISCU2-bound [2Fe-2S] clusters to [4Fe-4S] species. A SDUF Fe-S assembly reaction was initiated under Catalytic (no DTT) conditions by the slow addition of ^{57}Fe, incubated for an additional hour, the sample was split into two portions, and 50 mM DTT was incubated with one portion for an additional hour. Both portions were analyzed by LC-ICP-MS and Mössbauer spectroscopy. Samples with and without DTT exhibited retention times consistent with an ISCU2 monomer that coincides with the absorbance at all three wavelengths and with a small fraction (~10%) of the iron, whereas a larger fraction (~90%) of the iron associated with a low molecular weight species (LMWS) (Figure 3.20). The Mössbauer spectra for the sample without DTT revealed a strong signal (~90%) that was assigned based on its parameters (δ = 0.74 mm/s, ΔE_Q = 3.4 mm/s) to a high spin Fe(II) species coordinated to 4 thiol ligands, and weaker signals that correspond to high-spin Fe(II) bound to oxygen (δ = 1.3 mm/s, ΔE_Q = 3.5 mm/s) and a $[2Fe\text{-}2S]^{2+}$ cluster (δ = 0.3 mm/s, ΔE_Q = 0.7 mm/s) (Figure 3.21). The LMWS from the S-200 column may correspond to the high-spin Fe(II) species ligated by the 10 mM L-cysteine in the reaction mixture. The sample that included DTT exhibited Mössbauer features similar to the first sample except that a signal consistent with a $[4Fe\text{-}4S]^{2+}$ signal (δ = 0.4 mm/s, ΔE_Q = 1.15 mm/s) replaced the $[2Fe\text{-}2S]^{2+}$ signal as the minor (~15%) fraction of the Mössbauer spectrum (Figure 3.21B). This result suggests a stable [2Fe-2S] monomeric species converts to a [4Fe-4S] cluster upon the addition of DTT. To further test this hypothesis, a SDUF Fe-S assembly reaction was performed under DTT-free conditions to generate a CD signal that corresponds to a [2Fe-2S] cluster, DTT

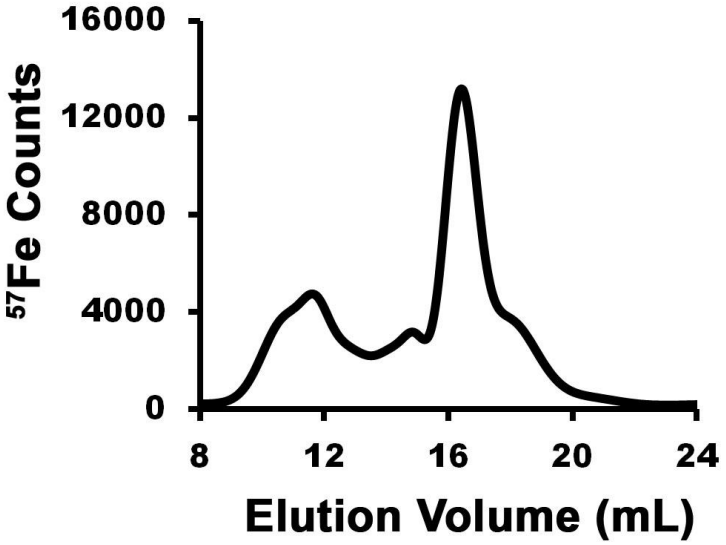

Figure 3.18. Formation of a $[2Fe\text{-}2S]^{2+}$ cluster bound to uncomplexed ISCU2. An SDUF Fe-S assembly reaction was performed under catalytic condition and applied to an anaerobic S-200 column in which the eluent was split to determine iron counts by ICP-MS. The majority of the iron counts coeluted with uncomplexed ISCU2 (16 mL).

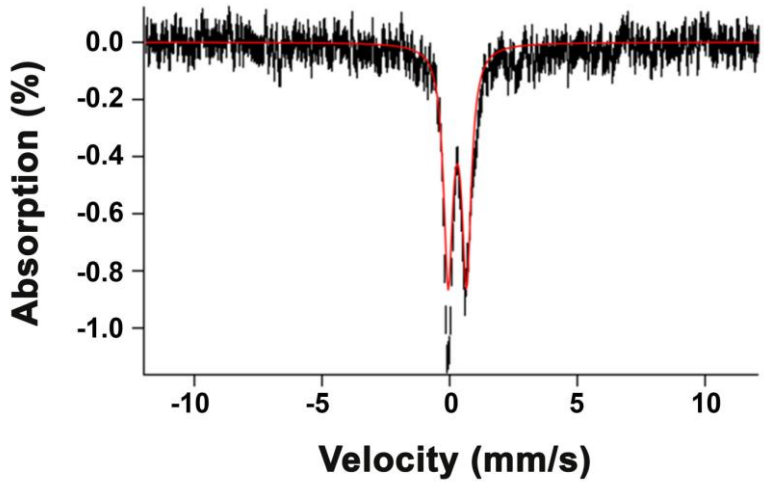

Figure 3.19. Formation of a $[2Fe\text{-}2S]^{2+}$ cluster bound to uncomplexed ISCU2. An SDUF Fe-S assembly reaction was performed under catalytic condition and was frozen for Mössbauer analysis. The quadruple doublet was fit (red) with parameters δ = 0.30 mm/s and ΔE_Q = 0.72 mm/s.

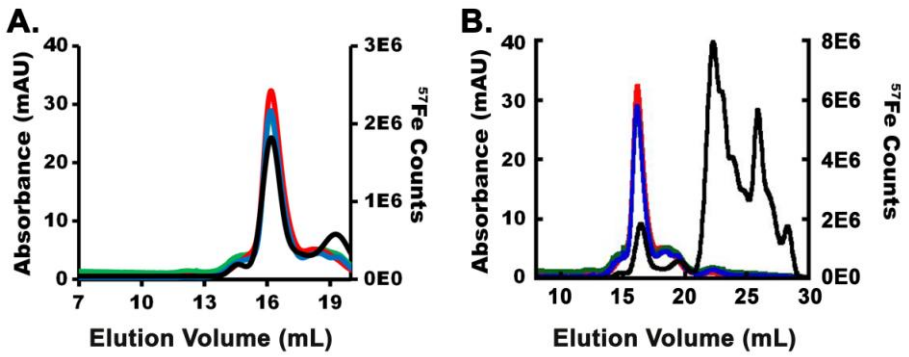

Figure 3.20. Formation of a $[2Fe\text{-}2S]^{2+}$ cluster bound to uncomplexed ISCU2. An SDUF Fe-S assembly reaction was performed under catalytic condition and applied to an anaerobic S-200 column in which the eluent was split to determine iron counts (black) by ICP-MS and absorbance at 280 (red, scaled down 10 fold for overlay), 400 (green), and 456 (blue) nm. (A) The chromatogram was cropped to highlight the uncomplexed ISCU2 that elutes at 16 mL. (B) Additional low molecular weight species (LMWS) eluted at 21-23 mL that contained >90% of the iron.

was added, and the CD spectra was followed as a function of time. This experiment revealed a DTT-dependent loss of Fe-S cluster CD signal until only the features from the PLP cofactor remained (Figure 3.22). The loss of the ISCU2-[2Fe-2S] signal could be due to conversion to a CD-silent [4Fe-4S] cluster, consistent with Mössbauer data (Figure 3.21), or transfer of the [2Fe-2S] cluster to DTT and generation of a CD silent species. Although this cluster conversion/transfer process is reproducible, the rate varies with some unknown factor (see Discussion). Interestingly, adding DTT at the beginning of the experiment resulted in HMWS Mössbauer features, whereas adding DTT after [2Fe-2S] cluster formation resulted in Mössbauer features consistent with a [4Fe-4S] cluster. Together, these data reveal that DTT can release sulfide from the Fe-S assembly complex that initiates Fe-S mineralization chemistry, can induce the conversion of

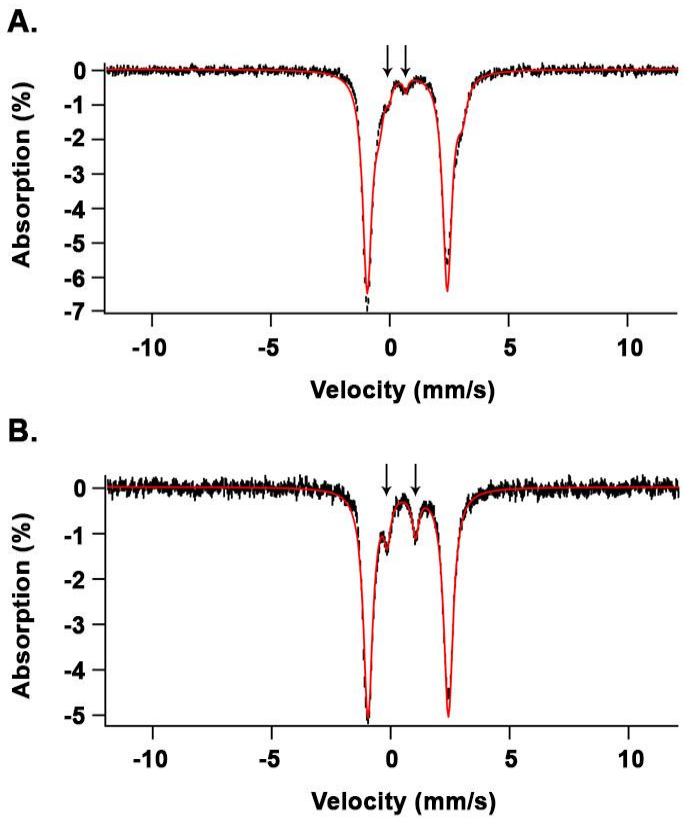

Figure 3.21. Mössbauer spectra determined for the ISCU2 monomer under catalytic conditions. Samples were prepared anaerobically (see Methods) under DTT-free conditions. (A) Half the sample was frozen for Mössbauer analysis where ~4% was $[2Fe\text{-}2S]^{2+}$ cluster (δ= 0.3 mm/s, ΔE_Q=0.7 mm/s; indicated by arrows) and 90% was high-spin Fe(II) bound to sulfur with 4 coordinate thiol ligation (δ= 0.74 mm/s, ΔE_Q=3.4 mm/s) and remaining 6% was unreacted high-spin Fe(II) bound to oxygen (δ= 1.3 mm/s, ΔE_Q=3.5 mm/s). (B)The other half of the sample was treated with 10 mM DTT and then frozen for Mössbauer analysis where 15% was $[4Fe\text{-}4S]^{2+}$ cluster (δ= 0.4 mm/s, ΔE_Q=1.15 mm/s; indicated by arrows) and 85% was high-spin Fe(II) bound to sulfur with 4 coordinate thiol ligation (δ= 0.74 mm/s, ΔE_Q=3.4 mm/s).

ISCU2-bound [2Fe-2S] clusters to [4Fe-4S] clusters, and may also be able to function in cluster transfer reactions as an acceptor molecule (similar to L-cysteine, above).

DTT mediates transfer of [2Fe-2S] clusters from ISCU2 to apo FDX. Here CD spectroscopy was used to monitor the transfer of Fe-S clusters generated by the SDUF complex under Acceptor (no DTT) conditions to apo FDX. Surprisingly, including

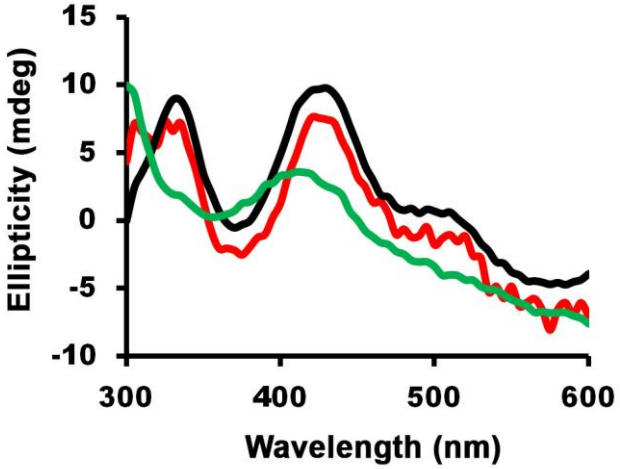

Figure 3.22. The SDUF Fe-S cluster assembly was monitored using CD under DTT-free conditions. Once the [2Fe-2S]-ISCU2 feature reached saturation (black), 4 mM DTT was added and at 2 min (red) or 5 min (green) the [2Fe-2S]-ISCU2 faded and all that was observed was the PLP from NFS1 (green). This indicated that ISCU2 transferred the cluster to DTT, and mineralization may have started to occur.

excess apo FDX in the assembly assay did not alter the Fe-S CD features and the same peaks developed at 330 and 430 nm (rate of 0.055 min^{-1}, Figure 3.23) that were previously assigned to ISCU2-bound [2Fe-2S] clusters (Figure 3.24A). The addition of DTT at the end of the reaction resulted in a slow change (rate of 0.02 min^{-1}; Figure 3.23B) in the CD features from those characteristic of the [2Fe-2S]-ISCU2 to features consistent with reduced FDX[114] (Figure 3.24B). Addition of DTT and apo FDX at the start of the Fe-S assembly reaction resulted in a fairly rapid (rate of 0.10 min^{-1}; Figure 3.23C) generation of the $[2Fe\text{-}2S]^{1+}$-FDX signal and no evidence for a [2Fe-2S]-ISCU2 intermediate species (Figure 3.24C). These data indicate the SDUF complex generates [2Fe-2S] species that can be transferred to thiol-containing acceptor molecules and that

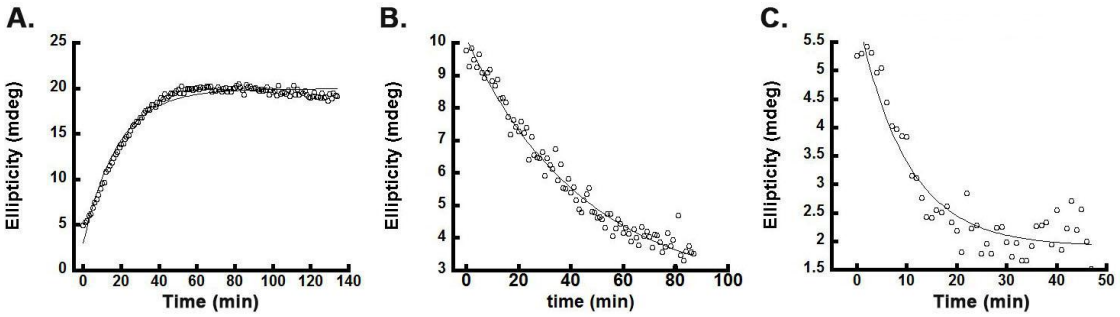

Figure 3.23. SDUF Fe-S cluster transfer reactions to apo FDX. The SDUF Fe-S assembly reactions were performed under Acceptor conditions (see Methods) that included apo FDX. (A) The cluster assembly reaction was initiated by L-cysteine in the absence of DTT and the CD spectrum was monitored for 130 minutes and fit to an exponential rise equation to yield a rate 0.055 min^{-1}. (B) After the reaction from (A) was complete, DTT was added and CD spectra were measured for 90 minutes which measured a rate of 0.022 min^{-1}. (C) The same reaction as (A) was performed in the presence of DTT. Rate was 0.10 min^{-1}. The Ellipticity was measured at 330 nm.

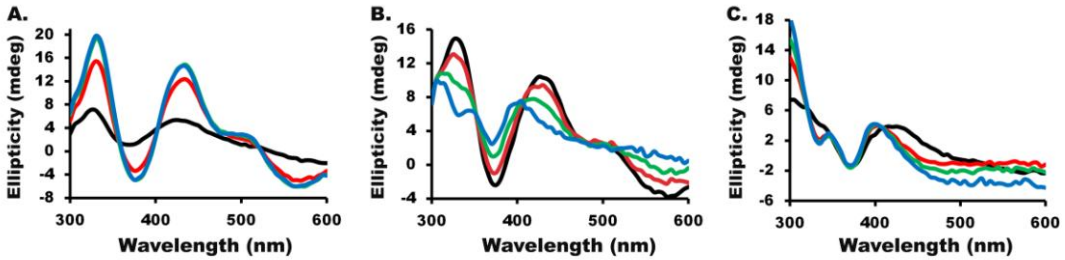

Figure 3.24. SDUF Fe-S cluster transfer reactions to apo FDX. The SDUF Fe-S assembly reactions were performed under Acceptor conditions (see Methods) that included apo FDX. (A) The cluster assembly reaction was initiated by L-cysteine in the absence of DTT and the CD spectrum was monitored at 0 (black), 20 (red), 40 (green) and 90 (blue) minutes. (B) After the reaction from (A) was complete, DTT was added and CD spectra were obtained at 0 (black), 20 (red), 40 (green), and 90 (blue) minutes. (C) The same reaction as (A) was performed in the presence of DTT. CD spectra were recorded at 0 (black), 10 (red), 20 (green), and 40 (blue) minutes.

DTT has a complex role in Fe-S assembly reactions that includes generating sulfide for Fe-S mineralization chemistry, facilitating [2Fe-2S] cluster to [4Fe-4S] cluster conversion, mediating [2Fe-2S] cluster transfer chemistry, and potentially functioning as an cluster acceptor.

Discussion

Experiments to identify reaction intermediates and elucidate mechanistic details of biosynthetic pathways often rely on monitoring reaction progress with kinetic measurements. This is challenging for Fe-S cluster biosynthesis as the substrates (iron, cysteine, and electrons) also undergo competing non-enzymatic Fe-S mineralization and self-assembly chemistry, plus the synthesized Fe-S clusters are capable of undergoing ligand exchange reactions. These competing reactions and chemistry have complicated the interpretation of results and limited mechanistic insight. It is therefore important to elucidate factors that partition reaction intermediates between these competing pathways and understand the types and properties of Fe-S species that are being generated. Here we identify conditions that favor pathways that compete with Fe-S cluster biosynthesis, uncover details of the surprisingly complex DTT-mediated chemistry for *in vitro* assays, and provide insight into human Fe-S cluster biosynthesis.

Fe-S assembly reactions under Standard *in vitro* assay conditions generate both Fe-S clusters by the assembly complex and a HMWS that has properties consistent with a solubilized Fe-S mineral. The HMWS is an iron, sulfide, and thiol-containing-protein dependent material that exhibits Mössbauer parameters (δ = 0.35 mm/s and ΔE_Q = 0.67

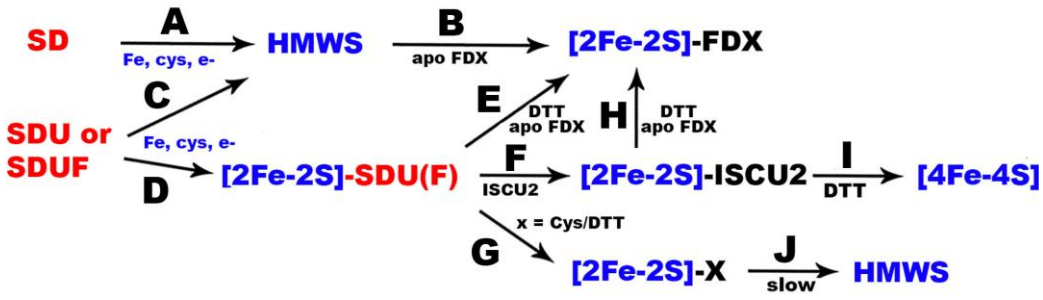

Figure 3.25. Model for competeing Fe-S cluster biosynthesis and mineralization pathways. (A) minealization of SD complex to generate HMWS. (B) Chemical reconstitution of apo FDX. Competing mineralization (C) and Fe-S biosynthetic (D) pathways for the SDU and SDUF complexes. Transfer of [2Fe-2S] cluster from the assembly complex to (E) apo FDX, (F) uncomplexed ISCU2, and (G) free thiol-containing molecules. The [2Fe-2S]-ISCU2 species can (H) transfer the cluster to apo FDX in a DTT mediate process and (I) reductive couple to generate [4Fe-4S]-ISCU2 species. (J) The [2Fe-2S] cluster bound to small molecule thiols can also slowly convert to HMWS. Protein complexes are displayed in red and iron-containing species in blue.

mm/s) similar to that of Fe-S minerals, such as pyrite (δ = 0.25-0.43 mm/s and ΔE_Q = 0.61-0.66 mm/s)[115], or superparamagnetic behavior consistent with mineral-like materials (Figure 3.10). The HMWS forms in the absence of the Fe-S catalytic subunit ISCU2 (Figures 3.6 and 3.25A) and can participate in the chemical reconstitution of apo target proteins (Figures 3.4 and 3.25B). In DTT-free conditions, both SDU and SDUF samples produce species with electronic absorbance and CD spectroscopic properties consistent with a [2Fe-2S] cluster (Figures 3.13 and 3.14). The partitioning between HMWS and [2Fe-2S] cluster biosynthetic pathways appears to be shifted toward the HMWS for SDUF compared to SDU samples, and for DTT compared to DTT-free assay conditions. SDUF is a more active cysteine desulfurase *in vitro* and DTT is more efficient at sulfide production than cysteine, suggesting increased HMWS formation (Figure 3.25C) relative to [2Fe-2S] cluster synthesis (Figure 3.25D) may at least

partially depend on the ability of a persulfide intermediate to be intercepted (by DTT and/or cysteine) and produce sulfide. Chemical reconstitution reactions for [4Fe-4S]-containing radical SAM enzymes generate a HMWS with similar spectroscopic properties.[113] Deconvoluting the enzymatic and mineralization processes is challenging as they exhibit comparable formation kinetics (both depend on cysteine turnover by NFS1), overlapping electronic absorbance properties, and the products coelute on desalting columns.

Fe-S cluster assembly assays under DTT-free conditions revealed [2Fe-2S]-cluster intermediate species. Mössbauer spectroscopy indicated [2Fe-2S] clusters were formed under cysteine-reducing (DTT-free) conditions (Figure 3.19). Fe-S assembly assays under similar conditions revealed the concurrent development of electronic absorbance and CD spectroscopic signals (Figures 3.13-3.15) and a concentration of [2Fe-2S] clusters that is significantly greater than the total ISCU2 concentration (Table 3.1). We suggest formation of both [2Fe-2S]-ISCU2 (Figure 3.25F) and [2Fe-2S]-X (Figure 3.25G) species, where X is a small molecule such as cysteine (in this reaction), DTT, or GSH. As [2Fe-2S]-GSH complexes do not exhibit significant Fe-S CD signals (Figure 3.11), we suspect [2Fe-2S] clusters bound to small molecule thiols like cysteine or DTT are also CD silent. At later time points the absorbance signal continues to increase and then slowly changed (> 2 hours) to a signal with HMWS rather than [2Fe-2S] features (Figure 3.17). In contrast, the CD signal plateaus (Figure 3.15A). This suggests a model in which cluster assembly on the complex is slow under cysteine-reducing conditions and readily and concurrently generates [2Fe-2S] clusters on ISCU2

(contributing to CD and absorbance properties) and cysteine (contributing primarily to absorbance properties), and that at longer time points the [2Fe-2S] bound to cysteine is slowly converted to the HMWS (Figure 3.25J). A model in which the SDUF complex generates a labile [2Fe-2S] cluster is further supported by the observations that the Fe-S CD signal intensity is proportional to the amount of excess ISCU2 that is added to the reaction (Figure 3.14) and LC-ICP-MS data that indicates most of the Fe-S species are associated with uncomplexed ISCU2 (Figures 3.18 and 3.20). This model is also consistent with the fact that IscU variants that are compromised in cluster transfer (D37A in *E. coli*), but not native IscU complexes, copurify with [2Fe-2S] clusters bound at the active site[47, 53]. It is unclear if ISCU2 subunits dissociate upon cluster formation or if the [2Fe-2S]-SDUF complex transfers clusters to uncomplexed ISCU2 through a ligand exchange mechanism.

We identified five different roles for DTT in Fe-S assembly reactions. First, DTT is commonly added as a surrogate electron donation system. Ferredoxin-ferredoxin reductase is thought to be the physiological electron donation system, but is not typically used in Fe-S assays because the absorbance and CD properties of ferredoxin, ferredoxin reductase, and NADPH complicate the ability to monitor cluster synthesis. Second, DTT is very effective at cleaving cysteine-persulfide intermediates and generating sulfide, which can undergo mineralization chemistry (Figure 3.25C). SDUF Fe-S assembly assays that include DTT rapidly generate HMWS absorbance features and are CD silent (Figure 3.15B). A simple explanation for this observation is that the SDUF complex exclusively partitions towards the mineralization (Figure 3.25C) rather than biosynthesis

(Figure 3.25D) pathway. This explanation would necessitate a correlation for the rates of the cysteine desulfurase and Fe-S assembly reactions. Recent results reveal Fe-S assembly complexes with ISCU2 variants ($SDU_{C35A}F$ and $SDU_{C61A}F$) exhibit native like cysteine desulfurase activities, but compromised Fe-S cluster assembly reactions (Chapter II). We therefore hypothesize that the addition of DTT at the beginning of the experiment results in both mineralization (Figure 3.25C) and biosynthetic cluster formation (Figure 3.25D), and that the third role of DTT is as a [2Fe-2S] cluster acceptor (Figure 3.25G) that can generate HMWS (Figure 3.25J). This hypothesis suggests the previously characterized $SDU_{C35A}F$ and $SDU_{C61A}F$ complexes undergo the mineralization pathway (explaining the slow increase in absorbance), but the biosynthetic route (Figures 3.25D, 3.25G, and 3.25J) to HMWS is compromised. Fourth, we show DTT addition results in the conversion of [2Fe-2S]-ISCU2 to [4Fe-4S]-ISCU2 species (Figures 3.21 and 3.25I). This type of reductive coupling has precedent in both biomimetic[3] and IscU literature[48]. The last role for DTT is in mediating the transfer of Fe-S clusters to apo FDX. Surprisingly, reactions that include apo FDX but no DTT generate [2Fe-2S]-ISCU2 species and transfer only occurs upon the addition of DTT (Figures 3.24 and 3.25H). It is unclear if DTT is required to reduce the cluster for transfer (the resulting holo-FDX appears to be reduced based on the CD spectra) or if DTT functions through a ligand exchange mechanism. Interestingly, the kinetics of cluster transfer from [2Fe-2S]-ISCU2 to apo FDX are much slower than the kinetics of cluster assembly and transfer using the SDUF complex, suggesting either the chemical reconstitution is faster than the enzymatic process and/or [2Fe-2S]-ISCU2 is not an

intermediate and is bypassed in cluster assembly on FDX (Figure 3.25E). Together, DTT appears to have *in vitro* roles in Fe-S assembly assays as a reductant, in persulfide cleavage, in [2Fe-2S] to [4Fe-4S] cluster conversion, in mediating [2Fe-2S] cluster transfer to apo FDX, and as a [2Fe-2S] cluster ligand.

Conclusion

In summary, we provide details of competing pathways for Fe-S cluster biosynthesis and Fe-S mineralization. Our data suggest a labile [2Fe-2S] cluster is generated on the native SDUF complex that can be transferred to thiol-containing acceptor molecules. Notably, this labile [2Fe-2S]-SDUF model is inconsistent with the proposal that mammalian Fe-S assembly complex forms a stable [4Fe-4S] species.[62] This stable [4Fe-4S]-SDUF proposal would also be inconsistent with the apparent requirement of additional protein factors in [4Fe-4S] cluster synthesis.[116] Moreover, even though our data supports a transient [2Fe-2S] intermediate on the SDUF Fe-S assembly complex, it does not rule out the possibility that additional protein factors affect the stability of Fe-S clusters on the assembly complex. Overall, the multiple roles for DTT complicate the interpretation of *in vitro* Fe-S assembly results and necessitate the development of new functional assays that monitor the kinetics of Fe-S cluster reactions using the native electron donation system and the ability to monitor Fe-S cluster assembly in an assay mixture with many different electronic absorbance and CD active chromophores.

CHAPTER IV

ALANINE SCANNING OF THE FRATAXIN (FXN) SURFACE IDENTIFIES A HOTSPOT FOR BINDING AND ACTIVATION WITH THE SDU COMPLEX

Introduction

Defects in the frataxin (FXN) protein have been shown to cause the neurodegenerative disease Friedreich's Ataxia (FRDA), a progressive degenerative disease of children and adolescents that ultimately leads to premature death. [88, 117, 118] Large research efforts to define the function of FXN and develop therapeutic approaches for the treatment of FRDA have been launched since the discovery of the link between FRDA and the *FXN* gene in 1996. Unfortunately, these efforts have not resulted in an effective FRDA therapy and the disease symptoms are often simply managed through chelation therapy to restrict mitochondrial iron accumulation and antioxidant treatment to limit ROS damage in patients. [119, 120] Although many roles have been proposed for the FXN family of proteins, emerging evidence suggests a regulatory role in Fe-S cluster biosynthesis. [22, 89, 121, 122] FXN is required to interact with the Fe-S cluster biosynthesis machinery to perform such a regulatory function. As mutations that decrease these protein-protein interactions might be linked to FRDA, it is essential to define these interactions both in terms of identifying FXN binding partners and also which residues on those proteins contribute to frataxin-based regulation.

Immunoprecipitation and pull-down assays by Cortopassi and coworkers suggest FXN interacts with the core components of the human Fe-S cluster assembly system

NFS1-ISD11 and ISCU2; as well as with the chaperones GRP75, HSP60, and HSC20. [123, 124] Many of these protein-protein interactions have been confirmed by others in the yeast and *E. coli* Fe-S cluster assembly systems. [125-127] We have shown a functional four protein complex between NFS1-ISD11, ISCU2, and FXN (named SDUF), which provides validation to the role of FXN in Fe-S cluster biosynthesis. [22, 62, 80] Taken together these results suggest that FXN interacts with a preformed NFS1-ISD11/ISCU2 (SDU) complex, and interaction of FXN with this complex significantly increases the rate of the cysteine desulfurase and Fe-S cluster assembly on the scaffold protein. Small-angle X-ray scattering data and structural analysis of the analogous *E. coli* IscS/IscU/CyaY complex (IscS, IscU, and CyaY are homologs of human NFS1, ISCU, and FXN, respectively) suggests that CyaY binds near the dimer interface of the cysteine desulfurase IscS, while the scaffold protein IscU binds near the periphery of the IscS dimer. [128] This arrangement not only allows for interaction of IscS with CyaY and IscU, but also allows for interaction between IscU and CyaY.

Several attempts have been made to identify residues involved in the interaction between FXN and either the intact SDU complex or components of the SDU complex. Based on pull-down assays Cortopassi *et al* suggest an interaction between FXN and ISD11 that is mediated through FXN residue I154 in the presence of nickel. [124] Mutation of the basic residues R220E/R223E/R225E on IscS or the acidic residues E18K/E19K/E22K on CyaY have been shown to disrupt the interaction of these two proteins, suggesting that the acidic ridge of the frataxin family serves as the binding surface for the cysteine desulfurase. [128] Further protein-protein interactions were

observed by Stemmler *et al*, who demonstrated that several residues on yeast Yfh1 are perturbed upon addition of the yeast scaffold protein Isu1. [129] Pull-down assays of yeast Yfh1 variants including N122K (human FXN_{N146K}), N122A/K123T/Q124A (human $FXN_{N146K/K147T/Q148A}$), and W131A (human FXN_{W155A}), suggest that the β-sheet region of the protein is involved in interactions with the yeast scaffold protein Isu1 and that W131 (human FXN_{W155}) is a hotspot for interaction. [125, 126] Furthermore *in vivo* studies of yeast Yfh1 by Foury *et al* suggest that Q129 (human FXN_{Q153}), W131 (human FXN_{W155}), and R141 (human FXN_{R165}) form a cluster of functionally important residues on the FXN surface, which could facilitate protein-protein interactions. [125] Puccio *et al* used pull-down assays of 15 FXN variants (Y95G, E96K, D104G, E108K, E111K, D115K, D122Y, D124K, G130V, N146A, N146K, I154F, W155A, W155R, & W173G) in the context of the SDU complex and further confirmed and expanded upon the results seen in yeast and *E. coli*; identifying six variants (E108K, E111K, D124K, N146K, W155A and W155R) that disrupted or abolished the FXN/SDU interaction. [80] The negatively charged acidic patch residues E108, E111, and D124 are suggested to interact with the basic residues on NFS1-ISD11, while the N146 and W155 β-sheet residues are proposed to interact with ISCU2. Furthermore the complete loss of interaction between SDU and the W155R variant or the less severe W155A variant support the findings in yeast that this residue is critical for interaction with ISCU2.[86, 87] The available biochemical, structural, and pull-down assay data suggest regions of the FXN β-sheet and α_1 helix, which appear to be important in protein-protein interactions with SDU. Here we build upon these results to examine the FXN side-chain contributions for

binding to the SDU complex and also establish the functional importance of FXN side-chains for the activation of the Fe-S assembly complex. These experiments provide vital information towards the design of peptide mimics as a FXN replacement strategy and potential FRDA therapeutic.

Experimental Procedures

Protein Preparation

All mutations were introduced into a pET11a plasmid containing a codon optimized human *FXN* gene (FXN Δ1-55), lacking the first 55 amino acids, using the QuikChange method (Stratagene). [22] Presence of the mutation was confirmed by DNA sequencing, performed by the Texas A&M University Gene Technology Laboratory. The plasmids containing each mutant were transformed into *E. coli* BL21(DE3) competent cells and grown at 37 °C, until an OD_{600} of ~0.7 was obtained. Protein expression was then induced with 0.5 mM isopropyl β-D-1-thiogalactopyranoside (IPTG), and cells were incubated at 16 °C for 16 hours. The cells were then harvested by centrifugation and lysed by sonication (Branson Sonifier 450) in 50 mM Tris pH 7.5. The supernatant was loaded onto an anion exchange column (26/20 POROS 60HQ, Applied Biosystems) and eluted with a linear gradient from 0 to 800 mM NaCl in 50 mM Tris pH 7.5. The fractions corresponding to monomeric frataxin were collected, concentrated, and loaded onto a Sepharcyl S100 (26/60, GE Healthcare) size exclusion column equilibrated with 50 mM HEPES, 150 mM NaCl pH 7.5. Protein concentrations for each variant were calculated using their absorbance at 280 nm with an extinction coefficient of 26030 $M^{-1}cm^{-1}$ used for all variants, except Y118A and W155A (ε =

24750 $M^{-1}cm^{-1}$ and ε = 20340 $M^{-1}cm^{-1}$, respectively).[130] The ISCU2 and NFS1-ISD11 proteins were purified as previously described and their protein concentrations determined using extinction coefficients of 10,900 $M^{-1}cm^{-1}$ (PLP) and 8250 $M^{-1}cm^{-1}$ at wavelengths of 420 nm and 280 nm, respectively.[22, 130]

Cysteine Desulfurase Activity Measurements

The number of equivalents of each FXN variant required to saturate the cysteine desulfurase activity was determined by titrating increasing amounts of each FXN variant into a standard reaction mixture, as previously described with a final volume of 800 μL.[22, 86, 107, 108, 131] Once the saturating about of each variant was determined reaction mixtures containing 0.5 μM NFS1-ISD11 (SD), 1.5 μM ISCU2, the saturating amount of FXN (or FXN variant), 10 μM pyridoxal-5'-phosphate (PLP), 2 mM dithiothreitol (DTT), 5 μM $Fe(NH_4)_2(SO_4)_2$, and 50 mM Tris, 250 mM NaCl pH 8.0 were incubated for 30 minutes in an anaerobic glovebox at ~14 °C.[22] The cysteine desulfurase reaction was initiated with the addition of 100 μM L-cysteine at 37 °C, and quenched with 100 μL each of 20 mM *N,N*-dimethyl-*p*-phenylenediamine in 7.2 N HCl and 30 mM $FeCl_3$ in 1.2 N HCl. Following 20 minute incubation at 37 °C and centrifugation for 5 minutes at 12,000 rpm, the methylene blue formation was measured at 670 nm and converted to sulfide production using a Na_2S standard curve. The rate is expressed in units of mol sulfide per mol SD per minute at 37 °C.

Michaelis-Menten Kinetics for Frataxin Variants in SDUF Complex

To a standard reaction mixture of 0.5 μM (SD), 1.5 μM ISCU2, 10 μM pyridoxal-5'-phosphate (PLP), 2 mM dithiothreitol (DTT), 5 μM $Fe(NH_4)_2(SO_4)_2$, and

50 mM Tris, 250 mM NaCl pH 8.0 was added the saturating amount of the FXN variants. [86, 131] Reactions were incubated for 30 minutes in an anaerobic glovebox before being initiated with the addition of 12.5 - 1000 μM L-cysteine. The rate of cysteine desulfurase activity was analyzed as above. The reaction rates were plotted verses L-cysteine concentration and fit with the Michaelis-Menten equation in KaleidaGraph. The k_{cat} was determined at varying FXN concentrations and used to determine the binding constant of FXN to the SDU complex using a weighted fit in Kaledagraph determined from k_{cat} error or replications. These results were fit as a type II allosteric activator using Eq. 4.1 in KaleidaGraph, where the [SDUF] is calculated as shown in Eq. 4.2. Alternatively, the rate was plotted verses [FXN] and also fit to the quadratic Eq. 4.2 and showed similar k_{cat} and K_d values.

$$k_{obs} = \frac{k_{SDU}([SDU]_{total} - [SDUF]) + k^{\infty}_{SDUF}[SDUF]}{[SDU]_{total}}$$

(Eq. 4.1)

$$[SDUF] = \frac{[SDU]_{total} + [FXN]_{total} + K_d - \sqrt{([SDU]_{total} + [FXN]_{total} + K_d)^2 - 4[SDU]_{total}[FXN]_{total}}}{2}$$

(Eq. 4.2)

Labeling of R97A FXN at Residue S202C for Fluorescence Anisotropy Measurements

Purified R97A, S202C FXN in 50 mM HEPES pH 7.5, 150 mM NaCl was aerobically combined with a 3-fold molar excess of 20 mM Texas Red® C_2 maleimide (Life Technologies) dissolved in DMSO. The labeling was allowed to proceed for approximately 3 days in a dark eppendorf tube at room temperature, and the excess fluorophore was removed by a 1 mL anion column (HiTrap™ Q HP) using 50 mM HEPES pH 7.5 for an extended wash of 50 mL before starting a linear salt gradient from 0-500 mM NaCl over a 50 mL time course. Labeled FXN elutes between 150-300 mM NaCl. The labeling efficiency of R97A FXN was estimated at 40 %, by dividing the absorbance due to the fluorophore at 596 nm (Texas Red ε_{596} = 85,000 $M^{-1}cm^{-1}$)(Life Technologies) by the absorbance at 280 nm due to FXN (native FXN ε_{280} = 26,030 $M^{-1}cm^{-1}$) and confirmed by a Bradford assay. 10 nM of labeled native FXN (FXN_{TX}) was anaerobically combined with 20 µM ISCU2 in buffer A and varied concentration of SD from a 30 µM stock solution of NFS1-ISD11 (SD), and 2 mM DTT to a total volume of 0.4 mL in a 1 mL anaerobic cuvette, and the cuvette was sealed and parafilmed. Each sample was prepared separately in an anaerobic glovebox, to keep the FXN concentration constant and centrifuged for 20 min. The fluorescence spectra was measured with a Fluoromax4 fluorimeter (Horiba Jovin-Yvon) at 16 °C. Fluorescence was measured using an excitation wavelength of 587 nm, an emission wavelength of 618 nm, a signal integration time of 30 s for 300 s, and slit width of 10 nm.

Results

Residues of the β-sheet Impair Interactions with the Fe-S Cluster Assembly Complex

A total of 39 alanine or glycine (used for proline residues) point variants were expressed in *E. coli* and purified to >95% homogeneity. During the protein purification process the Δ1-55 FXN construct spontaneously truncated to produce the mature (FXN^{81-210}) form of the protein. [132] The number of equivalents necessary to saturate the cysteine desulfurase activity for each variant was determined by maximum activity that no longer increases with the addition of more FXN variants. Michaelis-Menten parameters for all of the alanine scanning variants were determined (Table 4.1). The Michaelis-Menten parameters k_{cat} and K_M were determined, using the cysteine desulfurase activity at saturating FXN variant levels. The binding constants for all alanine scanning variants were determined by plotting the k_{cat} verses FXN variant concentration or NFS1 activity verses FXN variant and fitting the data with Eq. 4.2. The k_{cat} varied depending on batch on NFS1 and activity of that batch, the relative activity was used to standardize each batch for comparison of the different variants. The Log(activity) verse Log (K_d) was used to determine which variants affected activity and which affected binding (Figure 4.1A). Most of the variants were similar to wild type FXN or exhibited weaker binding as shown in orange (100 fold weaker binding than wild type) and red (1000 fold weaker binding than wild type). The red variants W155A and R165A and blue Q153A were significantly weaker binding than all other variants, which were modeled on Figure 4.1B to show a hotspot. In blue, Q148 and Q153A were

both affected weaker binding and were only variants that had a significant decrease in activity.

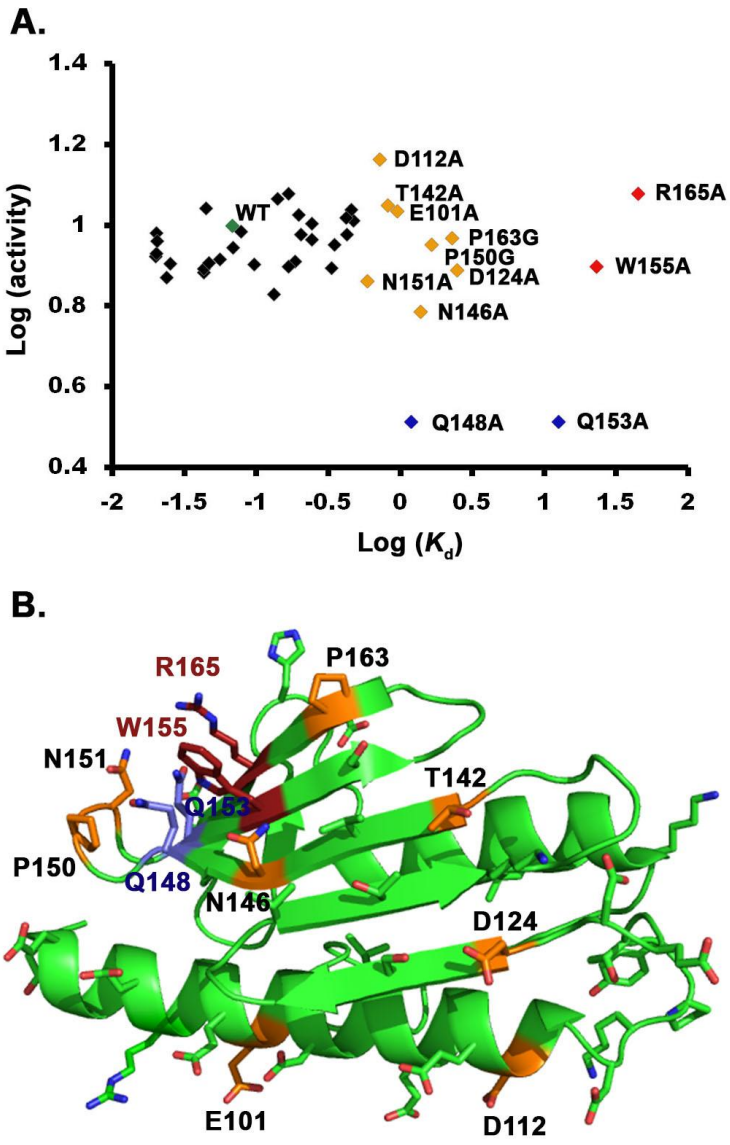

Figure 4.1. (A) The Log (activity) vs. Log (K_d). The variants that are severely affected in binding are colored in red, and modestly affected in binding colored in orange. In blue both activity and binding were affected. The wild type is in green. (B) Using PDB code: 1EKG all the mutants that were made are represented as sticks and were color coded according to (A).

Table 4.1. Kinetic Parameters for SDU with FXN Alanine Scanning Variants

Protein	Activity (min^{-1})	K_m^{Cys} (mM)	k_{cat}/K_m (M^{-1} s^{-1})	K_d (μM)
SDUF*	10.0	0.018	8981	0.09 ± 0.03
H86A*	7.7	0.015	12311	0.04 ± 0.01
D91A*	9.6	0.017	13614	0.02 ± 0.02
E92A*	11.7	0.018	15392	0.14 ± 0.04
E96A*	10.3	0.019	13019	0.47 ± 0.07
R97A*	10.1	0.018	15000	0.24 ± 0.07
E100A*	8.4	0.014	8322	0.02 ± 0.01
E101A*	10.9	0.025	7158	0.94 ± 0.12
D104A*	10.9	0.026	6850	0.45 ± 0.06
S105A	8.1	0.019	6013	0.02 ± 0.01
L106A	9.5	0.020	6740	0.20 ± 0.06
E108A*	9.0	0.020	7176	0.34 ± 0.04
E111A*	9.3	0.017	7558	0.24 ± 0.05
D112A*	14.6	0.030	7905	0.71 ± 0.10
D115A	10.6	0.019	9057	0.20 ± 0.04
K116A	11.1	0.032	4892	0.04 ± 0.03
P117G	8.0	0.020	5690	0.10 ± 0.03
Y118A	8.8	0.028	4468	0.07 ± 0.03
T119A	9.7	0.021	6534	0.08 ± 0.03
E121A*	8.3	0.010	11722	0.06 ± 0.03
D122A*	7.8	0.015	7392	0.04 ± 0.02
D124A*	7.8	0.016	7887	2.44 ± 0.20
S126A	8.6	0.021	5768	0.02 ± 0.03
V131A	6.8	0.023	4746	0.13 ± 0.03
T133A	9.5	0.021	7325	0.42 ± 0.10
K135A	8.1	0.021	5448	0.05 ± 0.03
T142A	11.3	0.026	6134	0.81 ± 0.19
V144A	8.1	0.021	6270	0.18 ± 0.05
N146A	6.1	0.019	5213	1.37 ± 0.18
Q148A*	3.3	0.012	7277	1.17 ± 0.58
P150G	9.0	0.014	10384	1.62 ± 0.22
N151A	7.3	0.027	4367	0.58 ± 0.08
Q153A*	3.3	0.014	6231	12.45 ± 4.62
W155A*	7.9	0.012	17639	22.72 ± 2.38

Table 4.1. Kinetic Parameters for SDU with FXN Alanine Scanning Variants Continued

Protein	Activity (min^{-1})	K_m^{Cys} (mM)	k_{cat}/K_m (M^{-1} s^{-1})	K_d (μM)
S157A	7.9	0.018	7071	0.33 ± 0.05
P163G	9.3	0.018	8379	2.27 ± 0.23
R165A	12.0	0.020	9708	44.28 ± 6.21
D167A	7.9	0.020	6407	0.16 ± 0.04
H177A	7.4	0.020	6017	0.02 ± 0.01
D178A	10.5	0.025	5937	0.41 ± 0.11
L190A	12.0	0.026	6542	0.17 ± 0.06
K195A	9.1	0.025	5184	0.02 ± 0.02

* Indicates the experiment was performed by Nicholas Fox

Discussion

Protein-protein interactions between FXN and the SDU complex have been demonstrated in the yeast, *E. coli*, and human systems; where interactions with ISCU and NFS1-ISD11 are proposed to occur through the FXN β-sheet and α_1-helix, respectively. [22, 80, 86, 124-126, 129, 131, 133] However, only limited information is known about the specific residues of interaction and the kinetic implications of these interactions. While attempts have been made to identify residues involved in the FXN/SDU interaction through loss of SDU pull-down or NMR amide backbone perturbation analysis, to our knowledge this is the first attempt to assess the functional importance of individual FXN residues to map the surface of interaction using the SDU complex *in vitro*.

Examination of the kinetic parameters of the 39 FXN variants suggests a hotspot for FXN interaction with SDU through the β sheet. Combination of alanine scanning with functional assessment through the cysteine desulfurase assay, identified 12 residues

of the FXN α_1 helix and β-sheet with significantly to moderate decrease in SDU binding and of those 12, 2 residues significantly affectedthe ability for FXN to activate NFS1. Drastic binding defects were observed upon mutation of the FXN residues Q153, W155, and R165 to alanine, while moderate impairment was seen for nine FXN residues (E101, D112, D124, T142, N146, Q148, P150, N151, and P163) of the α_1 helix and β-sheet regions (Figure 4.1, Table 4.1). Significant activation defects of the SDU complex were found upon mutation of two residues (Q148 and Q153) of the FXN β-sheet (Figure 4.1, Table 4.1). Impairment of the binding and/or activation of the FXN residues N146, Q148, Q153, W155, and R165 is consistent with previous findings by Barondeau *et al.*[86, 122] Furthermore pull-down assays in the yeast and human system support the findings that W155 and N146 are important for SDU interaction. [80, 125, 126] The NMR studies of Stemmler *et al*, showing perturbation of FXN residues Q148 and N151 in the presence of Isu1 support the role of these amino acids in SDU interactions.[129] Additionally the presence of FRDA clinical mutants at residues L106, N146, Q148, W155, and R165 provides further support for the importance of these residues in the proper *in vivo* function of FXN.[88] While disruption of the protein secondary structure cannot be ruled out as a factor for the kinetic defects of the P150G and P163G variants, lack of such effects with the other proline residue (P117) suggests that these β-sheet residues play a role in the binding or activation of SDU. Despite the presence of modest binding or activation defects of the acidic patch residues on α1, the level of impairment is significantly lower than expected for mutation of the iron binding site of an iron donor

protein; thus further supporting the allosteric activator role of FXN previously proposed by Barondeau *et al.* [22]

This improved understanding of FXN/SDU interactions must be considered in the development of new treatments for FRDA. Identification of the localized binding and activation hotspot on the β-sheet of FXN (residues N146, Q148, N151, Q153, W155, and R165), suggests that future drug design should be targeted to this region of the protein. We believe this to be a region that interacts with ISCU2 and residues E101 and D112 on the acidic path would interact with NFS1. In addition to the use of commercially available small molecule screening kits, the design of small cyclic peptides should be used to target the FXN hotspot. Since W155 and R165 appear to be the most important residues for binding SDU, and Q148 and Q153 are most important for activation, these residues should be included in cyclic peptide design. Finally this bank of FXN alanine scanning variants should also be applied to elucidating the FXN residues involved in interactions with the cluster transfer proteins.

Conclusion

FXN has been linked to the neurodegenerative disease Friedreich's ataxia (FRDA), which is the primary focus of current therapeutic efforts. Mutagenesis experiments were designed in which the FXN surface residues were replaced with alanine or glycine (proline residues) and the resulting variants were tested in binding and activity assays. These experiments revealed a localized hotspot, which included residues Q153, W155, and R165 that appear to be the most affected in binding and Q148 and Q153, which were severely affected in activity. This hotspot contains residues that are

all linked to FRDA and discovering the nature of the residues on the surface of FXN could aid in designing small peptide mimics for FRDA therapeutics.

CHAPTER V

CONCLUSION

In summary, we provide data that support a role for human FXN in accelerating the PLP-based chemistry of the cysteine desulfurase NFS1 and also in the interprotein sulfur transfer between NFS1 and scaffold protein ISCU2. Using enzyme kinetic studies and radiolabeled substrate, we have determined the catalytic cysteine on NFS1, generates a persulfide that is directly transferred to C104 on ISCU2. C104 is buried on an α-helix, so we believe this persulfide transfer event must be coupled to a helix-to-coil transition in order to expose C104 on ISCU2 to accept the persulfide sulfur. Additionally, evidence has been provided that the persulfide species transferred from NFS1 to ISCU2 is viable in Fe-S cluster assembly and can be transferred to apo ferredoxin. These studies are consistent with the mechanism of Fe-S cluster biosynthesis being sulfur first; ISCU2 can accept the persulfide sulfur in the absence of iron, following a transfer of persulfide from C104 to other cysteine residues on ISCU2, then ferrous iron can bind, and lastly, the sequential 2-electron reduction of each sulfane sulfur atom is required to complete cluster formation.

To further study the mechanism for Fe-S cluster biosynthesis, we designed experiments to determine the type of cluster the SDUF complex could synthesize. This became a challenging project due to the $Fe^{2+/3+}$ and S^{2-} easily interacting in solution causing an Fe-S mineralization. This effect can cause proteins to aggregate with this Fe-S mineralization resulting in a High Molecular Weight Species (HMWS) associated with

he complex that could also transfer to an apo target. This species can act as a chemical reconstitution for apo targets. We discovered through the use of gel filtration, CD, UV-Vis kinetics, and Mössbauer that the complex could synthesize a [2Fe-2S] that was rapidly transferred from the complex to free ISCU2 or small molecule thiols. Fundamentally, in order to study the mechanism for Fe-S cluster assembly we need to be careful in studying an enzymatic reconstitution versus a chemical reconstitution. Future experiments need to introduce the natural reductant of ferredoxin, ferredoxin reductase, and NADH, and other components like the iron donor and chaperones.

FXN has been linked to the neurodegenerative disease Friedreich's ataxia (FRDA), which is the primary focus of current therapeutic efforts. Our group designed mutagenesis experiments in which the FXN surface residues were replaced with alanine or glycine (proline) and the resulting variants were tested in binding and activity assays. These experiments revealed a localized hotspot, which included residues Q153, W155, and R165 that appear to be the most affected in binding and Q148 and Q153, which were affected in activity. This hotspot contains residues that are all linked to FRDA and discovering the nature of the residues on the surface of FXN could aid in designing small peptide mimics for FRDA therapeutics. These *in vitro* results suggest FXN may have a physiological function as a regulator and that FXN levels control Fe-S cluster assembly. Such a function would be consistent with the generally accepted role for FXN in Fe-S cluster assembly and explain the loss of Fe-S enzyme activity phenotype upon FXN depletion. Future experiments will focus on testing and expanding upon this model with the ultimate goal of developing new strategies to treat FRDA.

REFERENCES

[1] Johnson, D. C., Dean, D. R., Smith, A. D., and Johnson, M. (2005) Structure, function, and formation of biological iron-sulfur clusters, *Annu Rev Biochem 74*, 247-281.

[2] Lill, R., and Muhlenhoff, U. (2006) Iron-sulfur protein biogenesis in eukaryotes: components and mechanisms, *Annu Rev Cell Dev Biol 22*, 457-486.

[3] Beinert, H., Holm, R. H., and Münck, E. (1997) Iron-sulfur clusters: nature's modular, multipurpose structures, *Science 277*, 653-659.

[4] Rao, P. V., and Holm, R. H. (2004) Synthetic analogues of the active sites of iron-sulfur proteins, *Chemical Reviews 104*, 527-559.

[5] Lill, R. (2009) Function and biogenesis of iron-sulphur proteins, *Nature 460*, 831-838.

[6] Pierik, A. J., Netz, D. J. A., and Lill, R. (2009) Analysis of iron-sulfur protein maturation in eukaryotes, *Nat Protoc 4*, 753-766.

[7] Lill, R., and Mühlenhoff, U. (2008) Maturation of iron-sulfur proteins in eukaryotes: mechanisms, connected processes, and diseases, *Annu Rev Biochem 77*, 22.21-22.32.

[8] Holmes-Hampton, G. P., Miao, R., Garber Morales, J., Guo, Y., Munck, E., and Lindahl, P. A. (2010) A nonheme high-spin ferrous pool in mitochondria isolated from fermenting Saccharomyces cerevisiae, *Biochemistry 49*, 4227-4234.

[9] Frazzon, J., and Dean, D. R. (2003) Formation of iron-sulfur clusters in bacteria: an emerging field in bioinorganic chemistry, *Curr Opin Chem Biol 7*, 166-173.

[10] Johnson, D. C., Dean, D. R., Smith, A. D., and Johnson, M. K. (2005) Structure, function, and formation of biological iron-sulfur clusters, *Annu Rev Biochem 74*, 247-281.

[11] Frazzon, J., and Dean, D. R. (2002) Biosynthesis of the nitrogenase iron-molybdenum-cofactor from Azotobacter vinelandii, *Met Ions Biol Syst 39*, 163-186.

[12] Rees, D. C., and Howard, J. B. (2000) Nitrogenase: standing at the crossroads, *Curr Opin Chem Biol 4*, 559-566.

[13] Takahashi, Y., and Tokumoto, U. (2002) A third bacterial system for the assembly of iron-sulfur clusters with homologs in archaea and plastids, *J Biol Chem 277*, 28380-28383.

[14] Zheng, L., Cash, V. L., Flint, D. H., and Dean, D. R. (1998) Assembly of iron-sulfur clusters. Identification of an iscSUA-hscBA-fdx gene cluster from Azotobacter vinelandii, *J Biol Chem 273*, 13264-13272.

[15] Lill, R., and Kispal, G. (2000) Maturation of cellular Fe-S proteins: an essential function of mitochondria, *Trends Biochem Sci 25*, 352-356.

[16] Sheftel, A. D., and Lill, R. (2009) The power plant of the cell is also a smithy: the emerging role of mitochondria in cellular iron homeostasis, *Ann Med 41*, 82-99.

[17] Tsai, C., and Barondeau, D. P. (2010) Human frataxin is an allosteric switch that activates the Fe-S cluster biosynthetic complex, *Biochemistry 49*, 9132-9139.

[18] Ayala-Castro, C., Saini, A., and Outten, F. W. (2008) Fe-S cluster assembly pathways in bacteria, *Microbiol Mol Biol Rev 72*, 110-125, table of contents.

[19] Bulteau, A.-L., O'Neill, H. A., Kennedy, M. C., Ikeda-Saito, M., Isaya, G., and Szweda, L. I. (2004) Frataxin acts as an iron chaperone protein to modulate mitochondrial aconitase activity, *Science 305*, 242-245.

[20] Yoon, T., and Cowan, J. A. (2003) Iron-sulfur cluster biosynthesis. Characterization of frataxin as an iron donor for assembly of [2Fe-2S] clusters in ISU-type proteins, *J Am Chem Soc 125*, 6078-6084.

[21] Ding, H., Yang, J., Coleman, L. C., and Yeung, S. (2007) Distinct iron binding property of two putative iron donors for the iron-sulfur cluster assembly: IscA and the bacterial frataxin ortholog CyaY under physiological and oxidative stress conditions, *J Biol Chem 282*, 7997-8004.

[22] Tsai, C. L., and Barondeau, D. P. (2010) Human frataxin is an allosteric switch that activates the Fe-S cluster biosynthetic complex, *Biochemistry 49*, 9132-9139.

[23] Adinolfi, S., Iannuzzi, C., Prischi, F., Pastore, C., Iametti, S., Martin, S., Bonomi, F., and Pastore, A. (2009) Bacterial frataxin CyaY is the gatekeeper of iron-sulfur cluster formation catalyzed by IscS, *Nat Struct Mol Biol 16*, 390-396.

[24] Bridwell-Rabb, J., Iannuzzi, C., Pastore, A., and Barondeau, D. P. (2012) Effector role reversal during evolution: the case of frataxin in Fe-S cluster biosynthesis, *Biochemistry 51*, 2506-2514.

[25] Zheng, L., White, R. H., Cash, V. L., and Dean, D. R. (1994) Mechanism for the desulfurization of L-cysteine catalyzed by the nifS gene product, *Biochemistry 33*, 4714-4720.

[26] Behshad, E., and Bollinger, J. (2009) Kinetic analysis of cysteine desulfurase CD0387 from *Synechocystis* sp PCC 6803: formation of the persulfide intermediate, *Biochemistry 48*, 12014-12023.

[27] Behshad, E., Parkin, S. E., and Bollinger, J. M. (2004) Mechanism of cysteine desulfurase Slr0387 from Synechocystis sp. PCC 6803: kinetic analysis of cleavage of the persulfide intermediate by chemical reductants, *Biochemistry 43*, 12220-12226.

[28] Richards, T. A., and van der Giezen, M. (2006) Evolution of the Isd11-IscS complex reveals a single alpha-proteobacterial endosymbiosis for all eukaryotes, *Mol Biol Evol 23*, 1341-1344.

[29] Adam, A. C., Bornhövd, C., Prokisch, H., Neupert, W., and Hell, K. (2006) The Nfs1 interacting protein Isd11 has an essential role in Fe/S cluster biogenesis in mitochondria, *Embo J 25*, 174-183.

[30] Wiedemann, N., Urzica, E., Guiard, B., Müller, H., Lohaus, C., Meyer, H. E., Ryan, M. T., Meisinger, C., Muhlenhoff, U., Lill, R., and Pfanner, N. (2006) Essential role of Isd11 in mitochondrial iron-sulfur cluster synthesis on Isu scaffold proteins, *Embo J 25*, 184-195.

[31] Shan, Y., Napoli, E., and Cortopassi, G. A. (2007) Mitochondrial frataxin interacts with ISD11 of the NFS1/ISCU complex and multiple mitochondrial chaperones, *Hum Mol Genet 16*, 929-941.

[32] Shi, Y., Ghosh, M., Tong, W.-H., and Rouault, T. A. (2009) Human ISD11 is essential for both iron-sulfur cluster assembly and maintenance of normal cellular iron homeostasis, *Hum Mol Genet 18*, 3014-3025.

[33] Shi, Y., Ghosh, M., Kovtunovych, G., Crooks, D. R., and Rouault, T. A. (2011) Both human ferredoxins 1 and 2 and ferredoxin reductase are important for iron-sulfur cluster biogenesis, *Biochim Biophys Acta 1823*, 484-492.

[34] Sheftel, A. D., Stehling, O., Pierik, A. J., Elsässer, H.-P., Mühlenhoff, U., Webert, H., Hobler, A., Hannemann, F., Bernhardt, R., and Lill, R. (2010) Humans possess two mitochondrial ferredoxins, Fdx1 and Fdx2, with distinct roles in steroidogenesis, heme, and Fe/S cluster biosynthesis, *Proc Natl Acad Sci USA 107*, 11775-11780.

[35] Uzarska, M. A., Dutkiewicz, R., Freibert, S. A., Lill, R., and Muehlenhoff, U. (2013) The mitochondrial Hsp70 chaperone Ssq1 facilitates Fe/S cluster transfer from Isu1 to Grx5 by complex formation, *Molecular Biology of the Cell 24*, 1830-1841.

[36] Chandramouli, K., and Johnson, M. (2006) HscA and HscB stimulate [2Fe-2S] cluster transfer from IscU to apoferredoxin in an ATP-dependent reaction, *Biochemistry 45*, 11087-11095.

[37] Layer, G., Ollagnier de Choudens, S., Sanakis, Y., and Fontecave, M. (2006) Iron-sulfur cluster biosynthesis: characterization of Escherichia coli CyaY as an iron donor for the assembly of [2Fe-2S] clusters in the scaffold IscU, *J Biol Chem 281*, 16256-16263.

[38] Fontecave, M., Choudens, S. O. d., Py, B., and Barras, F. (2005) Mechanisms of iron-sulfur cluster assembly: the SUF machinery, *J Biol Inorg Chem 10*, 713-721.

[39] Ollagnier de Choudens, S., Mattioli, T., Takahashi, Y., and Fontecave, M. (2001) Iron-sulfur cluster assembly: characterization of IscA and evidence for a specific and functional complex with ferredoxin, *J Biol Chem 276*, 22604-22607.

[40] Mansy, S. S., Wu, G., Surerus, K. K., and Cowan, J. A. (2002) Iron-sulfur cluster biosynthesis. Thermatoga maritima IscU is a structured iron-sulfur cluster assembly protein, *J Biol Chem 277*, 21397-21404.

[41] Bencze, K. Z., Yoon, T., Millán-Pacheco, C., Bradley, P. B., Pastor, N., Cowan, J. A., and Stemmler, T. (2007) Human frataxin: iron and ferrochelatase binding surface, *Chem Commun (Camb) 14*, 1798-1800.

[42] Urbina, H. D., Silberg, J. J., Hoff, K. G., and Vickery, L. (2001) Transfer of sulfur from IscS to IscU during Fe/S cluster assembly, *J Biol Chem 276*, 44521-44526.

[43] Smith, A. D., Agar, J., Johnson, K. A., Frazzon, J., Amster, I. J., Dean, D. R., and Johnson, M. (2001) Sulfur transfer from IscS to IscU: the first step in iron-sulfur cluster biosynthesis, *J Am Chem Soc 123*, 11103-11104.

[44] Bonomi, F., Iametti, S., Morleo, A., Ta, D., and Vickery, L. E. (2011) Facilitated transfer of IscU-[2Fe2S] clusters by chaperone-mediated ligand exchange, *Biochemistry 50*, 9641-9650.

[45] Colin, F., Martelli, A., Clemancey, M., Latour, J. M., Gambarelli, S., Zeppieri, L., Birck, C., Page, A., Puccio, H., and de Choudens, S. O. (2013) Mammalian frataxin controls sulfur production and iron entry during de Novo Fe4S4 cluster assembly, *J Am Chem Soc 135*, 733-740.

[46] Huang, J., and Cowan, J. A. (2009) Iron-sulfur cluster biosynthesis: role of a semi-conserved histidine, *Chem Commun (Camb) 21*, 3071-3073.

[47] Shimomura, Y., Wada, K., Fukuyama, K., and Takahashi, Y. (2008) The asymmetric trimeric architecture of [2Fe-2S] IscU: implications for Its scaffolding during iron-sulfur cluster biosynthesis, *J Mol Biol 383*, 133-144.

[48] Agar, J., Krebs, C., Frazzon, J., Huynh, B. H., Dean, D. R., and Johnson, M. (2000) IscU as a scaffold for iron-sulfur cluster biosynthesis: sequential assembly of [2Fe-2S] and [4Fe-4S] clusters in IscU, *Biochemistry 39*, 7856-7862.

[49] Marinoni, E. N., de Oliveira, J. S., Nicolet, Y., Raulfs, E. C., Amara, P., Dean, D. R., and Fontecilla-Camps, J. C. (2012) (IscS-IscU)2 complex structures provide insights into Fe2S2 biogenesis and transfer, *Angew Chem Int Edit 51*, 5439-5442.

[50] Smith, A. D., Frazzon, J., Dean, D. R., and Johnson, M. (2005) Role of conserved cysteines in mediating sulfur transfer from IscS to IscU, *FEBS Lett 579*, 5236-5240.

[51] Zhang, B., Crack, J. C., Subramanian, S., Green, J., Thomson, A. J., Le Brun, N. E., and Johnson, M. K. (2012) Reversible cycling between cysteine persulfide-ligated [2Fe-2S] and cysteine-ligated [4Fe-4S] clusters in the FNR regulatory protein, *Proc Natl Acad Sci 109*, 15734-15739.

[52] Agar, J., Zheng, L., Cash, V. L., Dean, D. R., and Johnson, M. K. (2000) Role of the IscU protein in iron-sulfur cluster biosynthesis: IscS-mediated assembly of a [Fe2S2] cluster in IscU, *J Am Chem Soc 122*, 2136-2137.

[53] Foster, M. W., Mansy, S. S., Hwang, J., Penner-Hahn, J. E., Surerus, K. K., and Cowan, J. A. (2000) A Mutant Human IscU Protein Contains a Stable [2Fe2S]2+ Center of Possible Functional Significance, *J Am Chem Soc 122*, 6805-6806.

[54] Shimomura, Y., Wada, K., Fukuyama, K., and Takahashi, Y. (2008) The Asymmetric Trimeric Architecture of [2Fe-2S] IscU: Implications for Its Scaffolding during Iron-Sulfur Cluster Biosynthesis, *J Mol Biol 383*, 133-143.

[55] Kim, J., Fuzery, A., Tonelli, M., Ta, D., Westler, W., Vickery, L., and Markley, J. (2009) Structure and dynamics of the iron-sulfur custer assembly scaffold protein IscU and its interaction with the cochaperone HscB, *Biochemistry 48*, 6062-6071.

[56] Marinoni, E. N., de Oliveira, J. S., Nicolet, Y., Raulfs, E. C., Amara, P., Dean, D. R., and Fontecilla-Camps, J. C. (2012) (IscS-IscU)2 complex structures provide insights into Fe2S2 biogenesis and transfer, *Angew Chem Int Ed Engl 51*, 5439-5442.

[57] Agar, J. N., Krebs, C., Frazzon, J., Huynh, B. H., Dean, D. R., and Johnson, M. K. (2000) IscU as a scaffold for iron-sulfur cluster biosynthesis: sequential assembly of [2Fe-2S] and [4Fe-4S] clusters in IscU, *Biochemistry 39*, 7856-7862.

[58] Kato, S.-I., Mihara, H., Kurihara, T., Takahashi, Y., Tokumoto, U., Yoshimura, T., and Esaki, N. (2002) Cys-328 of IscS and Cys-63 of IscU are the sites of disulfide bridge formation in a covalently bound IscS/IscU complex: implications for the mechanism of iron-sulfur cluster assembly, *Proc Natl Acad Sci USA 99*, 5948-5952.

[59] Shi, R., Proteau, A., Villarroya, M., Moukadiri, I., Zhang, L., Trempe, J.-F., Matte, A., Armengod, M. E., and Cygler, M. (2010) Structural basis for Fe-S cluster assembly and tRNA thiolation mediated by IscS protein-protein interactions, *PLoS Biol 8*, 1-18.

[60] Shimomura, Kamikubo, Nishi, Masako, Kataoka, Kobayashi, Fukuyama, K., and Takahashi, Y. (2007) Characterization and crystallization of an IscU-type scaffold protein with bound [2Fe-2S] cluster from the hyperthermophile, aquifex aeolicus, *J Biochem 142*, 577-586.

[61] Wu, S.-p., Wu, G., Surerus, K. K., and Cowan, J. A. (2002) Iron-sulfur cluster biosynthesis. Kinetic analysis of [2Fe-2S] cluster transfer from holo ISU to apo Fd: role of redox chemistry and a conserved aspartate, *Biochemistry 41*, 8876-8885.

[62] Colin, F., Martelli, A., Clemancey, M., Latour, J. M., Gambarelli, S., Zeppieri, L., Birck, C., Page, A., Puccio, H., and Ollagnier de Choudens, S. (2013) Mammalian frataxin controls sulfur production and iron entry during de novo Fe(4)S(4) cluster assembly, *J Am Chem Soc 135*, 733-740.

[63] Iannuzzi, C., Adinolfi, S., Howes, B. D., Garcia-Serres, R., Clémancey, M., Latour, J.-M., Smulevich, G., and Pastore, A. (2011) The role of CyaY in iron sulfur cluster assembly on the E. coli IscU scaffold protein, *PLoS ONE 6*, 1-9.

[64] Smith, A. D., Jameson, G. N. L., Dos Santos, P. C., Agar, J., Naik, S., Krebs, C., Frazzon, J., Dean, D. R., Huynh, B. H., and Johnson, M. (2005) NifS-mediated assembly of [4Fe-4S] clusters in the N- and C-terminal domains of the NifU scaffold protein, *Biochemistry 44*, 12955-12969.

[65] Lawrence, N. S., Davis, J., Jiang, L., Jones, T. G. J., Davies, S. N., and Compton, R. G. (2000) The electrochemical analog of the methylene blue reaction: A novel amperometric approach to the detection of hydrogen sulfide, *Electroanal 12*, 1453-1460.

[66] Yoon, T., and Cowan, J. A. (2003) Iron-sulfur cluster biosynthesis. Characterization of frataxin as an iron donor for assembly of [2Fe-2S] clusters in ISU-type proteins, *J Am Chem Soc 125*, 6078-6084.

[67] Cook, J. D., Bencze, K. Z., Jankovic, A. D., Crater, A. K., Busch, C. N., Bradley, P. B., Stemmler, A. J., Spaller, M. R., and Stemmler, T. (2006) Monomeric yeast frataxin is an iron-binding protein, *Biochemistry 45*, 7767-7777.

[68] Cupp-Vickery, J. R., Urbina, H., and Vickery, L. E. (2003) Crystal structure of IscS, a cysteine desulfurase from Escherichia coli, *Journal of Molecular Biology 330*, 1049-1059.

[69] Shi, R., Proteau, A., Villarroya, M., Moukadiri, I., Zhang, L. H., Trempe, J. F., Matte, A., Armengod, M. E., and Cygler, M. (2010) Structural basis for Fe-S cluster assembly and tRNA thiolation mediated by IscS protein-protein interactions, *PLoS Biol 8*, 1-18.

[70] Cho, S. J., Lee, M. G., Yang, J. K., Lee, J. Y., Song, H. K., and Suh, S. W. (2000) Crystal structure of Escherichia coli CyaY protein reveals a previously unidentified fold for the evolutionarily conserved frataxin family, *Proc Natl Acad Sci USA 97*, 8932-8937.

[71] Dhe-Paganon, S., Shigeta, R., Chi, Y. I., Ristow, M., and Shoelson, S. E. (2000) Crystal structure of human frataxin, *Journal of Biological Chemistry 275*, 30753-30756.

[72] Rouault, T. A., and Tong, W. H. (2008) Iron-sulfur cluster biogenesis and human disease, *Trends Genet 24*, 398-407.

[73] Puccio, H., and Koenig, M. (2002) Friedreich ataxia: a paradigm for mitochondrial diseases, *Curr Opin Genet Dev 12*, 272-277.

[74] Ott, M., Gogvadze, V., Orrenius, S., and Zhivotovsky, B. (2007) Mitochondria, oxidative stress and cell death, *Apoptosis 12*, 913-922.

[75] Dimauro, S., and Davidzon, G. (2005) Mitochondrial DNA and disease, *Annals of Medicine 37*, 222-232.

[76] Kessler, D. (2006) Enzymatic activation of sulfur for incorporation into biomolecules in prokaryotes, *FEMS Microbiol Rev 30*, 825-840.

[77] Mueller, E. G. (2006) Trafficking in persulfides: delivering sulfur in biosynthetic pathways, *Nat Chem Biol 2*, 185-194.

[78] Cupp-Vickery, J., Urbina, H. D., and Vickery, L. (2003) Crystal structure of IscS, a cysteine desulfurase from Escherichia coli, *J Mol Biol 330*, 1049-1059.

[79] Bonomi, F., Iametti, S., Morleo, A., Ta, D. T., and Vickery, L. E. (2011) Facilitated transfer of IscU-[2Fe2S] clusters by chaperone-mediated ligand exchange, *Biochemistry 50*, 9641-9650.

[80] Schmucker, S., Martelli, A., Colin, F., Page, A., Wattenhofer-Donzé, M., Reutenauer, L., and Puccio, H. (2011) Mammalian frataxin: An essential function for cellular viability through an interaction with a preformed ISCU/NFS1/ISD11 iron-sulfur assembly complex, *PLoS ONE 6*, 1-12.

[81] Zheng, L., White, R. H., Cash, V. L., Jack, R. F., and Dean, D. R. (1993) Cysteine desulfurase activity indicates a role for NIFS in metallocluster biosynthesis, *Proc Natl Acad Sci USA 90*, 2754-2758.

[82] Shan, Y., Napoli, E., and Cortopassi, G. (2007) Mitochondrial frataxin interacts with ISD11 of the NFS1/ISCU complex and multiple mitochondrial chaperones, *Hum Mol Genet 16*, 929-941.

[83] Shi, Y., Ghosh, M., Tong, W. H., and Rouault, T. A. (2009) Human ISD11 is essential for both iron-sulfur cluster assembly and maintenance of normal cellular iron homeostasis, *Hum Mol Genet 18*, 3014-3025.

[84] Pandey, A., Golla, R., Yoon, H., Dancis, A., and Pain, D. (2012) Persulfide formation on mitochondrial cysteine desulfurase: enzyme activation by a eukaryote-specific interacting protein and Fe-S cluster synthesis, *Biochemistry 448*, 171-187.

[85] Pandey, A., Yoon, H., Lyver, E. R., Dancis, A., and Pain, D. (2012) Identification of a Nfs1p-bound persulfide intermediate in Fe-S cluster synthesis by intact mitochondria, *Mitochondrion 12*, 539-549.

[86] Tsai, C. L., Bridwell-Rabb, J., and Barondeau, D. P. (2011) Friedreich's ataxia variants I154F and W155R diminish frataxin-based activation of the iron-sulfur cluster assembly ccomplex, *Biochemistry 50*, 6478-6487.

[87] Bridwell-Rabb, J., Winn, A. M., and Barondeau, D. P. (2011) Structure-function analysis of Friedreich’s ataxia mutants reveals determinants for frataxin binding and activation of the Fe-S assembly complex, *Biochemistry 50*, 7265-7274.

[88] Campuzano, V., Montermini, L., Moltè, M. D., Pianese, L., Cossee, M., Cavalcanti, F., Monros, E., Rodius, F., Duclos, F., Monticelli, A., Zara, F., Cañizares, J., Koutnikova, H., Bidichandani, S. I., Gellera, C., Brice, A., Trouillas, P., De Michele, G., Filla, A., De Frutos, R., Palau, F., Patel, P. I., Di Donato, S.,

Mandel, J. L., Cocozza, S., Koenig, M., and Pandolfo, M. (1996) Friedreich's ataxia: autosomal recessive disease caused by an intronic GAA triplet repeat expansion, *Science 271*, 1423-1427.

[89] Lane, D. J. R., and Richardson, D. R. (2010) Frataxin, a molecule of mystery: trading stability for function in its iron-binding site, *Biochemistry 426*, e1-3.

[90] Xia, B., Cheng, H., Bandarian, V., Reed, G. H., and Markley, J. L. (1996) Human ferredoxin: overproduction in Escherichia coli, reconstitution in vitro, and spectroscopic studies of iron-sulfur cluster ligand cysteine-to-serine mutants, *Biochemistry 35*, 9488-9495.

[91] Bonomi, F., Iametti, S., Ta, D. T., and Vickery, L. (2005) Multiple turnover transfer of [2Fe2S] clusters by the iron-sulfur cluster assembly scaffold proteins IscU and IscA, *J Biol Chem 280*, 29513-29518.

[92] Flint, D. H. (1996) Escherichia coli contains a protein that is homologous in function and N-terminal sequence to the protein encoded by the nifS gene of Azotobacter vinelandii and that can participate in the synthesis of the Fe-S cluster of dihydroxy-acid dehydratase, *J Biol Chem 271*, 16068-16074.

[93] Liu, J., Oganesyan, N., Shin, D.-H., Jancarik, J., Yokota, H., Kim, R., and Kim, S.-H. (2005) Structural characterization of an iron-sulfur cluster assembly protein IscU in a zinc-bound form, *Proteins 59*, 875-881.

[94] Ramelot, T. A., Cort, J. R., Goldsmith-Fischman, S., Kornhaber, G. J., Xiao, R., Shastry, R., Acton, T. B., Honig, B., Montelione, G. T., and Kennedy, M. A. (2004) Solution NMR structure of the iron-sulfur cluster assembly protein U (IscU) with zinc bound at the active site, *J Mol Biol 344*, 567-583.

[95] Pandey, A., Gordon, D. M., Pain, J., Stemmler, T. L., Dancis, A., and Pain, D. (2013) Frataxin directly stimulates mitochondrial cysteine desulfurase by exposing substrate-binding sites, and a mutant Fe-S cluster scaffold protein with frataxin-bypassing ability acts similarly, *J Biol Chem 288*, 36773-36786.

[96] Kim, J. H., Tonelli, M., and Markley, J. L. (2012) Disordered form of the scaffold protein IscU is the substrate for iron-sulfur cluster assembly on cysteine desulfurase, *Proc Natl Acad Sci U S A 109*, 454-459.

[97] Dai, Z., Tonelli, M., and Markley, J. L. (2012) Metamorphic protein IscU changes conformation by cis-trans isomerizations of two peptidyl-prolyl peptide bonds, *Biochemistry 51*, 9595-9602.

[98] Hoff, K. G., Cupp-Vickery, J., and Vickery, L. (2003) Contributions of the LPPVK motif of the iron-sulfur template protein IscU to interactions with the Hsc66-Hsc20 chaperone system, *J Biol Chem 278*, 37582-37589.

[99] Hoff, K. G., Ta, D. T., Tapley, T. L., Silberg, J. J., and Vickery, L. (2002) Hsc66 substrate specificity is directed toward a discrete region of the iron-sulfur cluster template protein IscU, *J Biol Chem 277*, 27353-27359.

[100] Hudder, B., Morales, J., Stubna, A., Münck, E., Hendrich, M., and Lindahl, P. (2007) Electron paramagnetic resonance and Mössbauer spectroscopy of intact mitochondria from respiring Saccharomyces cerevisiae, *J Biol Inorg Chem 12*, 1029-1053.

[101] Mitou, G., Higgins, C., Wittung-Stafshede, P., Conover, R. C., Smith, A. D., Johnson, M., Gaillard, J., Stubna, A., Münck, E., and Meyer, J. (2003) An Isc-type extremely thermostable [2Fe-2S] ferredoxin from Aquifex aeolicus. Biochemical, spectroscopic, and unfolding studies, *Biochemistry 42*, 1354-1364.

[102] Münck, E., and Bominaar, E. L. (2008) Chemistry. Bringing stability to highly reduced iron-sulfur clusters, *Science 321*, 1452-1453.

[103] Miao, R., Martinho, M., Morales, J. G., Kim, H., Ellis, E. A., Lill, R., Hendrich, M. P., Munck, E., and Lindahl, P. A. (2008) EPR and Mossbauer spectroscopy of intact mitochondria isolated from Yah1p-depleted Saccharomyces cerevisiae, *Biochemistry 47*, 9888-9899.

[104] Pagani, S., Bonomi, F., and Cerletti, P. (1984) Enzymic-synthesis of the iron-sulfur cluster of spinach ferredoxin, *European Journal of Biochemistry 142*, 361-366.

[105] Sweeney, W. V., and Rabinowitz, J. C. (1980) Proteins containing 4Fe-4S clusters - an overview, *Annual Review of Biochemistry 49*, 139-161.

[106] Gao, H. Y., Subramanian, S., Couturier, J., Naik, S. G., Kim, S. K., Leustek, T., Knaff, D. B., Wu, H. C., Vignols, F., Huynh, B. H., Rouhier, N., and Johnson, M. K. (2013) Arabidopsis thaliana Nfu2 accommodates [2Fe-2S] or [4Fe-4S] clusters and is competent for in vitro maturation of chloroplast [2Fe-2S] and [4Fe-4S] cluster-containing proteins, *Biochemistry 52*, 6633-6645.

[107] Marelja, Z., Stöcklein, W., Nimtz, M., and Leimkühler, S. (2008) A novel role for human Nfs1 in the cytoplasm: Nfs1 acts as a sulfur donor for MOCS3, a protein involved in molybdenum cofactor biosynthesis, *J Biol Chem 283*, 25178-25185.

[108] Siegel, L. M. (1965) A direct microdetermination for sulfide, *Anal Biochem 11*, 126-132.

[109] Viollier, E., Inglett, P. W., Hunter, K., Roychoudhury, A. N., and Van Cappellen, P. (2000) The ferrozine method revisited: Fe(II)/Fe(III) determination in natural waters, *Appl Geochem 15*, 785-790.

[110] Fish, W. W. (1988) Rapid colorimetric micromethod for the quantitation of complexed iron in biological samples, *Methods in Enzymology 158*, 357-364.

[111] Stookey, L. L. (1970) Ferrozine - a new spectrophotometric reagent for iron, *Anal Chem 42*, 779-781.

[112] Cowart, R. E., Singleton, F. L., and Hind, J. S. (1993) A comparison of bathophenanthrolinedisulfonic acid and ferrozine as chelators of iron(II) in reduction reactions, *Anal Biochem 211*, 151-155.

[113] Lanz, N. D., Grove, T. L., Gogonea, C. B., Lee, K. H., Krebs, C., and Booker, S. J. (2012) RlmN and AtsB as models for the overproduction and characterization of radical SAM proteins, *Methods in Enzymology 516*, 125-152.

[114] Hall, D. O., Cammack, R., and Rao, K. K. (1973a) The plant ferredoxins and their relationship to the evolution of ferredoxins from primitive life, *Pure App Chem 34*, 533-577.

[115] Garg, V. K. (1980) Mössbauer studies of iron sulphide minerals, *Revista Brasileira de Fisica 10*, 535-558.

[116] Muhlenhoff, U., Richter, N., Pines, O., Pierik, A. J., and Lill, R. (2011) Specialized function of yeast ISA1 and ISA2 in the maturation of mitocondrial [4Fe-4S] proteins, *J Biol Chem 286*, 41205-41216.

[117] Chamberlain, S., Farrall, M., Shaw, J., Wilkes, D., Carvajal, J., Hillerman, R., Doudney, K., Harding, A. E., Williamson, R., and Sirugo, G. (1993) Genetic recombination events which position the Friedreich ataxia locus proximal to the D9S15/D9S5 linkage group on chromosome 9q, *American Journal of Human Genetics 52*, 99-109.

[118] Chamberlain, S., Shaw, J., Rowland, A., Wallis, J., South, S., Nakamura, Y., von Gabain, A., Farrall, M., and Williamson, R. (1988) Mapping of mutation causing Friedreich's ataxia to human chromosome 9, *Nature 334*, 248-250.

[119] Martelli, A., Napierala, M., and Puccio, H. (2012) Understanding the genetic and molecular pathogenesis of Friedreich's ataxia through animal and cellular models, *Disease Models & Mechanisms 5*, 165-176.

[120] Rouault, T. A. (2012) Biogenesis of iron-sulfur clusters in mammalian cells: new insights and relevance to human disease, *Disease Models & Mechanisms 5*, 155-164.

[121] Adinolfi, S., Iannuzzi, C., Prischi, F., Pastore, C., Iametti, S., Martin, S. R., Bonomi, F., and Pastore, A. (2009) Bacterial frataxin CyaY is the gatekeeper of iron-sulfur cluster formation catalyzed by IscS, *Nat Struct Mol Biol 16*, 390-396.

[122] Bridwell-Rabb, J., Iannuzzi, C., Pastore, A., and Barondeau, D. P. (2012) Effector role reversal during evolution: The case of frataxin in Fe-S cluster biosynthesis, *Biochemistry 51*, 2506-2514.

[123] Shan, Y., and Cortopassi, G. (2012) HSC20 interacts with frataxin and is involved in iron–sulfur cluster biogenesis and iron homeostasis, *Human Molecular Genetics 21*, 1457-1469.

[124] Shan, Y., Napoli, E., and Cortopassi, G. (2007) Mitochondrial frataxin interacts with ISD11 of the NFS1/ISCU complex and multiple mitochondrial chaperones, *Human Molecular Genetics 16*, 929-941.

[125] Leidgens, S., De Smet, S., and Foury, F. (2010) Frataxin interacts with Isu1 through a conserved tryptophan in its beta-sheet, *Human Molecular Genetics 19*, 276-286.

[126] Wang, T., and Craig, E. (2008) Binding of yeast frataxin to the scaffold for Fe-S cluster biogenesis, Isu, *J Biol Chem 283*, 12674-12679.

[127] Gerber, J., Muhlenhoff, U., and Lill, R. (2003) An interaction between frataxin and Isu1/Nfs1 that is crucial for Fe/S cluster synthesis on Isu1, *Embo Reports 4*, 906-911.

[128] Prischi, F., Konarev, P. V., Iannuzzi, C., Pastore, C., Adinolfi, S., Martin, S. R., Svergun, D. I., and Pastore, A. (2010) Structural bases for the interaction of frataxin with the central components of iron-sulphur cluster assembly, *Nature Communications 1*, 95-95.

[129] Cook, J. D., Kondapalli, K. C., Rawat, S., Childs, W. C., Murugesan, Y., Dancis, A., and Stemmler, T. L. (2010) Molecular details of the yeast frataxin−Isu1 interaction during mitochondrial Fe−S cluster assembly, *Biochemistry 49*, 8756-8765.

[130] Gill, S. C., and von Hippel, P. H. (1989) Calculation of protein extinction coefficients from amino acid sequence data, *Analytical Biochemistry 182*, 319-326.

[131] Bridwell-Rabb, J., Winn, A. M., and Barondeau, D. P. (2011) Structure-function analysis of Friedreich's ataxia mutants reveals determinants of frataxin binding and activation of the Fe-S assembly complex, *Biochemistry 50*, 7265-7274.

[132] Gakh, O., Bedekovics, T., Duncan, S. F., Smith, D. Y., Berkholz, D. S., and Isaya, G. (2010) Normal and Friedreich ataxia cells express different isoforms of frataxin with complementary roles in iron-sulfur cluster assembly, *J Biol Chem*.

[133] Prischi, F., Pastore, C., Carroni, M., Iannuzzi, C., Adinolfi, S., Temussi, P., and Pastore, A. (2010) Of the vulnerability of orphan complex proteins: The case study of the E. coli IscU and IscS proteins, *Protein Expression and Purification 73*, 161-166.

APPENDIX

ALANINE SCANNING OF THE FRATAXIN (FXN) SUPPLEMENTAL FIGURES

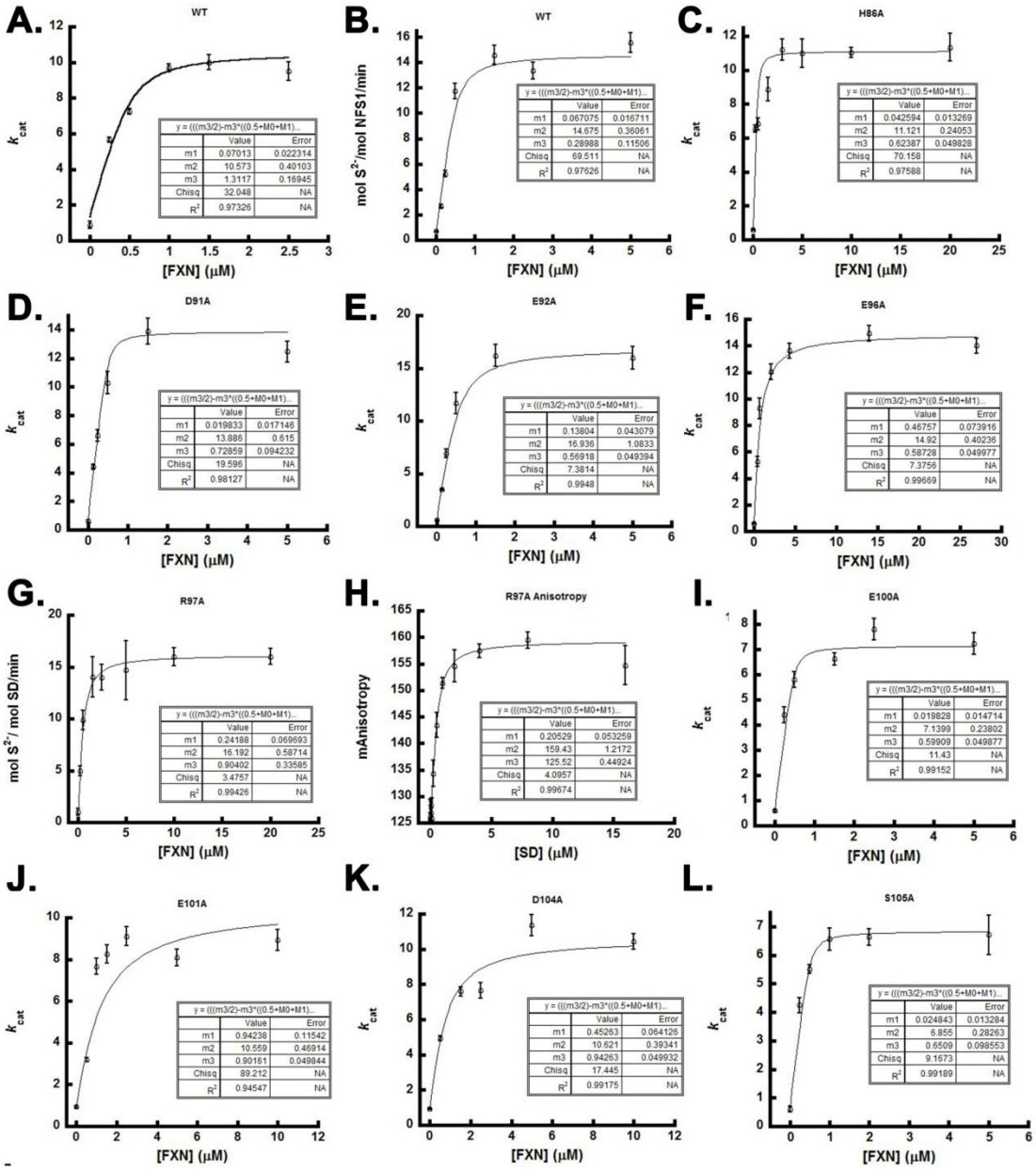

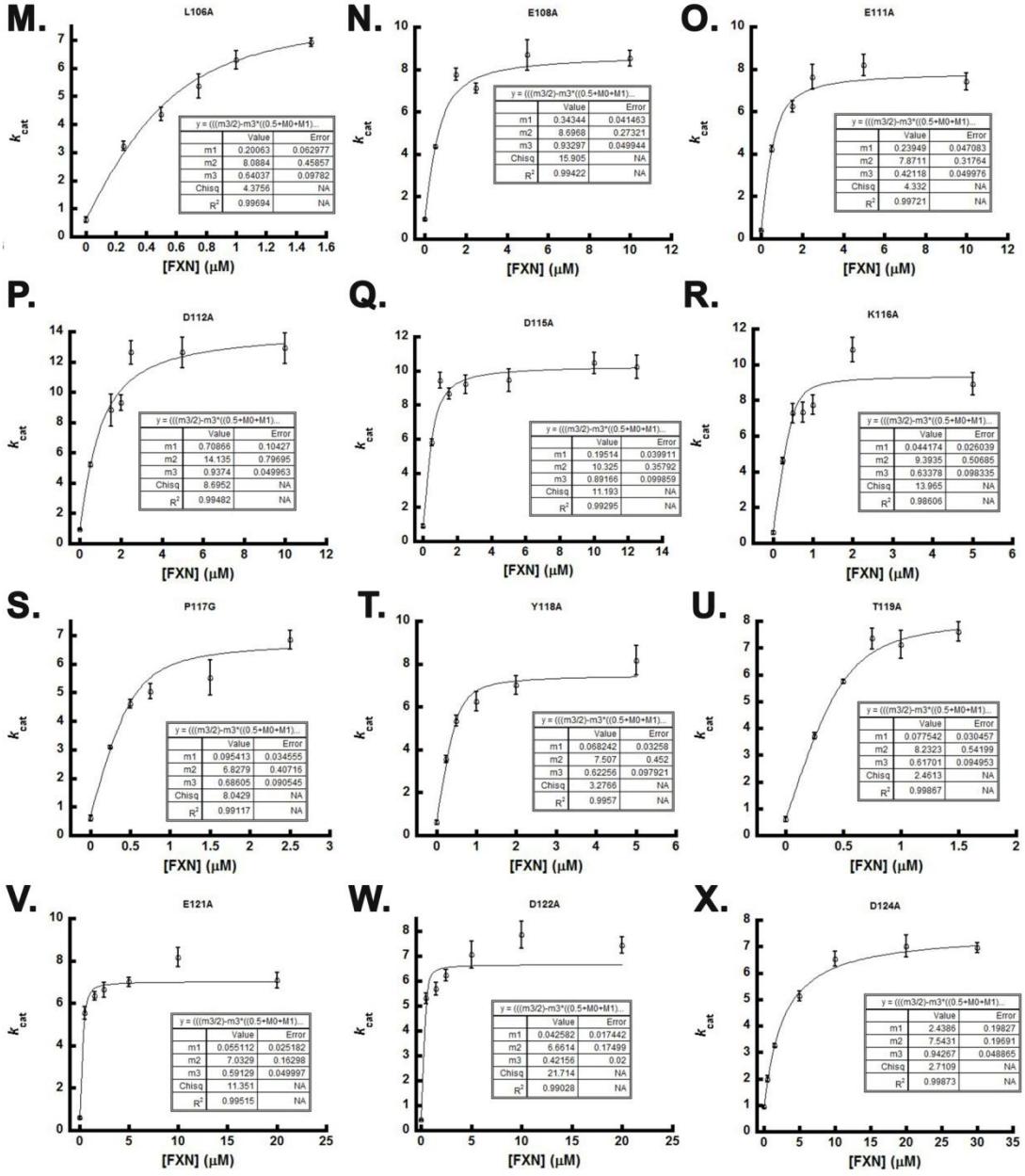
M.
L106A
y = (((m3/2)-m3*((0.5+M0+M1)...
Value Error
m1 0.20063 0.062977
m2 8.0884 0.45857
m3 0.64037 0.09782
Chisq 4.3756 NA
R² 0.99694 NA
N.
E108A
y = (((m3/2)-m3*((0.5+M0+M1)...
Value Error
m1 0.34344 0.041463
m2 8.6968 0.27321
m3 0.93297 0.049944
Chisq 15.905 NA
R² 0.99422 NA
O.
E111A
y = (((m3/2)-m3*((0.5+M0+M1)...
Value Error
m1 0.23949 0.047083
m2 7.8711 0.31764
m3 0.42118 0.049976
Chisq 4.332 NA
R² 0.99721 NA
P.
D112A
y = (((m3/2)-m3*((0.5+M0+M1)...
Value Error
m1 0.70866 0.10427
m2 14.135 0.79695
m3 0.9374 0.049963
Chisq 8.6952 NA
R² 0.99482 NA
Q.
D115A
y = (((m3/2)-m3*((0.5+M0+M1)...
Value Error
m1 0.19514 0.039911
m2 10.325 0.35792
m3 0.89166 0.099859
Chisq 11.193 NA
R² 0.99295 NA
R.
K116A
y = (((m3/2)-m3*((0.5+M0+M1)...
Value Error
m1 0.044174 0.026039
m2 9.3935 0.50685
m3 0.63378 0.098335
Chisq 13.965 NA
R² 0.98606 NA
S.
P117G
y = (((m3/2)-m3*((0.5+M0+M1)...
Value Error
m1 0.095413 0.034555
m2 6.8279 0.40716
m3 0.68605 0.090545
Chisq 8.0429 NA
R² 0.99117 NA
T.
Y118A
y = (((m3/2)-m3*((0.5+M0+M1)...
Value Error
m1 0.068242 0.03258
m2 7.507 0.452
m3 0.62256 0.097921
Chisq 3.2766 NA
R² 0.9957 NA
U.
T119A
y = (((m3/2)-m3*((0.5+M0+M1)...
Value Error
m1 0.077542 0.030457
m2 8.2323 0.54199
m3 0.61701 0.094953
Chisq 2.4613 NA
R² 0.99867 NA
V.
E121A
y = (((m3/2)-m3*((0.5+M0+M1)...
Value Error
m1 0.055112 0.025182
m2 7.0329 0.16298
m3 0.59129 0.049997
Chisq 11.351 NA
R² 0.99515 NA
W.
D122A
y = (((m3/2)-m3*((0.5+M0+M1)...
Value Error
m1 0.042582 0.017442
m2 6.6614 0.17499
m3 0.42156 0.02
Chisq 21.714 NA
R² 0.99028 NA
X.
D124A
y = (((m3/2)-m3*((0.5+M0+M1)...
Value Error
m1 2.4386 0.19827
m2 7.5431 0.19691
m3 0.94267 0.048865
Chisq 2.7109 NA
R² 0.99873 NA
k cat
[FXN] (μM)

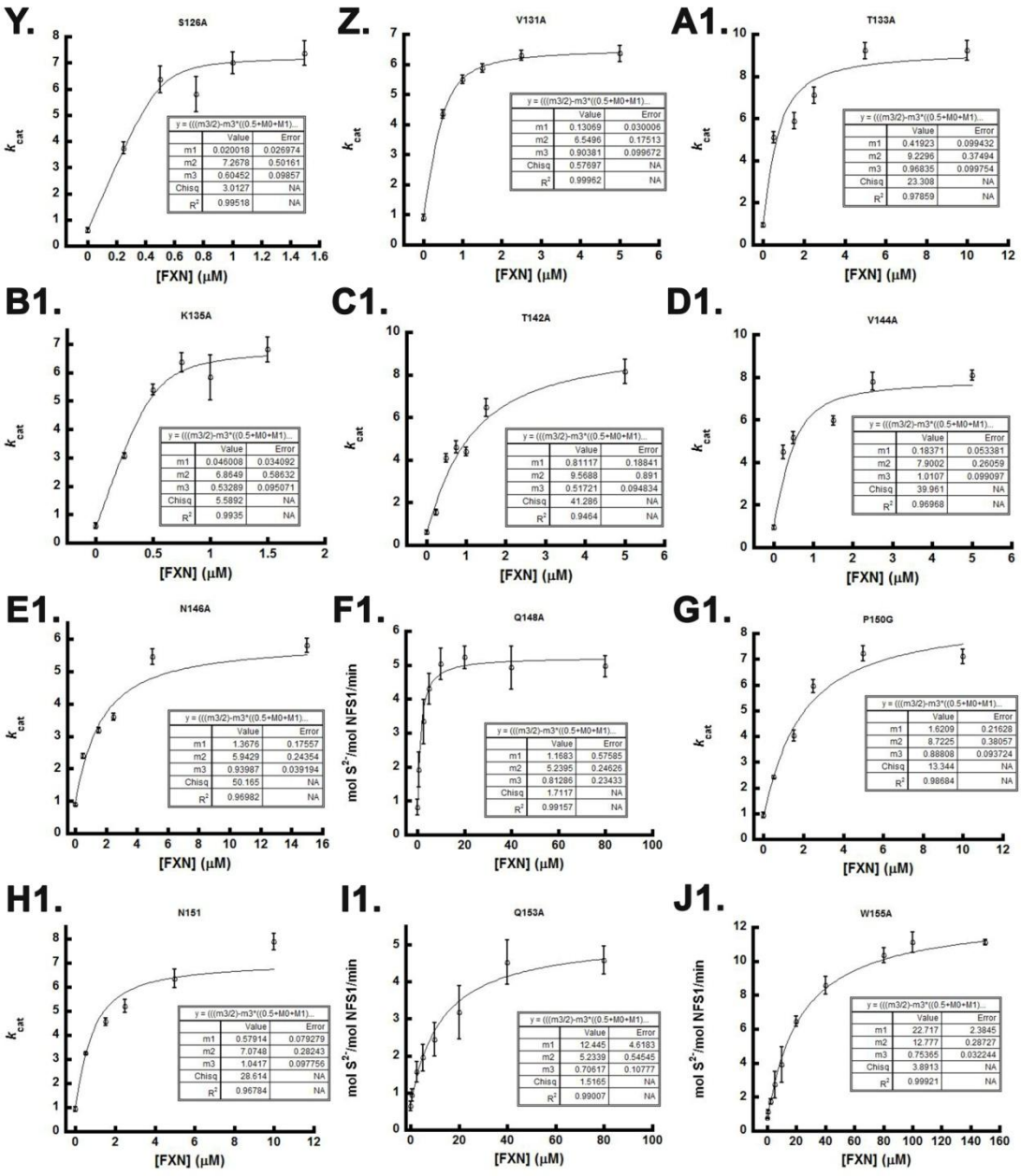
Y.
S126A
Z.
V131A
A1.
T133A
B1.
K135A
C1.
T142A
D1.
V144A
E1.
N146A
F1.
Q148A
G1.
P150G
H1.
N151
I1.
Q153A
J1.
W155A
k_{cat}
mol S^{2-}/mol NFS1/min
[FXN] (μM)
y = (((m3/2)-m3*((0.5+M0+M1)...
Value
Error
m1 0.020018 0.026974
m2 7.2678 0.50161
m3 0.60452 0.09857
Chisq 3.0127 NA
R^2 0.99518 NA
m1 0.13069 0.030006
m2 6.5496 0.17513
m3 0.90381 0.099672
Chisq 0.57697 NA
R^2 0.99962 NA
m1 0.41923 0.099432
m2 9.2296 0.37494
m3 0.96835 0.099754
Chisq 23.308 NA
R^2 0.97859 NA
m1 0.046008 0.034092
m2 6.8649 0.58632
m3 0.53289 0.095071
Chisq 5.5892 NA
R^2 0.9935 NA
m1 0.81117 0.18841
m2 9.5688 0.891
m3 0.51721 0.094834
Chisq 41.286 NA
R^2 0.9464 NA
m1 0.18371 0.053381
m2 7.9002 0.26059
m3 1.0107 0.099097
Chisq 39.961 NA
R^2 0.96968 NA
m1 1.3676 0.17557
m2 5.9429 0.24354
m3 0.93987 0.039194
Chisq 50.165 NA
R^2 0.96982 NA
m1 1.1683 0.57595
m2 5.2395 0.24626
m3 0.81286 0.23433
Chisq 1.7117 NA
R^2 0.99157 NA
m1 1.6209 0.21628
m2 8.7225 0.38057
m3 0.88808 0.093724
Chisq 13.344 NA
R^2 0.98684 NA
m1 0.57914 0.079279
m2 7.0748 0.28243
m3 1.0417 0.097756
Chisq 28.614 NA
R^2 0.96784 NA
m1 12.445 4.6183
m2 5.2339 0.54545
m3 0.70617 0.10777
Chisq 1.5165 NA
R^2 0.99007 NA
m1 22.717 2.3845
m2 12.777 0.28727
m3 0.75365 0.032244
Chisq 3.8913 NA
R^2 0.99921 NA

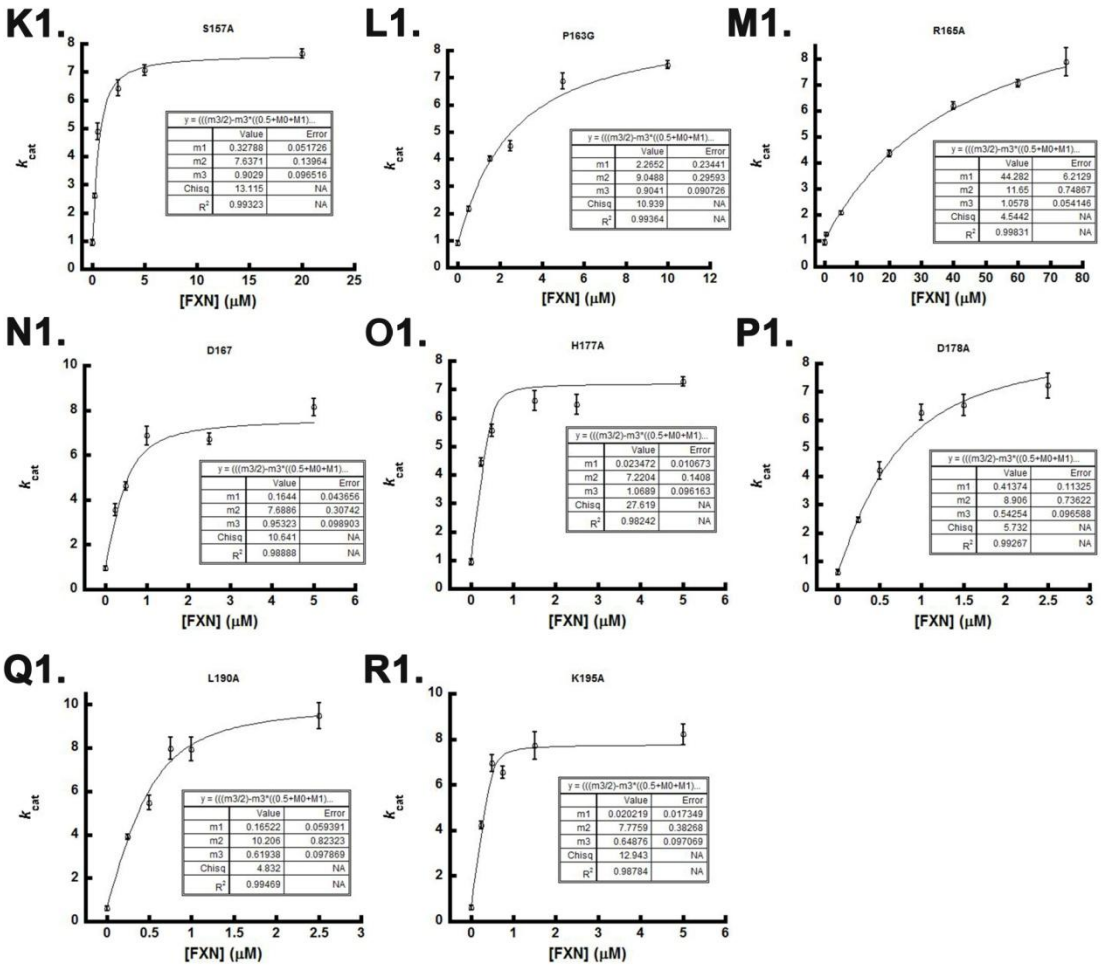
K1.
S157A
y = (((m3/2)-m3*((0.5+M0+M1)...
Value Error
m1 0.32788 0.051726
m2 7.6371 0.13964
m3 0.9029 0.096516
Chisq 13.115 NA
R² 0.99323 NA
L1.
P163G
y = (((m3/2)-m3*((0.5+M0+M1)...
Value Error
m1 2.2662 0.23441
m2 9.0488 0.29593
m3 0.9041 0.090726
Chisq 10.939 NA
R² 0.99364 NA
M1.
R165A
y = (((m3/2)-m3*((0.5+M0+M1)...
Value Error
m1 44.282 6.2129
m2 11.65 0.74867
m3 1.0578 0.054146
Chisq 4.5442 NA
R² 0.99831 NA
N1.
D167
y = (((m3/2)-m3*((0.5+M0+M1)...
Value Error
m1 0.1644 0.043656
m2 7.6886 0.30742
m3 0.95323 0.098903
Chisq 10.641 NA
R² 0.98888 NA
O1.
H177A
y = (((m3/2)-m3*((0.5+M0+M1)...
Value Error
m1 0.023472 0.010673
m2 7.2204 0.1408
m3 1.0689 0.096163
Chisq 27.619 NA
R² 0.98242 NA
P1.
D178A
y = (((m3/2)-m3*((0.5+M0+M1)...
Value Error
m1 0.41374 0.11325
m2 8.906 0.73622
m3 0.54254 0.096588
Chisq 5.732 NA
R² 0.99267 NA
Q1.
L190A
y = (((m3/2)-m3*((0.5+M0+M1)...
Value Error
m1 0.16522 0.059391
m2 10.206 0.82323
m3 0.61938 0.097869
Chisq 4.832 NA
R² 0.99469 NA
R1.
K195A
y = (((m3/2)-m3*((0.5+M0+M1)...
Value Error
m1 0.020219 0.017349
m2 7.7759 0.38268
m3 0.64876 0.097069
Chisq 12.943 NA
R² 0.98784 NA
kcat
[FXN] (μM)

Table A1. FXN Variant Activity Measurements w/o and w/ Fe^{2+}

Protein	mol S^{2-}/mol NFS1/min w/o Fe^{2+}	mol S^{2-}/mol NFS1/min w/ Fe^{2+}	*p* test df=4
SDUF*	5.80 ± 0.51	9.70 ± 0.55	9.01
H86A*	8.50 ± 0.03	10.70 ± 0.62	6.14
D91A*	**8.50 ± 0.70**	**8.80 ± 0.63**	**0.55**
E92A*	7.40 ± 0.50	11.20 ± 0.40	10.28
E96A*	8.00 ± 0.40	10.00 ± 0.54	5.15
R97A*	9.30 ± 0.30	16.01 ± 0.74	14.47
E100A*	5.00 ± 0.80	6.80 ± 0.40	3.49
E101A*	**6.60 ± 0.36**	**7.60 ± 0.75**	**2.08**
D104A*	7.90 ± 0.39	10.50 ± 0.24	9.83
S105A	4.38 ± 0.23	6.84 ± 0.15	15.52
L106A	3.53 ± 0.35	5.78 ± 0.34	7.99
E108A*	4.70 ± 0.70	7.00 ± 0.40	4.94
E111A*	7.20 ± 0.04	7.90 ± 0.27	4.47
D112A*	**6.90 ± 0.72**	**8.00 ± 0.09**	**2.63**
D115A	3.18 ± 0.14	5.68 ± 0.30	13.08
K116A	4.83 ± 0.16	7.24 ± 0.41	9.48
P117G	2.82 ± 0.15	5.59 ± 0.24	16.95
Y118A	3.98 ± 0.22	6.17 ± 0.40	8.31
T119A	2.87 ± 0.12	6.22 ± 0.31	17.46
E121A*	7.60 ± 0.50	9.60 ± 0.70	4.03
D122A*	6.30 ± 0.30	7.40 ± 0.30	4.49
D124A*	5.20 ± 0.07	7.20 ± 0.22	15.00
S126A	2.64 ± 0.15	5.71 ± 0.15	25.07
V131A	2.94 ± 0.37	4.86 ± 0.03	8.96
T133A	4.80 ± 0.38	6.91 ± 0.34	7.17
K135A	2.73 ± 0.42	5.80 ± 0.40	9.17
T142A	4.32 ± 0.57	6.99 ± 0.57	5.74
V144A	5.64 ± 0.72	9.34 ± 0.59	6.88
N146A*	6.50 ± 0.41	7.44 ± 0.28	3.33
Q148A*	2.50 ± 0.16	4.97 ± 0.08	23.88
P150G	2.47 ± 0.16	3.36 ± 0.16	6.81
N151A*	2.59 ± 0.26	7.36 ± 0.00	31.77
Q153A*	2.30 ± 0.29	4.59 ± 0.31	9.29
W155A*	5.46 ± 0.68	11.11 ± 0.17	14.03

Table A1. FXN Variant Activity Measurements w/o and w/ Fe^{2+} Continued

Protein	mol S^{2-}/mol NFS1/min w/o Fe^{2+}	mol S^{2-}/mol NFS1/min w/ Fe^{2+}	t test df=4
S157A	4.54 ± 0.27	8.12 ± 0.77	7.60
P163G	3.08 ± 0.13	5.08 ± 0.21	14.03
R165A	6.30 ± 0.22	8.55 ± 0.48	7.38
D167A	3.63 ± 0.12	6.24 ± 0.01	37.54
H177A	2.87 ± 0.18	5.92 ± 0.12	24.42
D178A	2.18 ± 0.31	5.66 ± 0.12	18.13
L190A	3.42 ± 0.36	6.81 ± 0.43	10.47
K195A	4.13 ± 0.37	6.23 ± 0.23	8.35

The *p* test was performed to see if there was a significant change in activity. In bold p>95% confidence, they are not different. * Indicates the experiment was performed by Nicholas Fox